



DIPLOMARBEIT

# Classification of satellite images by including spectral and textural information

zur Erlangung des akademischen Grades

**Diplom-Ingenieurin**

im Rahmen des Studiums

**Geodäsie und Geoinformation**

eingereicht von

**Madalina-Iasmina Gaina**

Matrikelnummer 01228554

ausgeführt am Department für Geodäsie und Geoinformation  
der Fakultät für Mathematik und Geoinformation der Technischen Universität Wien

Betreuung

Betreuer: Prof. DI Dr.techn. Josef Jansa

Mitwirkung: Univ.-Ass. Dr. Camillo Ressler

Wien, 10.05.2019

---

(Unterschrift Verfasser/in)

---

(Unterschrift Betreuer/in)



## **ACKNOWLEDGMENTS**

My special thanks and deep gratitude go to my supervisor Univ.Prof.Dipl.-Ing. Dr. Josef Jansa, who gave me not only the opportunity to do independent research but was also always open to exchanging thoughts and new ideas. I am grateful for patience, suggestions, constructive and inspirational conversations, but also for the guidance and advice throughout the duration of my thesis. I sincerely thank him for all support and also for the provided data and relevant information.

And last but not least, I express my sincere thanks to my mother, Gaina Sofia, who tirelessly sustained me from professional to emotional side but also for the financial support, because without her help, this work would not have been possible.

And thank God who gave me health, wisdom, and work power to complete this master thesis.



## ABSTRACT

*Keywords: high-resolution, spectral, texture, standard classification, quality assessment.*

With the advance in sensor technology in the field of remote sensing from space, new challenges emerge. The high-resolution images offer a wide range of new applications, but at the same pace, the interpretation requires new approaches, from pure spectral interpretation to a more holistic one. This thesis focuses only on a small aspect of that sort of interpretation and on one specific application, which has been gaining increasing importance nowadays, where the carbon dioxide balance has become an issue. Forests are important CO<sub>2</sub> sinks, and therefore, it makes sense to concentrate on the interpretation of forest stands, in this case in the area of central Europe. Thus, the principal objective of this investigation is to focus on forest classification and to interpret different types of forest stands in high-resolution satellite images.

The used images have been captured by Pléiades 1B satellites, whose spatial resolution provides quite good textural information, which may be utilized to distinguish between different types of forest patches. Together with the spectral information, one may expect even an improvement of the classification quality compared to the interpretation of sole multispectral object properties. Therefore, this research concentrates on assessing standard strategies for image classification if the spectral and textural information is to be taken into consideration.

The key for characterizing texture in forest areas was found in using a set of Haralick textural features known already for many decades, therefore for the special purpose a thorough investigation of generating suitable textural features has been carried out and their properties have been studied.

One of the standard classification algorithms in remote sensing is the Maximum Likelihood classification. The question arises of course, whether the Maximum Likelihood classification would be appropriate enough for the textural classification. Therefore, the distribution of the classes in the feature space for the textural parameters has been investigated and then the decision has been made to use the Maximum Likelihood for classifying the multispectral as well as for textural parameters, from which Mean, Contrast, and Entropy delivered promising results, which have proved of value in previous research with other satellite data.

Further, the quality assessment of the data has been made, where the resulted accuracies are quite high, around 80%, and lie in the expected range, although a significant improvement by including textural features cannot be observed.

In the frame of these investigations, commercial software (ENVI Image Analysis (the Environment for Visualizing Images)), open source products, and a few other minor tools have been used for visualization, analysis, and processing, besides own software developments.

There are still a few open issues for future work, whose investigation would have exceeded the effort for a diploma thesis, in particular, the influence of combining various Haralick features and of varying the parameters for their generation.

## KURZFASSUNG

*Schlüsselwörter: hochauflösend, spektral, Textur, Standardklassifikation, Qualitätsbeurteilung*

Mit den Fortschritten in der Sensortechnologie auf dem Gebiet der Fernerkundung aus dem Weltraum tauchen neue Herausforderungen auf. Die hochauflösenden Bilder eröffnen einen weiten neuen Anwendungsbereich, aber im gleichen Tempo erfordert die Interpretation neue Ansätze, von reiner spektralen Interpretation hin zu einer mehr ganzheitlichen. Diese Arbeit stellt nur einen kleinen Aspekt der Interpretationsart in den Mittelpunkt und nur eine spezielle Anwendung, welche heute wichtig geworden ist, wo die Kohlendioxid-Bilanz ein Anliegen wurde. Wälder sind wichtige CO<sub>2</sub> Verbraucher und deshalb ist es sinnvoll sich auf die Interpretation von Waldbeständen zu konzentrieren, in diesem Fall auf ein Gebiet in Mitteleuropa. Der Hauptzweck dieser Untersuchung richtet sich auf die Waldklassifizierung und auf die Interpretation von verschiedenen Arten von Waldbeständen aus hochauflösenden Satellitenbildern.

Die verwendeten Bilder wurden durch den Satelliten Pléiades 1B aufgenommen, der für eine gute Texturinterpretation geeignete räumliche Auflösung bietet, mit deren Hilfe man zwischen verschiedenen Waldbereichen unterscheiden kann. Zusammen mit der spektralen Information erwartet man sogar eine Verbesserung der Klassifizierungsqualität im Vergleich zur Interpretation der reinen multispektralen Objekteigenschaften. Daher befasst sich diese Studie mit der Beurteilung von Standardstrategien der Bildinterpretation, wenn sowohl spektrale auch texturale Information berücksichtigt wird.

Der Schlüssel für die Texturcharakterisierung von Forstgebieten wurde in den Haralick Texturmerkmale gefunden, die seit Jahrzehnten bekannt sind, daher wurde für den speziellen Zweck eine gründliche Untersuchung durchgeführt in Bezug auf die Ableitung geeigneter Texturmerkmale und das Studium ihrer Eigenheiten.

Einer der Standardklassifizierungsalgorithmen ist die Maximum Likelihood Klassifikation. Natürlich stellt sich die Frage, ob die Maximum Likelihood Klassifikation für Texturklassifikation gut genug wäre. Daher wurde die Verteilung der Klassen im Merkmalsraum der Texturmerkmale untersucht und es wurde dann entschieden, Maximum Likelihood für die Klassifizierung sowohl der multispektralen als auch der texturalen Parameter zu verwenden, von denen Mean, Contrast und Entropy vielversprechende Ergebnisse lieferten, welche auch schon in früheren Forschungen mit anderen Satellitendaten sich als wertvoll erwiesen.

Des Weiteren wurde eine Qualitätsbeurteilung der Daten durchgeführt, bei welcher die erhaltenen Genauigkeiten recht hoch waren, um die 80%, und im erwarteten Rahmen lagen, wenn auch eine signifikante Verbesserung der Genauigkeiten durch Einbeziehung der Texturinformation nicht beobachtet werden konnte.

Für diese Untersuchungen wurde kommerzielle Software (ENVI Bildanalyse (The Environment for Visualizing Images)), Open Source Produkte und andere kleinere Werkzeuge für die Visualisierung, Analyse und Prozessierung verwendet nebst selbst entwickelter Software.

Es gibt noch ein paar offene Fragen für zukünftige Forschung, deren Untersuchung den Rahmen einer Diplomarbeit gesprengt hätte, und zwar den Einfluss bei der Kombination verschiedener Haralick-Merkmale und beim Variieren der Parameter für deren Herleitung.





## Contents

1	Introduction.....	3
1.1	Goal of the research.....	4
1.2	State of the art.....	5
2	Study area and description of satellite data.....	8
2.1	Study area.....	8
2.2	Satellite data.....	9
2.2.1	Pléiades Satellite imagery.....	9
2.2.2	Panchromatic images.....	10
2.2.3	Multispectral images.....	10
2.2.4	Pan-Sharpended Data.....	12
2.2.5	Image resolution.....	13
3	Characteristics of spectral signatures.....	16
3.1	Interpretation of spectral signature regarding vegetation.....	16
3.2	The spectral signature in the acquired image.....	17
4	Introductory remarks on texture and the Gray Level Co-occurrence Matrix (GLCM).....	19
4.1	Introductory remarks on texture.....	19
4.2	The interpretation of textural signatures regarding forest.....	21
4.3	The Gray Level Co-occurrence Matrix (GLCM) and the textural features.....	21
4.4	Parameters for deriving GLCM and texture images.....	25
5	Image classification.....	31
5.1	Supervised and unsupervised classification.....	31
5.2	Choosing a supervised approach.....	32
5.2.1	Selecting the classification algorithm.....	33
5.2.2	Maximum Likelihood classification (ML classification).....	33
6	Investigation methodology.....	35
6.1	Selection of ground truth areas.....	35
6.2	Image texture measures.....	36
6.3	Separability analysis.....	37
6.4	Maximum Likelihood classification process.....	37
6.5	Quality assessment.....	37
7	Practical example.....	39
7.1	Selection of ground truth areas.....	39
7.2	Results of separability analysis.....	39

7.3	Assessment of the cluster distributions in feature space.....	43
7.3.1	Spectral case .....	44
7.3.2	Textural case .....	47
7.4	Visual comparison of the real distribution with the normal distribution.....	55
7.5	Classification.....	63
7.5.1	N-W area: Spectral case.....	64
7.5.2	N-W area: Textural case.....	66
7.5.3	N-W area: Combination of spectral and textural properties.....	68
7.5.4	S-E area: Spectral case .....	69
7.6	Results of the quality assessment .....	71
7.6.1	N-W area: Spectral case.....	71
7.6.2	N-W area: Textural case.....	77
7.6.3	N-W area: Combination of spectral and textural properties.....	83
7.6.4	S-E area: Spectral case .....	88
7.7	Combination of spectral and textural classifications.....	91
8	Conclusions.....	96

# 1 Introduction

Along with the important technological developments in recent years, imaging devices and general purpose computing systems have become more and more powerful and prevalent.

Naturally, the desire to have autonomous systems gets increasingly in the focus of current developments. Solutions which have looked unrealistic in the past, suddenly begin to dominate many fields of our every day's life. Just looking at satellite imaging, the task of preparing big data for optimal visualization and automated interpretation has gradually moved to optimal automatic analysis, interpretation, and understanding. Image processing and analysis include a set of techniques and methods of acquisition, storage, visualization, modification, and exploitation of visual information contained in images. In particular, image analysis refers to the ability to describe, understand and recognize scenes, scene objects, and links between them. From a functional point of view, image analysis transforms an input image into a description.

The work on this thesis is targeting at the satellite image analysis from a spectral and textural perspective, as well as on the quality evaluation of the classification result.

The visual interpretation of remotely sensed data has always relied on spatial image properties to separate image components into similar groups (Lillesand T. M., and Kiefer R. W., 2000). This visual process takes advantage of an interpreter's ability to perceive spatial and tonal differences rapidly (for instance such as texture and color) and group areas with similar spatial structure with little ambiguity (Franklin S.E. et al., 2001). Image texture is a complex visual perception (Coburn C. A., and Roberts A. C. B., 2004).

For a long time, neither in remote sensing nor in photogrammetry, textural interpretation has not been used in image interpretation tasks. In the 90's, all these investigations, and classifications appear with the introduction of the digital workstations and powerful digital imaging systems. That was the time when in photogrammetry, where digital high-resolution imagery increasingly became standard, texture analysis, and feature detection has begun to emerge in order to automatize the sometimes rather cumbersome 3D object restitution tasks.

On the other hand, in remote sensing, this objective occurred earlier, because digital imaging became standard in early 1970 when space-borne digital acquisition systems commenced their successful area. Due to their fairly low spatial resolution at the very beginning, the interpretation mainly focused on multispectral properties.

Landsat satellite imaging may be the most important episode in the history of remote sensing and Earth observation. In 1972, Landsat satellite imaging systems had a resolution of 60 to 80 meters, which means, that the textural properties of objects were rarely an issue and hence in general the interpretation of textural characteristics could easily be ignored.

With the appearance of the second Landsat generation in 1980, the imaging system Thematic Mapper was introduced and more object details become visible and in one or the other case one could even think of taking texture into consideration. Nevertheless, the multispectral interpretation was still more important, but appropriate sophisticated interpretation methods became more established in practice. Since then, digital imaging systems rapidly became more powerful as far as the spatial, the radiometric, and the spectral resolutions are concerned. In the meantime, many space-borne sensors deliver

spatial resolutions up to several decimeters and radiometric resolutions far beyond the typical 8-bit intensity range.

As a consequence, the importance of traditional spectral interpretation decreased slightly because of the disturbing effects of minor elements like, for instance, micro shadows. Suddenly textural aspects started to become more important, but due to missing reliable and powerful software in remote sensing and in particular in photogrammetry, the human interpreter could not entirely be replaced, although theoretical research has been carried out for many decades and practical approaches for special applications implemented in dedicated hardware, especially for military and surveillance purposes and in manufacturing, already existed.

In remote sensing texture issues become more and more important with the occurrence of high-resolution satellite imaging systems. These high-resolution satellite images show a lot of detail, thus being able to recognize much more characteristics of a certain object class so that, not only the color but also textural properties started to play an increasingly important role. One may define the begin of high resolution in remote sensing with the launch of the French satellite SPOT1 in 1986, which carried a panchromatic sensor on board providing an image with a ground resolution of 10m. In 1996 the Indian Satellite IRC-1C had a Pan sensor on board providing an amazing spatial resolution of 6m (though at the cost of radiometric resolution). But the panchromatic images of IKONOS(2) are considered to mark the real milestone of high-resolution satellite imaging. Their sensor footprint has a size of some 80 cm to 1 m. Then shortly one after the other, systems have been launched reaching high-resolution of 50 cm and less nowadays. Finest object details and precision, together with a rapid and reliable data distribution system cover practical interests in many fields of every day's life, such as environmental observations, precision farming, monitoring urban sprawl, forest inventory and many others ([1] [http://www.landinfo.com/products\\_satellite.htm](http://www.landinfo.com/products_satellite.htm)).

Haralick R.M. was one of the first who has introduced texture in image processing. From his perspective, color alone is not that what is important and therefore he has been taking into consideration texture as well. Hence he created the Grey-Level-Co-occurrence Matrix (abbreviated GLCM) where the neighborhood of intensity values in images are analyzed. Traditionally, texture has been defined as the spatial variation in image tones or colors (Haralick R.M.et al., 1973).

Hall-Beyer M. (2017) writes: "Texture as defined visually has long been an important element in visual image interpretation, allowing operators to separate spectrally similar image regions. In visible and infrared-wavelength remotely sensed images, texture provides information that is independent of spectral reflectance values." [...]

"Haralick's texture measures remain widely implemented in software and are able to incorporate multiple elements of texture." [...]

"As noted by Wang L. et al. (2016), the primary improvements in GLCM since the 1970s have resulted in faster calculation algorithms, rather than changes in the statistics themselves".

## 1.1 Goal of the research

In the context of the thesis it is intended to evaluate the applicability of standard digital image processing methods by including spectral information together with the textural information in order to improve the quality of the classification result.

Choosing and acquiring satellite imagery is one of the most important phases of a project based on remote sensing. This step is the most important because the final results are influenced by the quality of the input data. A cloudless view with maximum visibility can be considered a very good source. Secondly, it is very important to keep in mind the purpose for which satellite images are used, because many types of images and sensors have different spectral and spatial features. There are many types of platforms on which a remote sensor can be built or mounted.

The discussions in the following chapters will focus on commercial platforms and known sensors used in remote sensing applications and available to the public. Thereby, in this study processing of the digital images acquired by the Pléiades satellites ([2] <https://directory.eoportal.org/web/eoportal/satellite-missions/p/pleiades>) are evaluated with the concentration on the assessment of areas covered by forests. This is justified because forests are the green lungs on Earth and, hence their state of health, distribution, and composition plays a very important role for estimating the carbon dioxide balance in the context of climate change issues.

The main objective of this research is to investigate whether standard classification methods, which have proved to deliver good results in the case of multispectral images, are able to be utilized with channels of textural features or in combination with spectral bands so that the quality of the final result may be improved. In the course of this investigation, Haralick's approach is analyzed in the context of forest classification, in order to obtain deeper understanding and better know-how for further similar projects.

All these being said, the reason for choosing this subject is, beside curiosity, a challenge and has been formed and developed from the interest of finding out more details about the impact of texture on the interpretation of high-resolution satellite images. On the basis of all these principle examinations, it has been considered that it would be very stimulating to find out more information about the texture analysis.

## 1.2 State of the art

In the past, many approaches, which focus on segmentation or classification of texture in remote sensing applications, have been developed and/or investigated. In the following, a concise collection of different approaches will briefly be presented in order to prove that Haralick's features are important but they are by far not the only way of including texture in classifications. Even though the current thesis concentrates on utilizing Haralick's concept, other approaches must not be overseen and they may even be the primary choice for other research.

Standard texture classification techniques have been proposed by Grigorescu S.E. et al., 2002, where the Gabor filters are taken into consideration. Gabor energy, complex moments, and grating cell operator features are examined. In order to produce distinct feature vector clusters for different textures, two methods are presented: the Fisher criterion (Fisher A., 1923) and the classification result comparison. The results are satisfactory, the grid cell operator is the only one that selectively reacts only to the texture and does not give the false response to the non-texture characteristics, such as the contours of the object, accordingly, the best discrimination and segmentation result is provided by the cell grills.

Another Textural Approach for Land Cover Classification of Remotely Sensed Image is presented by Jenicka S. and Suruliandi A., 2014, describing the Local binary pattern (LBP). In the described study, texture models should be capable of capturing and discriminating even minute pattern differences. A multivariate texture model is introduced with four discrete output levels for efficient analysis of land covers. Land cover classification of the remotely sensed image has been achieved using the multivariate texture model MDLTP (Multivariate Discrete Local Texture Pattern) and Support Vector Machine (SVM) classifier. Hence, the classification accuracy of the classified image obtained is found to be 93.46%.

Kerroum M.A. et al., 2009, discuss "A method based on the Gaussian mixture model (GMM) in calculating Shannon's mutual information between multiple features and the output class labels". This is applied to a textural feature selection algorithm for multispectral image classification. The extracted features are from an HRV-SPOT image of a forest area in Morocco, using Wavelet Packet Transform (WPT) and the Gray Level Co-occurrence Matrix (GLCM), and the purposed classifier is the Support Vector Machine (SVM). The concluded results show that the selected textural features are more beneficial to the classification accuracy than the ones provided by mutual information between individual variables and the use of spectral information delivers poor performances.

Haralick R.M. et al., 1973, describe a method with a technique for computing texture features using the GLCM and is well summarized by Puetz A.M. and Olsen R.C., 2006 in "Haralick Texture Features Expanded Into The Spectral Domain". A gray-scale image is being quantized by the standard GLCM in a limited number of discrete gray-level bins, and the gray-levels in an image are statistically analyzed. Accordingly, the GLCM's technique result is a gray-scale image with values correlated to the intensity of the statistical measure.

Two different approaches are described. The first one is determined using the Haralick Texture Method, while in the second approach, the Spectral Texture Method is adopted. In the Haralick Texture Method, the quantization range is defined as the range of reflectance values in a particular spectral band. In the Spectral Texture Method, a spectral image is quantized based on discrete spectral angle ranges. Both texture approaches provide good results when creating a classified image that characterizes land cover types, but the Spectral Texture Method provides an increase over the Haralick Texture Method.

An important issue in classifying images from a textural point of view is using different sizes of the processing window. Coburn C.A. and Roberts A.C.B., 2004, "discuss a multiscale approach to image texture where first and second-order statistical measures were derived from different sizes of processing windows and were used as additional information in supervised classification". Different window sizes (from 5 x 5 to 15 x 15) were used for a single spectral band, thus, the classification accuracy increased. The results are improved when this multi-scale approach is adopted, compared to the current single-band approach to analyzing image texture.

Regions were classified based on using color information alone to using texture and color texture information by Vansteenkiste E. et al., 2004. In this paper, the effect of color space reduction and a 2D and 3D extension of the co-occurrence matrix is being evaluated, along with the parameters derived from them. Despite the fact that color features achieve best in the simple classification exercise, very high-resolution classification rates are collected using color texture features and the fragmentation degree in the classified areas is smaller.

Zhao P. et al., 2016 apply three different classifiers when they classify SPOT satellite images of forest. The three classifiers are: the support vector machine (SVM), the k-nearest neighbor algorithm (KNN), and the classification and regression tree (CART). Like others, for texture information they use GLCM and Haralick features, but together with features derived from Grey Level Difference Vectors (GLDV), which represent normalized 1D-histograms (i.e. vectors) of grey value differences between pairs rather than 2D-histograms (i.e. matrices) of grey values pairs as it is the case in GLCM. The best classifier applied to the forest classifications and analysis was the SVM, providing an Overall Accuracy of 78% and a Kappa coefficient of 0.737. This paper presents a fast and simple method to forest classification and lays the foundation for forest management and forest resource surveys.

Summarizing the aforementioned publications, one can see that heaps of methods concerning textural parameters have been proposed, but perhaps the most popular of these is the utilization of the GLCM and therefrom derived features.

The central focus of this study is on applying GLCM's features, and the main objective of this investigation is to develop a strategy by taking into account the textural classification using the Haralick textural features with the intention to find out a possible advantage when classifying high-resolution imagery.

Although there has been ample research regarding the analysis and inclusion of texture in high-resolution images, these investigations should concentrate on the utilization of the widely implemented classification methods, which have become standard for multispectral classification in medium resolution satellite images. Eventually, two questions arise:

- Firstly, is it appropriate to apply these classic methods, in particular, the Maximum Likelihood algorithm, to datasets of textural features either alone or in combination with spectral information?
- Secondly, is it possible to improve, hopefully significantly, the quality of a pure multispectral classification by adding textural features or by combining textural and multispectral classification results?

These are the major questions, which should be answered at the end.



## 2 Study area and description of satellite data

### 2.1 Study area

The study areas have been selected in a mainly forested region some 60 km south of Vienna, in the Rosalia, the eastern low foothills of the Alps. Their elevation ranges from some 500 m to 700 m a.s.l. To a great part, the vegetation cover consists of a mixed forest of coniferous (dominated by spruce, pine, and larch) and deciduous trees (dominated by beech and oak) ([3] <https://pannatuara.at/wald/daten-und-fakten/>).

The first test area is situated in the central part of the Austrian province Burgenland, while the second test area lies some 5 km apart in the north-westerly direction almost entirely in the province of Lower Austria, only a few kilometers south-east of the city of Wiener Neustadt (see figure 1).

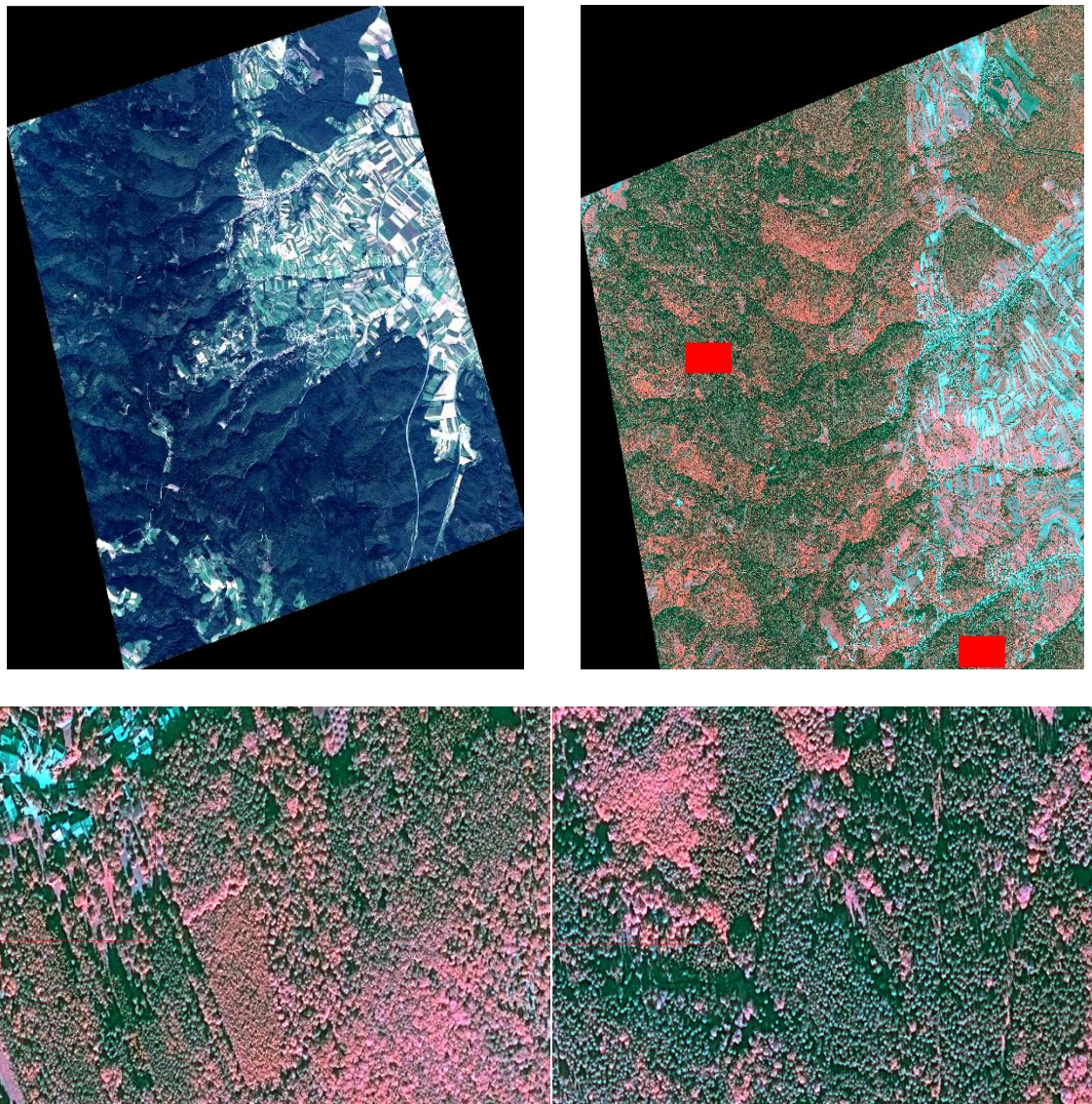


Fig.1: Study area (LU: true color composite of full scene, RU: study areas marked in red, LL: study area S-E, RL: study area N-W, both as color-infrared composites)



In addition, Rosalia region is an area that offers many wonderful opportunities for relaxation to tourists due to its beautiful natural park, but there are also interesting offers that introduce tourists to aspects of ecological and cultural education, ([4] <http://region-rosalia.at>). The selected areas have been acquired by high-resolution satellite sensors and two areas (area North-West and area South-East) have been chosen, which seem to be best suited for the planned investigations.

## 2.2 Satellite data

### 2.2.1 Pléiades Satellite imagery

Nowadays a great number of satellites with highly resolving instruments on board are in orbit. Among them are two Pléiades Satellites, called Pléiades 1A and Pléiades 1B, which complement each other. The image used in the case study has been acquired by 1B on 24 September 2014 at 9:59 local time. Both satellites belong to a greater number of satellites which are operated by the Airbus Defence and Space company. Figure 2 shows an overview of these Earth observation satellites. Among them are the well-known SPOT satellites, which have been playing an important role in Earth observation since the mid-eighties. In fact, the very last SPOT satellites 6 and 7 are part of a quartet whose remaining players are the Pléiades.

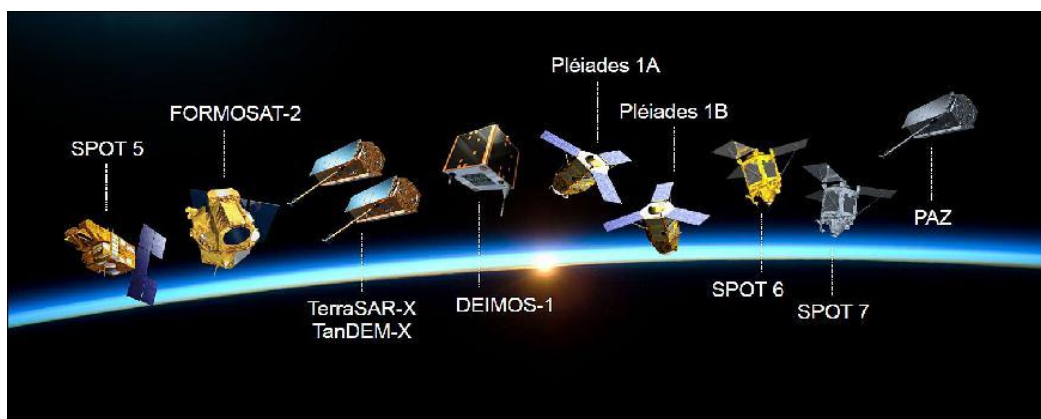


Fig.2: Spacecraft fleet operated by Airbus Defense and Space (image credit: Airbus Defence and Space) eoPortal 2017 ([2] <https://directory.eoportal.org/web/eoportal/satellite-missions/p/pleiades>)

The Pléiades program was initiated and managed by the French Space Agency - Centre National d'Etudes Spatiales. The technical part of the space segment is Airbus Defence and Space (formerly EADS). Partners of the Pléiades program are the space-agencies of France, Sweden, Belgium, Spain and Austria, and therefore, for Austria special conditions apply for data order.

Both satellites were launched from the Kourou Space Center in French Guyana: Pléiades 1A on 17 December 2011, Pléiades 1B on 1 December 2012. The planned duration of the mission was 5 years. Figure 3 shows an artist's view of a Pléiades satellite.

Pléiades 1A and Pléiades 1B operate on the same orbit, 180° apart from each other, and on the same orbit as Spot 6 and Spot 7, which are positioned exactly in between. It is an orbit with an average altitude of 695 km and an inclination of 98.2°. All four satellites offer

various acquisition modes, even with tilted instruments so that this constellation, with four satellites at a distance of 90° in orbit, provides a double daily revisit over the same point on Earth in high-resolution (SPOT) and very high-resolution (Pléiades), respectively.

The technical performances of the Pléiades satellites are as follows:

- Geometric resolution: 50 cm
- Spectral bands:
  - a. Pan: 470-830 nm;
  - b. Blue (B): 430-550 nm;
  - c. Green (G): 500-620 nm;
  - d. Red (R): 590-710 nm;
  - e. Near Infrared: 740-940 nm.

([5] [http://www.intelligence-airbusds.com/files/pmedia/public/r49228\\_9\\_pleiades\\_product.pdf](http://www.intelligence-airbusds.com/files/pmedia/public/r49228_9_pleiades_product.pdf))

Terrestrial receiving stations provide a direct connection and data delivery. Two military stations are used for receiving data, one in France and one in Spain, and two civilian stations, from Toulouse (France) and Kiruna (Sweden). Upon request, additional regional stations are installed. Pléiades images can be obtained in less than 6 hours after purchase.

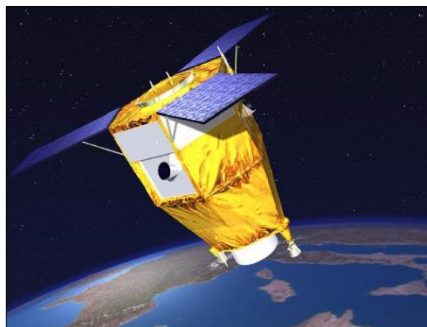


Fig.3: Artist's conception of the Pléiades spacecraft in orbit (image credit: CNES)  
ESA 2000 - 2018

([6] <https://earth.esa.int/web/eoportal/satellite-missions/p/pleiades>)

### 2.2.2 Panchromatic images

Panchromatic images have monochrome continuous tone characteristics. They are recorded over a wider range of wavelengths in the electromagnetic spectrum, typically including a large portion of the visible spectrum and even a portion of the near infrared. Due to this wide range in the spectrum, a high amount of energy arrives at the sensor. Therefore, panchromatic images can be exposed to rather small sensor elements with sufficient signal/noise ratio, thus enabling the collection of, as it is called, very high-resolution images. Since the advantage is not given for multispectral images with their narrow spectral bands, their resolution is worse.

### 2.2.3 Multispectral images

By the term multispectral image, we usually understand a set of images of generally the same geometric behavior acquired through a set of spectral filters. Each image of this set, therefore, represents the reflectance or emittance properties of the observed objects. This

narrow definition has been a bit extended in the meantime, in particular since high-resolution panchromatic images have become state of the art. SPOT 1 in 1986 and Landsat 7 in 1999 began to include, in addition to narrow spectral bands, also one geometrically higher resolving wide panchromatic band, which is treated as part of the multispectral dataset. In the meantime, all modern high-resolution satellite missions acquire both, the narrow spectral bands and one wide panchromatic band. So do the Pleiades, which are used in this investigation.

According to a commonly used definition of multispectral images, the original image contains the reflectance or emittance properties of the imaged objects so that by analyzing the multispectral datasets and by knowing true object properties it should be possible to immediately classify the image with respect to the classes of the observed objects.

Unfortunately, there are a series of reasons why this is not so easy at all.

- Firstly, the sensors provide only a selection of more or less narrow spectral bands without the guarantee that they represent the typical spectral object behaviors. Hyperspectral sensors exist which try to avoid this drawback, not without introducing another drawback with regard to geometric resolution. For the investigations in this thesis, one needs not to take care of a possible lack of spectral bands. The typical bands for vegetation studies, i.e. green, red and near infrared, exist in the Pleiades data.
- Secondly, the illuminating radiation passes through the atmosphere twice on the way from the sun to the Earth surface and back to the satellite. The radiation also interacts with the contents of the atmosphere causing scattering (air light, skylight, extinction) and absorption effects. Scattering is especially present in the short wavelength range towards the blue spectrum and ultraviolet, and not taking it into account would easily lead to wrong interpretations. Scattering in this study could be an issue, but the most important bands are red and near infrared which are least influenced by scattering, and they are not significantly influenced by absorption either.
- Thirdly, the shape of observed object surfaces causes varying incidence and exitance angles of the illuminating sun rays thus producing shades and shadows. Dependent on the bi-directional reflectance properties of the object materials shading effects are more or less dominant. Dominant, in particular in high-resolution images, are cast shadows. Satellite images can never be taken at a diffuse lighting condition, which would be the optimum illumination and which in the real world exists only at overcast skies. Satellite images require cloudless sky, thus producing significant cast shadowing. Shades and shadows are an issue in this investigation. Without regard to effects caused by the shape of the terrain, they, on the one hand, provide us with nicely shaded forest canopies and therefore with typical textures for certain forest varieties, on the other hand, in less dense forests they produce cast shadows of trees which negatively influence both the spectral and the textural interpretation. Since there is no feasible and sound possibility to take into consideration this illumination effect, one has to live with it. An acceptable workaround is a classification into different classes of same object varieties with different illumination effects and the fusion of those intermediate classes into one object class in a post-processing step.

The Pléiades collect together with the panchromatic images (in PA mode) also multi-spectral images (in XS mode). A multispectral Pléiades image consists of four data bands. For digital classification algorithms and if appropriate, these four bands can be used simultaneously, but as soon as visual interpretation is involved, color composites of three selected bands

must be created. Two sorts of composites may be considered: first, by assigning the blue, green and red channel to the respective display colors, a natural color image is generated, and second, by assigning the green, red and near-infrared channel to the blue, green and red display colors, a color infrared image is generated. While the first is compliant with our real-world experience, the latter is the preferred composite if vegetation studies are to be carried out, like in our studies. Due to the unusual color impression, one must be familiar with the spectral reflectance properties of the object under investigation in order to avoid misinterpretation and, as a possible consequence, wrong classification results. In the case of digital analysis, the entire spectral information content of the image is used in interpretation. In order to improve the visual quality, the panchromatic images are frequently used to artificially enhance the resolution of the multispectral bands through merging algorithms. New sensors, like that of the Pléiades, acquire panchromatic and multispectral images simultaneously and therefore resolution merging has become standard for these sort of satellite images. Merged images are offered as own products. In practice, resolution merged products have become by far more important than the original panchromatic image (Kidiyo K. et al., 2014).

#### 2.2.4 Pan-Sharpended Data

As mentioned afore, very highly resolving panchromatic images may be merged with the less resolving multispectral images in order to make them look like highly resolving products. This process is commonly called pan-sharpening (also known as “image fusion” and “resolution merging”, the first a bit confusing and misleading, the latter quite appropriate). It has become a terminus technicus for various methods in the field of digital imaging, in particular for airborne and spaceborne imagery. Figure 4 shows an example of pan-sharpening. A variety of algorithms have been developed in recent years for data from different sensors and with different resolutions and with different effects on the original multispectral information (Buntilov V.M., 2013). One should be aware that pan-sharpening never produces an image whose spectral information is equivalent to an original high-resolution multispectral image. The spectral property has been deteriorated in a more or less significant way, dependent on the merging algorithm. To express it a bit negatively, one could call these data pseudo-multispectral. If the spectral reflectance properties of objects play the central role in an interpretation task, pan-sharpened products are certainly not the first choice. The Pleiades image used here belong to this sort of images. For the investigations planned in this study, the focus is more on texture and color and, therefore, pan-sharpened images are well suited.

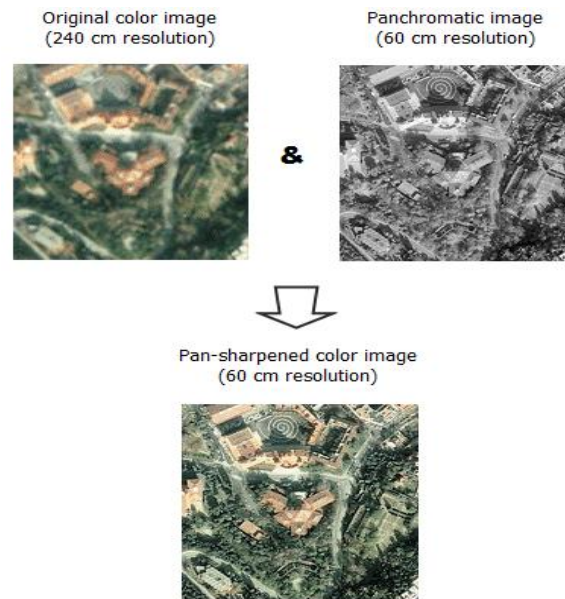


Fig.4: An example for Pan-sharpening

([7] <http://desktop.arcgis.com/en/arcmap/latest/manage-data/raster-and-images/fundamentals-of-panchromatic-sharpening.htm>)

### 2.2.5 Image resolution

The availability of large and very high-resolution satellite imagery has led to the development of applications unimaginable some decades ago. The quality of satellite imagery can be summed up to spatial, spectral, radiometric and temporal resolutions. In addition, radiometric, topographic or atmospheric corrections may be applied to improve the results.

The Pléiades satellite mission provides optical images for civil use at VHR (very-high-resolution) of any point of the Earth surface. Each of the two Pléiades satellites carries a CCD (charge-coupled device) camera, named HiRi, which is a Korsch telescope with an aperture diameter of 65 cm and a focal length of 12.9 m. Each HiRi acquires images in pushbroom mode using 5x6000 pixel arrays and 20 integration lines (for TDI forward-motion compensation) for the panchromatic band (480–830 nm) and 5x1500 pixel arrays for the multispectral bands (blue, green, red and near-infrared). The native resolution of Pléiades 1A and 1B is 0.7 m in the panchromatic and 2.8 m in the multispectral mode in the vertical direction, which in the orthorectified products are resampled to 0.5 m and 2.0 m, respectively (Poli D. et.al., 2015).

Featuring a daily revisit to any location on the planet, the Pléiades constellation separates itself from the competitors for site monitoring and projects requiring rapid imagery acquisitions, ([8] <https://apollomapping.com/imagery/high-resolution-imagery/pleiades-1>) Figure 5 shows the first image from Pléiades 1B.

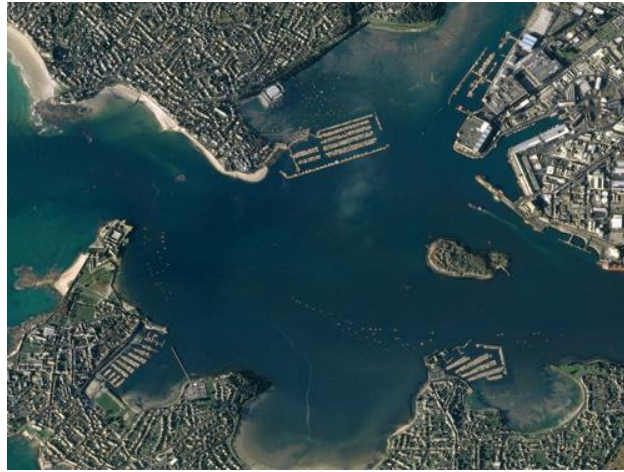


Fig.5: First image from France's Pléiades 1B high-resolution imaging satellite ([8] <https://apollomapping.com/imagery/high-resolution-imagery/pleiades-1>)

It has been mentioned that the Pleiades sensors are very high resolution instruments. This statement is not unambiguous, since various kinds of resolutions may be found in the specifications of an image sensor. To the term resolution a bit more attention needs to be paid, and therefore, in the following more detailed explanations should be provided and related to the Pléiades sensors.

- **Spatial resolution** is defined by the ability to just recognize neighboring small objects as two different objects. The spatial resolution also depends on the respective intensities of the neighboring objects. Therefore, the spatial resolution cannot be defined by a unique value but by the Modulation Transfer Function, which relates a recognized spatial wavelength to its amplitude. In practice, however, the spatial resolution simply represents the linear dimension of the smallest object in the field present in an image. It can also be considered as the line width separating two small neighboring objects in a picture such as a car and a building. In digital images, commonly the spatial resolution corresponds to the field size of a pixel's side, the smallest element constituting that image ([9] <https://www.sciencedirect.com/topics/earth-and-planetary-sciences/spatial-resolution>). As for the panchromatic orthorectified images the spatial resolution is 0.5 m. In other words, by one pixel an area on ground of 0.5 m x 0.5 m is covered.
- **Spectral resolution** may be defined in two ways. Once it is the spectral range or wavelength range (i.e. the band width) within which an image has been recorded. The narrower the band width, the higher the spectral resolution. And secondly, in the case of multispectral images, the spectral resolution is expressed equally by the number of bands or spectral intervals in which images of the same terrain surface were simultaneously acquired. The more bands, the higher the spectral resolution. A great number of bands allows the identification of an object or phenomenon in the field through the reflected electromagnetic radiation, even if its spectral signature is rather complex. There is a loose dependence between bandwidth and number of bands. If a great number of bands can be recorded by an instrument, only very narrow bandwidths make sense ([10] <https://www.sciencedirect.com/topics/earth->

and-planetary-sciences/spectral-resolution). As for the Pléiades sensor, the panchromatic one has a poor spectral resolution, i.e. a very wide band width of roughly 400 nm ranging from visible to near infrared, and only one band. The multispectral resolution is better with four bands and an average band width of some 100 nm.

- **Radiometric resolution** refers to the dynamic range of the recording, that is, to the possible number of distinguishable different intensity values (often referred to as noise-equivalent reflectance (or radiance) difference (NeDL, where DL stands for “delta radiance”) for recording the radiometric response between the just recognizable lowest intensity (where the signal-to-noise ratio approaches 1.0) to the maximum just not overexposing intensity (where the signal-to-noise ratio reaches its maximum). In digital images also the number of bits to store intensity values are often referred to as radiometric resolution of the sensor, though not correct in the sense of instrument specification. Again there is a sort of relationship between radiometric sensor resolution and number of bits reserved to store an intensity value. For a highly resolving sensor a great number of bits should be provided in order not to lose captured information, while for a poorly resolving sensor a high number of bits would not make sense and would just increase the amount of data without contributing to image information. As for the Pléiades sensor no reliable physical specification of NeDL could be found. The data are delivered with 16 bits/intensity value allowing to store 65536 different intensity values. In practice only maximal 12 bits are used, resulting in 4096 different shades of intensities. Still, concluding from this value to the actual radiometric resolution of the sensor hardware is not possible. ([11] <https://www.sciencedirect.com/topics/earth-and-planetary-sciences/radiometric-resolution>).
- **Temporal resolution** refers to the frequency of revisits over a site, depending on the orbitography of the platform or satellite on which the sensor is located, and on the geographic latitude of the investigated area. Before flying over the same area at the same image shooting conditions (26 days for Pléiades), the satellite has to go through a number of orbits (that is, a complete revolution around the Earth). The temporal resolution is defined by the duration of an orbital cycle or the number of revolutions required before returning to the starting point. With the emergence of the agile satellites, such as Pléiades satellites, which can tilt the viewing angle in any directions, the revision period can be reduced, making it possible to get the image of the same geographical area before the end of the full orbital cycle. The images obtained may show strong geometric disparities due to different imaging angles, even if the pictured area is the same. The acquisition conditions are different as far as geometry as well as radiometry are concerned. The Pléiades satellite is able to lower the revisit period to about 7 days above the equator if someone tolerates a viewing angle of the sensor of 20°. With the existence of two equivalent satellites and instruments in orbit, Pléiades 1A and 1B, the temporal resolution can even be further increased. ([12] <https://www.sciencedirect.com/topics/earth-and-planetary-sciences/temporal-resolution>).



### 3 Characteristics of spectral signatures

The notion of “spectral signature” in remote sensing covers an area where very complex phenomena are involved. All objects of the environment reflect and emit energy flux in the form of electromagnetic radiation. The relative variation of the reflected or emitted energy as a function of the wavelength is what we call the spectral signature of the considered object. Thus a given object, in a certain state, must correspond to a unique spectrum. This spectrum can be used to identify the object and its state. For a satellite that makes measurements in a certain number of bands, the spectral signature of an object corresponds to different radiometric levels, levels recorded in each band.

The spectral signatures of vegetation vary dependent on the plants` vitality due to seasonal influences, diseases or environmentally induced damage. As a typical example, where seasonal changes play the major role, are the changes in the deciduous forest. During winter time the trees are without leaves, their reflection in near-infrared does not exist, during spring the young leaves are sprouting with very high vitality, the reflection in near-infrared slowly reaches a maximum, in summer the vitality is stable until autumn approaches, where the near infrared reflection goes down dramatically. This sort of variation may be typical for certain varieties and may be utilized in multi-temporal data acquisition. Similar variations apply for agricultural crops, pastures, meadows, etc. The term spectro-temporal phenology is often used when the seasonal variations of reflection play a major role for classification. Unfortunately, in practice, spectral signatures of natural and anthropogenic objects are overlaid by effects due to illumination parameters, observation angle, atmospheric conditions, and others.

As the following investigations concentrate on forest classification, suited satellite images may be captured during the growing season, i.e. between late spring and early autumn (with a certain dependency on the geographic location), even though an acquisition in early summer is preferred due to the high elevation of the sun. As for illumination and observation influences the users have not many degrees of freedom for their decision. Even the possible time of the day depends very much on the satellite`s orbit parameters, and weather conditions are further reasons for limited acquisition possibilities. The image used in this study has been captured in late September almost at the end of the optimum period. Due to the long vegetation period in the Rosalia area, this image is still well suited.

#### 3.1 Interpretation of spectral signature regarding vegetation

The spectral signatures of vegetation leaves, independent of the actual plant, whether grass or bushes or tress, even coniferous trees, show a typical and similar shape with a small local maximum in the green portion of the spectrum and a significant maximum in the near infrared, and further local maxima in the mid-infrared around 1.6  $\mu\text{m}$  and 2.2  $\mu\text{m}$ . The signatures of vegetation objects mainly differ just by their amplitude in three typical regions of the spectrum, in visible light, in near-infrared and mid-infrared.



Factors that can influence the spectral response of vegetation are:

- Type, anatomy or phenological phase of vegetation (flowering, fructification, etc.);
- Age of vegetation;
- The condition in which plants are found in terms of water;
- Deficiency of minerals;
- Reflection from the ground or other nearby object within the sensor's footprint.

If the vitality of the plant or the concrete species were in the focus of the investigation, these items would be of interest. What is needed is a rough classification of the vegetation, in particular in forests, independent of their health conditions. Therefore, one just needs to know the major differences between the classes deciduous and coniferous forest, other vegetation and something else. In other words, it is good to know about the differences in reflectance behavior, but it is not necessary to investigate in detail the fine difference of the vegetation object in the area of interest. The texture is at least as important if classes of forest stands have to be found with the help of digital image analysis.

### **3.2 The spectral signature in the acquired image**

In the previous section, the spectral signature as object properties has been explained. It is derived in situ or in the laboratory and it provides valuable information for reference catalogues. Remote sensing is the science of capturing and analyzing object properties by not getting in physical contact with the object. The analyses and classifications in remote sensing rely on the analysis of images and, therefore, for the image interpreter usually not the real world's spectral signature is on the first position, but the spectral signature as it has been mapped into the image during the capturing process. The following list gives an overview of what sort of influences impair the real object properties on its way to the digital image:

- The incidence angle of illuminating rays on the object surface, causing shading effects, a significant parameter!
- The observation angle of the object surface, i.e. the exitance angle of the reflected ray, a less significant parameter!
- The atmospheric condition, such like haze and other microscopic particles in the air, causing various sorts of scattering, commonly known as skylight and air light, may be quite significant and dependent on the wavelength, i.e. the spectral band!
- Mutual illumination, a less significant influence, which may be ignored in practice!
- Cast shadows, i.e. areas with no direct illumination due to light hidden by large or very small objects or by clouds. Shadowed areas may just be illuminated by the skylight or marginally by mutual illumination by nearby bright objects. Cast shadow can be quite dominant and annoying in satellite images due to the bright direct sun illumination!
- Influences which happen as soon as the ray enters the imaging system, such as transparency of the optical system, influences in the electric system, i.e. the detector's, and the amplifier's, and digital-analogue converter's performance. It may be ignored in practice because of today's excellent sensor quality and a priori internal calibration procedures!

The first two items are also largely determined by the shape of the terrain where the objects grow on, or in detail, by the shape of the forest canopy or individual tree crowns. The

difference between the objects' real spectral signature and the imaged spectral signature is modelled by the bi-direction reflectance distribution function, the BRDF. The BRDF is a very complex mapping function, which may in part be determined in the laboratory. The theoretically ideal BRDF models the ray from the illumination source, usually the sun, via the object surface to the sensor element for each illumination and observation angle. For applications in practice, one has to significantly simplify this function. In many cases, even a BRDF is not considered at all. When analyzing the image, apparent shading is taken into consideration by introducing intermediate classes like objects in cast shadow, in heavily shaded areas, in slightly shaded areas, and in sunlit areas. After the classification objects in the just mentioned classes are combined in respective one object classes. This study does not apply a BRDF and if it would have turned out necessary the just explained simplified approach would have been used. Taking into consideration cast shadows through modelling would even be more complicated, because it needed, in addition to illumination and observation angles, careful ray tracing based on a very accurate surface model.

## 4 Introductory remarks on texture and the Gray Level Co-occurrence Matrix (GLCM)

### 4.1 Introductory remarks on texture

“There is no precise definition for the notion of texture because natural textures have contradictory properties (regularity to disorder, homogeneity, distortion) that are very difficult to describe in a unitary way” (Sidhu A.S. and Dillon T.S., 2009).

Texture is an important help in interpreting visual images, especially in high resolution space imagery. Texture is not a pixel related property, since one individual pixel never forms a texture. Texture parameters may be stored in an individual pixel, but they need to be derived from a more or less large surrounding area. In this sense, an image which represents the textural context on a pixel bases may be seen as the result of a moving texture-describing filter. In digital image processing one tries to characterize the textural aspects from a numerical point of view, using algorithms for the discrimination of different textures by deriving numerical characteristics, which are assumed to be able to sufficiently describe certain types of texture.

Texture is described in linguistic terms by roughness, contrast, fineness, regularity, terms whose mathematical translation is not clear.

One can easily recognize an image with texture, but it is difficult to give a rigorous texture definition. If the elements that make up the texture are identical and precisely ordered, then the texture is called deterministic. If the elements are not identical, but they are similar, and their arrangement is based on certain statistical laws, then it is called random texture. Intermediary, between the deterministic model and the random model, there is an observable texture pattern. In general, uniform textures exist, which contain a large number of uniform small spots (primitive elements), arranged according to a placement rule, and the forms of this spots and their positions are governed by random variables. An important step in building mathematical models for textures is to identify the perceptible qualities of the texture.

In order to appreciate the fact that there is texture in an image, a number of properties have to be intuitively assessed. The most important properties of the textures are the following:

- the texture is a domain property;
- the texture involves a spatial distribution of the gray levels. Texture existence must involve changes in gray or color values in image windows. The size of these windows depends on the type of texture or the size of primitives that define the texture, and, on the one hand, they must be large enough to represent the typical spatial pattern of a texture, on the other hand, they should be small enough not to include an unnecessary amount of redundant data at the cost of resolution;
- the texture of an image can be seen at various resolutions of the image;

- a region of the image is perceived as having a texture when the number of elementary (primitive) objects adjacent and grouped in the region is very large (Chen C.H. et al., 1998).

There is much literature available for texture analysis and texture classification and for all who wants to go closer in this topic the book: "Texture Analysis" by Chen C.H., et al., (1998), In The Handbook of Pattern Recognition and Computer Vision (2nd Edition), is recommended.

Texture analysis means extracting features and image coding. The extraction of features refers to identifying and selecting a set of distinctive and sufficient features to characterize a texture. Thus, image coding leads to a compact description of the texture of the selected characteristics. Automatic texture processing is possible if a complex texture is represented by a small number of parameters. In recent years, different texture analysis methods have been proposed. Among the available methods are the geometric method, model-based and signal processing methods (Sidhu A.S. and Dillon T.S., 2009).

There are two main ways of describing the texture:

- descriptive method - derives a quantitative description of a texture with respect to a range of manageable property measures
- generic method - creates a geometric or probabilistic model for texture description (Sidhu A.S. and Dillon T.S., 2009).

Sidhu A.S. and Dillon T.S., 2009, wrote with regard to texture the following, which is summarized in the item list below:

- (1) "Moreover, the descriptive approach can be divided into statistical and spectral methods, due to the techniques used in the selection of the characteristics. Statistical methods use spatial image signal statistics as feature descriptors. The most commonly used statistics are 1D histograms, moments, gray co-occurrence matrices (GLCM), etc".
- (2) "Typically, inferior image statistics, especially first and second order statistics, are used in texture analysis. First-order statistics (average, standard deviation, and high-order histogram moments) work with the individual pixel properties".
- (3) "Second order statistics also account for spatial interdependence or the co-occurrence of two pixels at specific positions".
- (4) "Grayscale co-occurrence matrices, gray level differences, auto-correlation function, and local binary model operator are the most commonly applied second-order texture descriptors".
- (5) "The Haralick features derived from the GLCM, is one of the most popular feature set".

The texture may contain important information about the surfaces and describe the relationship between the analyzed area and the environment.

Textural properties include granulation, contrast, direction, linearity, regularity, and relief (asperity). Texture description is primarily based on the interpretation of pixel values as the achievements of randomly correlated processes. The descriptions will therefore be of the type of distribution of some features (value, energy, variation) in the spatial image area or in the frequency domain (spectral characterization).

The four major categories of texture algorithms are as follows:

- statistical techniques - characterize textures according to the different gray levels of pixels that make up a surface.
- geometric techniques - characterize textures as being composed of simple primitives in structural units, called textures, placed on a surface on a regular basis.
- spectral techniques - based on Fourier spectrum properties to describe the overall periodicity of gray levels on a surface by identifying high energy points.
- model-based techniques - use statistical distribution approaches based on random pixel parameters (Markov random fields).

There are different methods for texture analysis and texture classification, these approaches are very well described in Digital Image Processing, by Gonzales R.C. and Woods R.E., 2001.

This previous paragraph regarding introductory remarks on texture stands here only as a sort of introduction, but the following, the Gray Level Co-occurrence Matrix is the main focus used in this investigation.

## 4.2 The interpretation of textural signatures regarding forest

In the case of the textural approach, class names have been chosen to get a rough idea of the kind of texture. The intention was to provide distinct classes names rather than accurate descriptions. Therefore, for better understanding, a translation table has been created, that references the class names to terms and descriptions used in forestry (see table 1):

<i>working classes</i>	<i>real life of forestry</i>	<i>translation</i>
<i>rough</i>	<i>packed</i>	<i>The crown of the trees is irregular, overlap and is not smooth.</i>
<i>coarse</i>	<i>closed</i>	<i>Coarse and rough are two slightly different textures. Coarse texture means that the crowns all touch, but do not overlap.</i>
<i>fine</i>	<i>spacey/gappy</i>	<i>Fine and foliar are mostly similar. Fine is the equivalent of a refined and unmixed crown. There are many clearing in between.</i>
<i>foliar</i>	<i>spacey/gappy</i>	<i>The crown is more dominant, close to each other, but do not overlap when looked from above.</i>
<i>dense</i>	<i>dense</i>	<i>The crown is compact with a few spaces in between.</i>
<i>rarefied</i>	<i>individuals</i>	<i>When there are a few unconnected trees.</i>
<i>flat</i>	<i>-</i>	<i>Regular and smooth surfaces. Non-forest area.</i>

Table 1: Translation table

Further information about forest stands, crown closure as well as crown cover can be found under ([13] [https://en.wikipedia.org/wiki/Stand\\_level\\_modelling](https://en.wikipedia.org/wiki/Stand_level_modelling)) and ([14] [https://en.wikipedia.org/wiki/Crown\\_closure](https://en.wikipedia.org/wiki/Crown_closure)).

## 4.3 The Gray Level Co-occurrence Matrix (GLCM) and the textural features

The Gray Level Co-occurrence Matrix consists of second-order spatial relationship (since usually the matrix is normalized, its elements are also referred to as probabilities of the

appearance of some pairs of gray values in the texture). The elements of the GLCM( $c,r$ ) are the number of color pairs ( $i,j$ ) taken from a reference pixel (with color  $i$ ) and a partner pixel (with color  $j$ ), which are separated by a given distance  $d$ , along a given direction  $a$ , more generally expressed by pixel pairs at a given neighborhood  $H(d,a)$ . Thus, the term neighborhood in this context is related not only to immediate pixel neighbors, but also to distant neighbors. In the end, this descriptor will be a square matrix of size equal to the number  $N$  of possible distinct pixel values. Hence, the number of columns  $c=N$  is equal to the number of rows  $r=N$ , with the column index  $i \in [1,N=i_{max}]$  and the row index  $j \in [1,N=j_{max}]$ . The concept of co-occurrence matrix can also be applied to color pairs, not just to images with gray levels, using different levels of color space quantization. One term in the context of GLCMs should be briefly explained here. One may come across the attributes symmetric and non-symmetric. The following formulas are valid for the both kinds of a GLCM, but it must be mentioned here, that the column and row related values for Mean and Variance are usually different. In the case of symmetric GLCMs the column and row values are always identical. A GLCM is called non-symmetric if the neighbourhood is counted in a given direction, it is called symmetric if it is counted also in the opposite direction. There is, for instance, a non-symmetric GLCM for  $0^\circ$  and another one for  $180^\circ$ , but there is only one symmetric GLCM for  $0^\circ$  because the calculation also includes the direction  $180^\circ$ .

In practice, to reduce calculations and even to make them more reliable, the number of gray levels  $N$  in the original image is reduced usually to 8, 16, 32 or 64 by an appropriate gray-scaling techniques, often called quantization. One should be aware, that there is not only one unique GLCM for a certain texture.

For the same texture, the eventually obtained co-occurrence matrix depends on the size and orientation of the region considered, the translation vector, and the degree of reduction expressed by the gray level quantization factor.

The distinction between different textures can be done primarily by inspecting the 2-dimensional co-occurrence matrix which contains in its elements the frequencies of the respective pairing of gray value  $i$  and  $j$ . In other words, a GLCM could also be called a 2-dimensional frequency histogram of grayscale pairs. In general the frequencies are normalized, i.e. the sum of the frequencies over the entire matrix yields 1.0. In the following, therefore,  $P_{i,j}$  is to be interpreted as normalized frequency, where  $i$  defines the matrix column,  $j$  the matrix row. The normalized frequencies are sometimes also called probabilities. A series of statistical indices have been defined by Haralick (1973), also known as Haralick features, that characterize the distribution within the co-occurrence matrix. In the formulas below, which show a selection of textural features, the following definitions of the variables apply:

$P_{i,j}$  is the probability of values in GLCM element  $i$  and  $j$ ;

$i$  and  $j$  are the labels of the columns and rows (respectively) of the GLCM. Because of the construction of the GLCM,  $i$  refers to the digital number (=gray value) of a target (or reference) pixel, and  $j$  is the digital number of the partner pixel whose neighbourhood has been defined by direction and distance.

$\mu$  is the mean and  $\sigma$  the standard deviation, both as defined by the equations for GLCM Mean and GLCM Variance in the list of equations below;

N is the number of rows or columns, which is identical to the number of gray levels in the image:

- Mean :

Represents the mean column  $i$  or row  $j$  by applying as weight the pairing frequencies of the GLCM projected onto the column axis  $i$  and the row axis  $j$ , respectively. As mentioned above, in case of symmetric GLCMs both means are identical.

$$\mu_i = \sum_{i=0}^{N-1} \left( i \sum_{j=0}^{N-1} P_{i,j} \right) \quad \mu_j = \sum_{j=0}^{N-1} \left( j \sum_{i=0}^{N-1} P_{i,j} \right)$$

Equation 1. Mean of Column and Mean of Row

- Contrast:

Similar to the later mentioned feature Dissimilarity the GLCM elements are weighted by their distance from the diagonal. While Dissimilarity uses the linear distance, Contrast applies the square distance. Diagonal elements do not contribute to Contrast. There is a strong reverse relationship to Homogeneity, as one can easily see later on:

$$\sum_{i,j=0}^{N-1} P_{i,j} (i - j)^2$$

Equation 2. Contrast

- Entropy:

As defined in digital image processing, the entropy represents the information contents of the GLCM. The more different values within a GLCM the higher the entropy. Due to the fact that the content of symmetric and asymmetric GLCMs are different, also the Entropies must be different.

$$\sum_{i,j=0}^{N-1} P_{i,j} (-\ln P_{i,j})$$

Equation 3. Entropy

- Variance of Columns and Variance of Rows:

Describes the scattering of GLCM values around the mean values. As with the Mean, the variances with respect to column and rows are identical in case of symmetric GLCMs.

$$\sigma_i^2 = \sum_{i,j=0}^{N-1} P_{i,j} (i - \mu_i)^2;$$

$$\sigma_j^2 = \sum_{i,j=0}^{N-1} P_{i,j} (j - \mu_j)^2 ;$$

Equation 4. Variance

- Correlation:

Shows the correlation between the rows and columns. The correlation is positively high (i.e. close to +1) if the filled elements in the GLCM are ordered along the positive GLCM diagonal, is low (i.e. close to 0) if the filled elements are spread out over the entire GLCM, is negatively high (i.e. -1) if the filled elements are ordered along the negative GLCM diagonal.

$$\sum_{i,j=0}^{N-1} P_{i,j} \left[ \frac{(i - \mu_i)(j - \mu_j)}{\sigma_i \sigma_j} \right]$$

Equation 5. Correlation

- Homogeneity:

The GLCM elements are weighted by the reciprocal of their squared distance from the matrix diagonal, where i equals j. The Homogeneity is the higher the closer the GLCM elements gather around the matrix diagonal. As a certain contrast to Homogeneity see Dissimilarity.

$$\sum_{i,j=0}^{N-1} \frac{P_{i,j}}{1 + (i - j)^2}$$

Equation 6. Homogeneity



- Dissimilarity:

The GLCM elements are weighted by their distance from the matrix diagonal, where  $i$  equals  $j$ , i.e. where a gray value is identical to its partner, where the pairs have the highest similarity. The higher the difference between the column/row index the higher the weight and the higher the dissimilarity. The Dissimilarity ranges from 0 to  $d_{\max}$ . It is 0 if reference and partner are equal.  $d_{\max}$  is the greatest grey value difference. Dissimilarity reaches  $d_{\max}$  if the GLCM contains only one element located in the last column of the first row or in the last row of the first column.:

$$\sum_{i,j=0}^{N-1} P_{i,j} |i - j|$$

Equation 7. Dissimilarity

- Angular Second Moment (also known as Energy or Uniformity):

Energy needs a few more words of explanation: In several publications, Energy is defined as square root of Angular Second Moment. Both, Angular Second Moment (often abbreviated as ASM) and Energy need  $P_{i,j}$  as a weight for themselves. When the window is very orderly, ASM and Energy yield high values. The ASM and Energy are always less or equal 1.0. There is only one case, where it reaches 1.0. There must be only one single non-zero element in the GLCM, and if this is the case it must be located in the matrix diagonal, or in other words, if all gray values in the original image window are identical. The less used term Uniformity becomes understandable. In practice, the Energy is always significantly less than 1.0. As for Entropy, the Angular Second Moment yields different results for symmetric and asymmetric GLCMs.

$$\text{Energy} = \sqrt{ASM}$$

Equation 8: Angular Second Moment and Energy or Uniformity

$$\sum_{i,j=0}^{N-1} P_{i,j}^2$$

Equation 9: Angular Second Moment

For further detailed explanations of calculations regarding the Gray Level Co-occurrence Matrix, see Hall-Beyer M., 2017 and Gonzales R.C. and Woods R.E., 2001.

## 4.4 Parameters for deriving GLCM and texture images

For the extraction of the Haralick features, from the Gray Level Co-occurrence Matrix (GLCM) four important parameters need to be considered:

- the grayscale quantization levels;

- the size of the window moved over the image to be analysed;
- the orientation angle for the direction of neighborhood analysis;
- the distance of neighborhood.

### **1. The grayscale quantization levels:**

Images as they are acquired by high quality imaging systems contain an overabundance of tonal shades of gray or colours. Quite often ranges of several thousands or even ten thousands of intensity values may be available. In general digital images are stored as positive integer values within a certain value range, thus representing a discrete quantisation of the natural continuous grey scale. High resolution satellite imagery may provide a range from 0 to 4095 (i.e. 12 bit representation) or even more.

As mentioned afore, the size of a GLCM depends on the range of intensities of the image under investigation. In the case of a 12-bit image, the GLCM would end up in a size of 4096 by 4096 elements, by far too big to be feasibly processed. Therefore, a re-quantisation is usually applied, which in the software tools is set by a parameter just called “quantisation”. The quantisation in this sense is a rescaling of the intensity range to a smaller range, quite often to 6 bits (64 intensity values), 5 bits (32 intensity values), or 4 bits (16 intensity values). The question arises, what the optimum quantisation setting would be. In the following a few basic considerations should be listed.

If the full image information is preserved, very likely many neighbourhood relationships do not appear at all in large GLCMs, which eventually leads to a statistically less reliable sparsely filled huge matrix. On the other hand, the smaller the range after the quantization, the more information gets lost in the image under investigation. Minor variations in textures are erased and there are no variations in the distribution within the GLCM, everything is compressed (grey values of neighbouring pixels become identical). The information content is getting smaller, the more the level of quantization is reduced. Though the matrix elements are not empty, the information is gone.

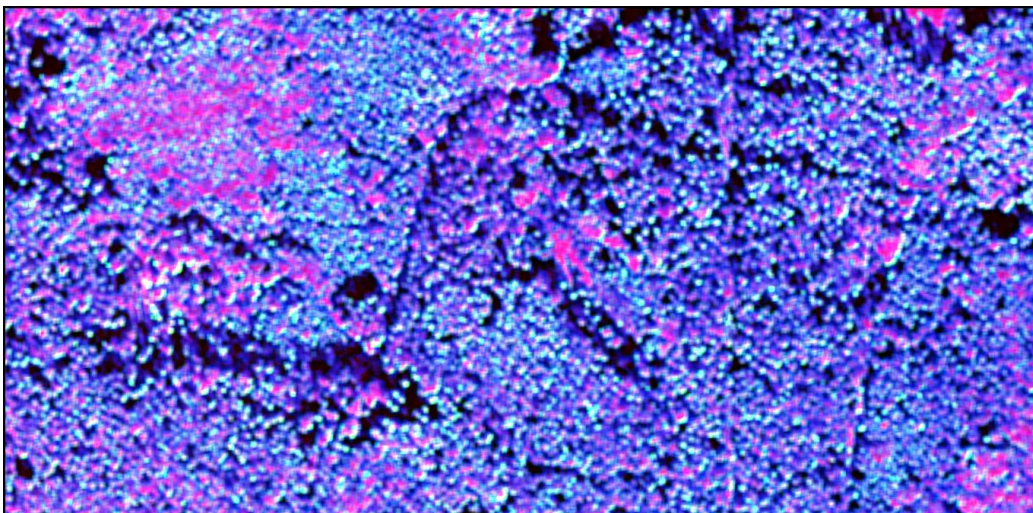
### **2. The size of a window moved over the image:**

A GLCM may be derived for the whole image. For texture classification this would not make much sense, therefore a moving window is shifted over the image, and in each window a GLCM is generated, which in the following is used to calculate Haralick features. This process can be called non-linear texture filtering in spatial domain. A parameter of filtering in spatial domain is the size of the moving window. In the following are a few considerations with regard to finding an optimum window size:

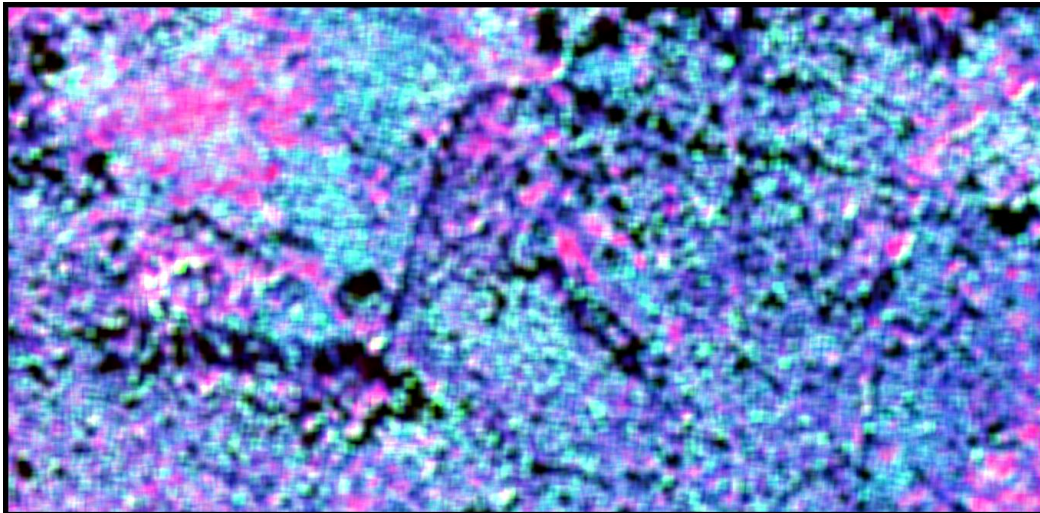
- The smaller the size of the window, the less information exists about the neighborhood and therefore, less information about the characteristics of a texture, but due to the small window size the process is sensitive to spatially changing texture characteristic. Boundaries between different textures could be detected more reliably.
- The larger the size of the window, the more information exists for describing the texture and therefore, unfortunately, the process is less sensitive to boundaries between different textures. In other words, smaller windows deliver sharper results and larger windows deliver greater transition zones between changes of texture.

- When small window sizes are applied, coarser textures, i.e. textures with a longer repetition wavelength, cannot be analysed and, hence, are not detected, while for detecting high frequency texture small windows are well suited.
- If coarse texture frequently appears in an image, larger window sizes are a must, at the cost of good boundary detection. On the other hand, it is likely that boundaries between coarse textures are not so well defined anyway.
- If all sorts of textures, fine as well as coarse ones, are present in images, one should consider separate analyses by applying different window sizes (there are suggestions in literature (e.g. Coburn C.A. and Roberts A.C.B., 2004)), or as an alternative approach, it possible to analyse several levels in image pyramids. One should be aware, that larger windows and coarser pyramid levels may deliver similar results, but they are not equivalent, although the size of the GLCM may be equal.

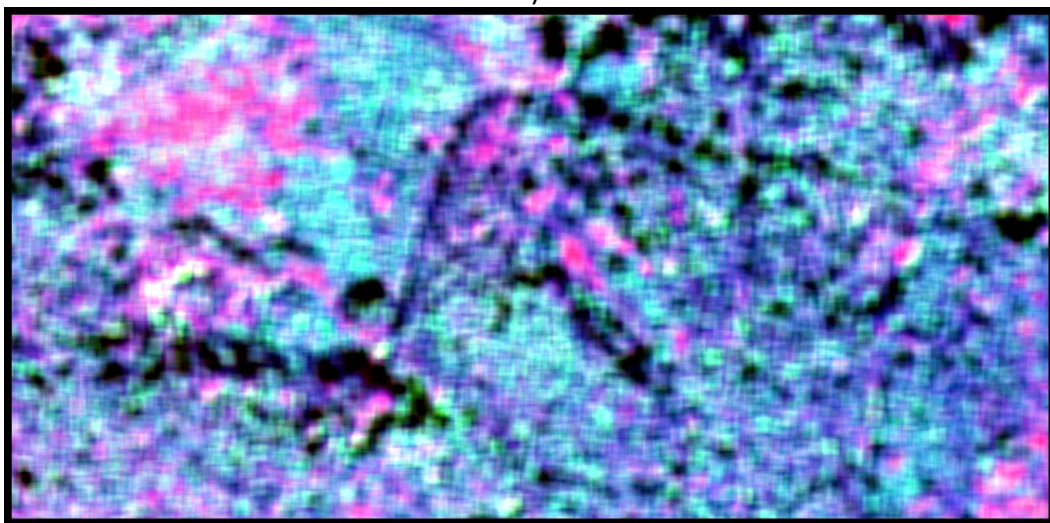
In the figure below (figure 6) a sample from Pléiades 1B has been tested, where the Haralick texture features Mean, Contrast and Entropy have been applied, with a quantisation of 64 gray levels, using three different window sizes, i.e. a) 7x7, b) 15x15 and c) 21x21. One may watch the tooth-like pink feature right in the centre of the image. The shape in the image a) clearly shows two extensions, the boundaries to the neighbouring textures are sharp. In image b) the boundaries are already blurred, while in image c) the original shape has been significantly generalized; the two extensions are separated by only a narrow gap. On the other hand, in image a) the forested cyan-blue dotted area below the above mentioned pink feature appears to be rather noisy. Obviously small image details are extracted as individual textures. As a matter of fact, the entire region has a more coarse texture. If one compares this region with the feature extracted in image c) a by far more uniform cyan patch can be recognized, which seems to represent more accurately the type of texture in this area. This example already indicates, that the combination of textural images derived with different parameters may render possible a more accurate classification of textured objects.



a)



b)



c)

Fig.6: Haralick texture measures: Mean, Contrast and Entropy  
 Image with: a) Window Size: 7x7, Quantization Level: 64  
 b) Window Size: 15x15, Quantization Level: 64  
 c) Window Size: 21x21, Quantization Level: 64

### 3. The orientation angle for the direction of neighborhood analysis:

A matrix has eight major directions, which can be expressed by  $0^\circ$ ,  $45^\circ$ ,  $90^\circ$ ,  $135^\circ$ ,  $180^\circ$ ,  $225^\circ$ ,  $270^\circ$ ,  $315^\circ$ , in other words, along rows, columns, and along diagonals, all in both directions, yielding a total of eight directions for analysis. In non-symmetric GLCMs these eight directions deliver different results, in symmetric GLCMs only the four main directions are relevant. The direction is an essential parameter of the GLCM in cases of non-isotropic textures, for instance, when in farmlands crops are arranged in lines in various directions, or in reforestation areas where trees may be restocked in certain patterns.



#### 4. The distance of neighborhood:

Another major parameter that influences the discrimination capabilities of the GLCM is the separation distance between pixels. If the neighbourhood distance is equal to 1, it means that the partner pixel is the immediate neighbour of the reference pixel. It is likely that the immediate neighbour contains a gray value that is very close to that of the reference pixel, therefore in the GLCM the elements along the (i=j)-diagonal are more frequently filled and eventually contain great values. The feature Correlation is positive and might lie close to 1.0. In the case that the distance value is increased, it tends to reflect a decreasing degree of correlation between distant pixels. Therefore, it would be advisable before the texture analysis and classification starts, to calculate the GLCM for different partners in different distances, like for five or even ten pixels distance.

An example of an asymmetric GLCM (figure 7), with a 4x4 pixel neighbourhood, direction 0° (row left to right) and 45° (left lower corner to right upper corner) and distance 1 is illustrated below (reference coordinate = row number, partner coordinate = column number):

1	2	3	4
1	2	3	0
4	3	4	1
0	1	2	3

(a)

	0	1	2	3	4
0	0	1	0	0	0
1	0	0	3	0	0
2	0	0	0	3	0
3	1	0	0	0	2
4	0	1	0	1	0

(b)

	0	1	2	3	4
0	0	0	0	1	0
1	0	0	1	0	1
2	0	1	0	1	0
3	0	0	0	1	1
4	1	0	1	0	0

(c)

Fig.7: (a): original image;  
 (b): GLCM in 0°, distance 1;  
 (c): GLCM in 45°, distance 1

In this study, different processing windows and grayscale quantization levels were investigated. In regard to the direction and distance, as in the previous case, several directions and distances have been tested, but in all cases, very small differences were noticed. Therefore, varying the parameters is of minor importance, and it has been decided to select a fixed setting of a 45 direction and the distance 1 in order to perform the further analysis.

## 5 Image classification

Image classification is a task of image analysis to assign distinct object classes to parts of the image by spatial subdivision according to typical local image characteristics, such as texture, colour, geometric shape, etc. The resulting classified image is a thematic dataset whose elements bear the name of the respective class. In the huge field of image interpretation and image understanding, classification is a basic process, and therefore, a great many approaches and algorithms have been developed in the past and standard procedures exist. In the field of remote sensing, the classification of multispectral or multichannel images have belonged to the core procedures of each image processing system from the very beginning. The multispectral images of the Landsat series and their successors led to standard procedures, which have proved successful and which are still widely used, although the challenges of modern high-resolution imagery captured from space platforms require more sophisticated approaches. Both texture and colour are going to play a major role. Whether the well-known algorithms, like Maximum Likelihood, Minimum Distance, k-Means or Isodata, are able to yield satisfying results, need more detailed investigation. The current work is not intended to provide a general answer.

### 5.1 Supervised and unsupervised classification

To start with classification, first, two widely used terms for characterizing classification approaches should be explained: the supervised and the unsupervised classifications.

The classification process may be supported by the user who is responsible for teaching the algorithm what sort of image characteristics should be searched for by providing training or ground truth samples. These samples may be taken from a sample library, but quite often the samples are extracted from the image under investigation by selecting regions of interest (widely known as ROIs) for each class. In this case, the approach is called supervised classification.

To perform a supervised classification, one must follow rigorously certain steps.

These are:

- adopting a classification scheme;
- selecting representative test areas (samples);
- statistical analysis of the samples of the spectral data must be carried out;
- a suitable classification algorithm must be selected;
- the accuracy of the classification must be statistically assessed by validating the classified result against the samples of “field data”.

More sophisticated approaches leave it to the algorithm to find regions of identical or at least very similar data characteristics. A priori analysis and learning are carried out without or with minor interaction by a user. This group of approaches is called unsupervised classification.

The unsupervised classification does not need too much knowledge about the data in advance, though each algorithm needs some initial settings and these settings need to be estimated. As an example, the k-Means algorithm asks for an estimated number of classes to be classified. If this number is not realistic at all, because it is too high or too low, the result may not be very useful. The Isodata algorithm, on the other hand, is an extension of k-Means and the user has to provide a few further settings which control an automatic joining or splitting in order to lead to an extension or reduction of an a priori estimated number of classes. Basically, the algorithms are based on finding clusters, i.e. areas of high point density, in the multichannel feature space followed by their statistic analysis. Clusters are expected to represent prominent classes in the original data set.

Besides the fact, that there exists a great number of very different algorithms for both approaches, there is no clear indication, which tells a user, which approach should be preferred. One just needs to be aware, that a supervised approach always needs a sort of human visual interpretation in advance. After classification, at least, the pixels of the classified image are already assigned the classes which the user has provided. One should keep in mind, that only classes can be found for which ground truth samples exist. Classes which obviously are present in an image but have not been selected for training are either assigned to the next best ground truth class or are rejected into a not classifiable background class. In cases of multichannel images, such as multispectral images, it is quite difficult to visually find sufficient and well separable class samples. The classified result may then be incomplete or inaccurate.

On the contrary, a good unsupervised algorithm is capable of finding by far more classes, because it analyses the complete image for distinct characteristics even in a multichannel image. The resulting classified image does not have assigned class names, just category numbers. The assignment of class names according to the real world's objects has to be done manually in an independent post-processing step by the user, what would need a quite cumbersome process. If the parameters of the unsupervised classification algorithm were not optimally set, the number of resulting categories could be rather high, i.e. the separation criteria were too sensitive, or the number of categories might be rather low, i.e. the separation criteria were too insensitive. Finding the optimum number of classes can usually be set by adjusting the initial parameters of the algorithm, possibly in a trial and error feedback loop.

Though at a first sight, the unsupervised approach looks more convenient and even more reliable, the supervised approach might be superior in cases where the classes looked for are very limited and where the image has only a few channels so that classes are visually well separable during the training phase. Additionally, it has to be emphasized, that the major difference between a supervised and an unsupervised approach is the way of finding the class representatives in the multichannel feature space. The eventual subdivision of the space into class relevant portions may be carried out by the same algorithms, for instance, by Maximum Likelihood, Minimum Distance, Support Vector Machine, etc.

## 5.2 Choosing a supervised approach

For all following investigations, a supervised approach has been chosen in order to facilitate the comparison between the computer assisted classification and human based interpretation. The operator has to select ground truth data, first, for training and, second, for quality assessment. Since the ground truth areas are known, they can, in a separate step,



easily been investigated with respect to their multi-channel characteristics. This is particularly important for getting more information about the behaviour and nature of textural parameters. In the unsupervised approach, where the software makes its class assignment independently, investigations of that kind would be more cumbersome or even not possible at all.

### 5.2.1 Selecting the classification algorithm

Numerous classification methods can be used to assign a pixel to a particular class. Choosing a custom grading classification method depends on the nature of the input data and desired data.

Some of the most used classifications in remote sensing so far are: Parallelepiped classification; Minimum Distance classification; Maximum Likelihood classification and Mahalanobis Distance. Common for all these classification methods is that the typical class representation is given by the mean value of the cloud. The Mahalanobis Distance and Maximum Likelihood are approximately the same, it is just a matter of scaling the distances. The cloud is statistically represented by a mean value and a normal distribution. The Parallelepiped classification uses the Gaussian curves as representatives for the distribution of each channel individually, while the Minimum Distance analysis just depends on Euclidean distances from the mean to a pixel to be classified. Accordingly, it means that the Mahalanobis Distance and Maximum Likelihood algorithm have very similar prerequisites. These two classifications assume that the distributions of the classes in the multi-channel feature space, come close to a normal distribution. Parallelepiped and Minimum Distance even assume that clouds form an isotropic distribution.

Maximum Likelihood is a very often implemented algorithm, therefore it would be very interesting to investigate, whether this type of classification would be successfully applicable for fused textural and spectral information. For this reason, in this investigation the Maximum Likelihood algorithm plays an important role and since it is installed more or less in all image processing systems dedicated to remote sensing applications (also in the ENVI software which is used for this investigation), minor a priori implementations were necessary and the work could concentrate on the image analysis almost immediately.

### 5.2.2 Maximum Likelihood classification (ML classification)

A powerful and commonly used method of supervised classification in remote sensing is the Maximum Likelihood, which assumes that a pixel is assigned to a class depending on the probability density of a particular class whose mean and variance-covariance behavior can be described by a normal distribution in the multispectral feature space. In other words, the Maximum Likelihood decision rule is based on probability density and therefore, its procedure assumes that each class in each band are normally distributed. Training data with bimodal or n-modal histograms in a single band are not ideal. In such cases, the individual modes probably represent unique classes that should be trained upon individually and labeled as separate classes. A set of  $m$  classes is calculated, and the pixel is then assigned to the class for which the probability density is the highest.

In the 1-dimensional case the normal distribution is represented by the well-known Bell Curve, which can be defined by the two parameters mean and the standard deviation. In the N-dimensional case mean and standard deviation are replaced by the N-dimensional mean vector and by the  $N \times N$ -dimensional variance-covariance matrix.

“This approach to classification is extremely useful and flexible and, under certain conditions, provides what is probably the most effective means of classification given the constraints of supervised classification” (Richards J.A., 1999).

As already mentioned above, this classification method is based on the use of probability theory to compare the spectral values of each pixel in part with the statistical “footprint” in each sample chosen during the classification preparation phase. The higher the probability density for a certain point, the more likely that point belongs to the respective class.

Calculations are slower due to the complexity of the used algorithms. Depending on the importance of the project and the precision required for classification, it is recommended to choose this classification method, because it is based on a sound statistical theory. It needs more computer resources than the more simpler approaches, but with nowadays’ powerful hardware this is not a limitation any more. In nature, the areas to be classified show a certain variation in spectral responses. In addition, occlusions, cast shadow, topographic shading, system noise, and mixed pixel effect increase this variability.

Nevertheless, the classification needs careful preparation by the user. If the ground truth samples are not well selected with respect to the method’s requirements, the final quality will certainly not fulfill the high expectations independent of the theoretically high quality of the algorithm.

ENVI operator also allows to select a probability threshold. “This means that if the probability that the test pixel is below the operator input value then the pixel will remain unclassified” (Richards J.A., 1999). No probability threshold has been chosen in this work, which means that all pixels are classified into one of the reference classes and no pixel remains unclassified.

## 6 Investigation methodology

In order to obtain results which allow a qualitatively sound assessment of the investigation's objective, a strategy has been put together, which eventually allows various comparisons. Therefore, three basic processing lines have been worked out to be evaluated: Classification with spectral data alone, classification with textural features alone, and finally, as a sort of fusion, classification with both spectral data and textural features together. The processing framework is illustrated below in figure 8.

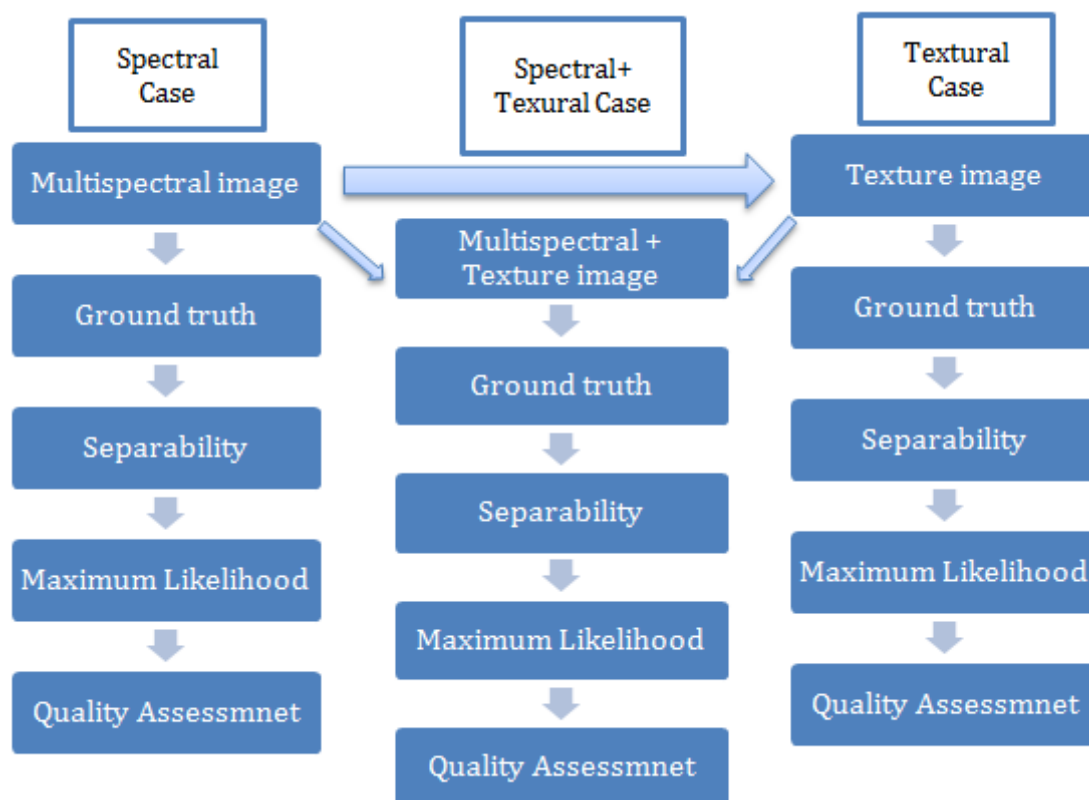


Fig.8: A general framework of the investigation methodology

### 6.1 Selection of ground truth areas

Ground truth areas are those regions in the image of which one knows the object class in the real world. Ground truth is usually gathered by visual interpretation of the image under investigation. Areas (often called Regions of Interest, or ROIs) need to be defined, from which the interpreter is sure to know the class of the real world object below. Ground truth samples, in the ideal case, must contain only one class and therefore their collection must be carried out very carefully. They are needed in two cases:

1. If a supervised classification is to be applied, ground truth provides information for teaching the algorithm the typical spectral properties of the classes to be classified. These ground truth areas are often called "training areas".
2. The quality assessment of a classification is based on the comparison of the classification result with ground truth data. There exist several strategies for that

comparison. One would be the comparison of the classes at randomly selected points. At each selected point the user has to interpret the class in the original image or in any other appropriate dataset. Another way would be the use of ground truth areas of the same type as they have been used by the algorithm for learning. As they must not be geometrically the same areas as the training areas, they may be called “checking areas”.

The current classification of multispectral images is very automated. In many cases, the choice of ground truth areas is both scientific and intuitive. The interaction between analyst and image data is needed. Substantial references and good knowledge of the geographic area to which data is applied are also needed.

## 6.2 Image texture measures

Haralick famously proposed a technique for evaluating textural features, that are divided into two categories, namely occurrence texture measures and co-occurrence texture measures. For this investigation, the co-occurrence-based filters have been tested and employed.

As for the important textures measures, there is a total number of five occurrence measures, these are: data range, mean, variance, entropy and skewness and eight co-occurrence filters, namely: mean, variance, homogeneity, contrast, dissimilarity, entropy, second moment respectively correlation.

“Occurrence measures use the number of occurrences of each gray level within the processing window for the texture calculations” (Anys H. et al., 1994). These measures are also known as 1st order statistics.

“Co-occurrence measures use a gray-tone spatial dependence matrix to calculate texture values. This is a matrix of relative frequencies with which pixel values occur in two neighboring processing windows separated by a specified distance and direction. It shows the number of occurrences of the relationship between a pixel and its specified neighbor” (Haralick R.M. et al., 1973). These measures are also known as 2nd order statistics.

The occurrence measures are based on statistical moving window filters in the spatial domain. They are not directly sensitive to neighborhood variations and to directional behavior of textures and therefore it has been decided, not to use them in the current investigation, and to concentrate on co-occurrence measures only.

## 6.3 Separability analysis

Before the classification is carried out, there are a few possibilities for estimating the expected quality of the classification result. Among the most important ones is the analysis of the separability of the classes. There exist several approaches, among them the well-known Jeffries-Matusita Distance (JMD). Like the Maximum Likelihood Classification itself, the calculation of the separability is based on class samples which can be represented by a normal distribution in feature space, i.e. by representative mean values and associated variance-co-variance functions. The JMD is a sort of probability estimation rather than a distance in feature space. It is derived from a multiplicative comparison of normalized distributions. The separability is always carried out between two classes only. If there are more than two classes, all class combinations are evaluated separately. In case of  $n$  classes,  $n(n-1)/2$  separabilities must be calculated. The JMD cannot exceed a maximum value. A bit dependent on the actual implementation this theoretical maximum is 2.000. The worst separability is given if the two normal distributions overlap 100% yielding a separability 0.000. If the two distributions form distinct clouds, the separability reaches 2.000. One should be aware, that the JMD is rather sensitive, in other words, only values close to 2.000 indicate a good separability. ENVI suggests interpreting values greater than 1.9 as excellent separability. The threshold in practice is somewhere at 1.5. In particular values below 1.000 indicate a not acceptable separability and a thorough check of the samples must be carried out. By analyzing the JMD for the dataset of the samples, one can easily find which classes will not be separable by the classification, thus causing wrong class assignments. As a consequence, the ground truth samples need to be revisited and its boundaries edited. In some cases, a bad separability may even be accepted, for instance, if the two classes are not distinct classes in the real world, but two subclasses, which at the end will be combined, anyway. As mentioned before, there are other separability measures used in remote sensing. Mausel et al. (1990) investigate several of them in order to find the optimal band for supervised classification of multispectral data.

## 6.4 Maximum Likelihood classification process

For classification, the supervised Maximum Likelihood approach has been selected. It has been one of the standard procedures in multispectral remote sensing from the very beginning of image processing and thus, it is implemented in almost all dedicated remote sensing software tools. It is also available in ENVI, the toolbox of our choice, as already mentioned earlier. The question arises whether the Maximum Likelihood approach is well suited for the particular investigation. As already mentioned in section 5.2.2 certain preconditions apply for successful use. As for texture classification and the combined classification of texture and multispectral data, it will, therefore, be necessary to check whether these conditions are fulfilled.

## 6.5 Quality assessment

The accuracy assessment analyzes the comparison with the help of confusion matrix between two sorts of information:

- pixels or polygons from a classification map derived from remotely sensed data and
- ground reference test information, i.e. checking information (Jensen J.R., 2005).

A confusion matrix is a table that compares the relationship between the two sets of information. From a confusion matrix, the following can be determined: the Overall Accuracy, Producer's Accuracy, Omission Errors, User's Accuracy and Commission Errors. It contains rows and columns, and in order to create it, we need classes of interest. Since it is not generally defined, in the following the confusion matrices are written in the way ENVI does: the columns include the reference data while the rows are composed of the classified information. "The intersection of the rows and columns summarize the number of sample units (i.e. pixels, clusters of pixels, or polygons) assigned to a particular category (class) relative to the actual category as verified in the field" (Jensen J.R., 2005). Along the diagonal of the matrix, the numbers represent the number of pixels, or samples which have been correctly classified, while the numbers in the non-diagonal matrix elements are considered as erroneous.

The Overall Accuracy is a figure that expresses the percentage of the correctly classified pixels. The Overall Accuracy includes all classes at once. From the confusion matrix, it is derived by dividing the sum of the diagonal elements by the sum of all matrix elements. The disadvantage of the Overall Accuracy is obvious: it does not show the classification quality of the individual classes. Therefore, the Producer's Accuracy and the User's Accuracy provide a more detailed quality assessment.

The Producer's Accuracy (PA) is a statistical figure that expresses for each class the percentage of pixels of the ground reference data that have been correctly classified. In practice, there are certain ground reference pixels that have incorrectly been classified. These pixels are missing for a correct coverage. Therefore, the percentage of the omitted pixels is called "Error of Omission" (EoO). It is the complement of the Producer's Accuracy, thus  $EoO=1-PA$ . PA for a certain class is calculated by dividing the respective diagonal element by the all pixels of the reference class under investigation.

The User's Accuracy (UA) is a figure which is intended as information for the data user. It is derived from the classification result and it provides information of what percentage for each classified class may be assumed as correctly classified. In practice, there will certainly be more pixels in each class. Those are incorrect since they have erroneously been assigned. The percentage of erroneous pixels of a certain class is therefore called the "Error of Commission" (EoC). It is the complement of the User's Accuracy. Thus,  $EoC=1-UA$ . UA for a certain class is calculated by dividing the respective diagonal element by all pixels of the classified class under investigation.

The Kappa coefficient expresses whether the classification is more a random assignment or a deterministic assignment. The higher the Kappa coefficient, the more organized the classification. In general, a Kappa coefficient greater than 0.7 is said to indicate a good classification. In fact, there are cases where even much smaller values indicate a systematic and not a random assignment.

## 7 Practical example

### 7.1 Selection of ground truth areas

In this practical section, it will be investigated whether the data is appropriate for the Maximum Likelihood classification, therefore, firstly, the selection of the ground truth areas is introduced. To successfully achieve a good digital image classification, the ground truth areas must be carefully selected and defined. Regarding the supervised classification process, the selection of ground truth areas was essential in this study and had to be extracted from the imagery data.

As already mentioned in section 2.1, two study areas (N-W and S-E) were investigated, both of them located in the Rosalia region, in a mainly forested region some 60 km south of Vienna.

It needs to be noted, that for the S-E area only the multispectral classification was applied, while for the N-W area, both multispectral information and texture have been taken into consideration. The main reason for this choice is that the N-W area offers much more different textures in forests, therefore it was more interesting for this study and the more thorough investigation by using spectral and texture at once has been applied.

The areas were classified with the help of supervised classification. The following list shows which classifications have been carried out:

#### 1) N-W area:

- a) Multispectral classification: 6 classes with training and checking areas for each class;
- b) Textural classification: 7 classes with training and checking areas for each class;
- c) Spectral classification combined with textural classification: 7 classes with training and checking areas for each class.

#### 2) S-E area:

- a) Multispectral classification: 8 classes, with training and checking areas for each class.

### 7.2 Results of separability analysis

It has to be mentioned that for the spectral classification three channels of the satellite image are the most important ones and have been used for the separability analysis, these are Red, Green and Near-Infrared and for the textural classification Mean, Contrast and Entropy have been chosen. Theoretically, there is the possibility to use all co-occurrence measures but a first quick check showed that there are partly high correlations in this case of forest patterns and therefore, it has been decided to use only three parameters, which also Hall-Beyer M. (2017) has used for the investigation of Landsat and which delivered quite good results. Although in this current investigation, high-resolution images have been analyzed, these three parameters might deliver good results.

#### N-W area:

Tables 2 to 4 describe the pair separation with the help of Jeffries Matusita distance, applied to the spectral, textural and combined spectral-textural case. In addition, the separability has been calculated for the training and for the checking areas. For a good separation of the region-of-interest, values should reach 1.9, the range down to 1 represents a poor, but still acceptable separation and less than 1 is very poor and thus forgettable.

Table 2 shows the separability results in the spectral case. Numbers in red represent a very poor separation, in yellow are the acceptable results, while green indicates an excellent separation of the classes.

Pair Separation					
Training			Checking		
Class		Separability	Class		Separability
conifers 1	larch	0.9	conifers 2	larch	0.89
conifers 1	conifers 2	1.13	conifers 1	larch	1.26
deciduous old	larch	1.3	deciduous old	meadow	1.3
conifers 2	larch	1.4	conifers 1	conifers 2	1.33
conifers 2	shadow	1.59	conifers 2	shadow	1.52
conifers 1	deciduous old	1.63	conifers 1	deciduous old	1.68
deciduous old	meadow	1.75	deciduous old	larch	1.75
meadow	larch	1.8	shadow	larch	1.79
conifers 1	meadow	1.84	conifers 1	shadow	1.83
conifers 2	meadow	1.85	meadow	larch	1.93
conifers 1	shadow	1.88	deciduous old	conifers 2	1.93
deciduous old	conifers 2	1.88	conifers 1	meadow	1.97
shadow	larch	1.94	conifers 2	meadow	1.98
meadow	shadow	1.98	deciduous old	shadow	1.99
deciduous old	shadow	1.98	meadow	shadow	1.99

Table 2. Spectral case: results of separabilities of training and checking areas, respectively

Legend:

	<i>very good separation</i>
	<i>acceptable</i>
	<i>poor</i>



Table 3, gives an overview of the separability for the textural case. One can clearly see that shadow 1 is not able to be separated from shadow 2 and falls into the category forgettable. This is not a serious problem since these two classes will finally be unified anyway.

Pair Separation					
Training			Checking		
Class		Separability	Class		Separability
shadow 1	shadow 2	<b>0.56</b>	shadow 1	shadow 2	<b>0.88</b>
rough texture	flat texture	<b>1.01</b>	coarse texture	fine texture	<b>1.02</b>
coarse texture	fine texture	<b>1.17</b>	rough texture	flat texture	<b>1.49</b>
fine texture	foliar texture	<b>1.23</b>	foliar texture	shadow 1	<b>1.66</b>
rough texture	coarse texture	<b>1.5</b>	fine texture	foliar texture	<b>1.66</b>
foliar texture	shadow 1	<b>1.65</b>	rough texture	coarse texture	<b>1.81</b>
coarse texture	foliar texture	<b>1.67</b>	coarse texture	foliar texture	<b>1.89</b>
rough texture	foliar texture	<b>1.84</b>	coarse texture	flat texture	<b>1.91</b>
rough texture	fine texture	<b>1.89</b>	rough texture	foliar texture	<b>1.94</b>
foliar texture	shadow 2	<b>1.9</b>	rough texture	fine texture	<b>1.96</b>
coarse texture	flat texture	<b>1.91</b>	fine texture	flat texture	<b>1.97</b>
fine texture	shadow 1	<b>1.96</b>	fine texture	shadow 1	<b>1.97</b>
foliar texture	flat texture	<b>1.98</b>	foliar texture	flat texture	<b>1.98</b>
fine texture	flat texture	<b>1.99</b>	foliar texture	shadow 2	<b>1.98</b>
fine texture	shadow 2	<b>1.99</b>	coarse texture	shadow 1	<b>1.99</b>
coarse texture	shadow 1	<b>1.99</b>	fine texture	shadow 2	<b>1.99</b>
rough texture	shadow 1	<b>1.99</b>	rough texture	shadow 1	<b>1.99</b>
rough texture	shadow 2	<b>1.99</b>	flat texture	shadow 1	<b>1.99</b>
coarse texture	shadow 2	<b>1.99</b>	coarse texture	shadow 2	<b>1.99</b>
flat texture	shadow 1	<b>1.99</b>	rough texture	shadow 2	<b>1.99</b>
flat texture	shadow 2	<b>1.99</b>	flat texture	shadow 2	<b>2</b>

Table 3. Textural case: results of separabilities of training and checking areas respectively

Table 4 lists the separability of the combined spectral-textural case. Shadow 1 and shadow 2, as in the previous case, are difficult to be separated.

Pair Separation					
Training			Checking		
Class		Separability	Class		Separability
shadow 1	shadow 2	0.47	shadow 1	shadow 2	0.44
conifers very dense	conifers less dense	1.02	conifers very dense	conifers less dense	0.59
conifers very dense	larch rarefied	1.17	conifers very dense	larch rarefied	1.07
conifers less dense	larch rarefied	1.24	conifers less dense	larch rarefied	1.15
conifers less dense	shadow 1	1.86	old deciduous very dense	flat	1.36
conifers less dense	shadow 2	1.87	old deciduous very dense	larch rarefied	1.64
old deciduous very dense	larch rarefied	1.87	conifers less dense	shadow 1	1.8
conifers very dense	shadow 1	1.89	larch rarefied	flat	1.88
conifers very dense	shadow 2	1.9	conifers very dense	shadow 1	1.89
old deciduous very dense	flat	1.92	larch rarefied	shadow 1	1.93
old deciduous very dense	conifers very dense	1.95	conifers less dense	shadow 2	1.94
larch rarefied	flat	1.95	larch rarefied	shadow 2	1.95
larch rarefied	shadow 1	1.96	old deciduous very dense	conifers very dense	1.96
larch rarefied	shadow 2	1.97	conifers very dense	shadow 2	1.97
conifers very dense	flat	1.99	old deciduous very dense	conifers less dense	1.99
old deciduous very dense	conifers less dense	1.99	conifers very dense	flat	1.99
conifers less dense	flat	1.99	conifers less dense	flat	1.99
old deciduous very dense	shadow 2	1.99	old deciduous very dense	shadow 1	1.99
old deciduous very dense	shadow 1	1.99	old deciduous very dense	shadow 2	1.99
shadow 1	flat	1.99	shadow 1	flat	1.99
shadow 2	flat	1.99	shadow 2	flat	1.99

Table 4. Spectral combined with texture: results of separabilities of training and checking areas respectively

It need to be mentioned that despite the poor separability between some classes, the results are encouraging. Many of the yellow marked separabilities are rather close to the upper limit and may be considered as highly acceptable. If we look at the results marked in red, like for instance shadow 1 and shadow 2, these would normally not be acceptable at all, but the central focus of this study is not shadow, therefore, the results are tolerable and fully acceptable. Shadow 1 and shadow 2 have been introduced to express the different appearance of the areas, rather than to treat them as individual classes. Hence, separating shadow 1 from shadow 2 is not an issue.

#### **S-E area:**

Table 5 displays the results of spectral separability for the training and checking samples. It can clearly be observed that most of the classes have been well separated thus indicating that the classes and their ground truth samples were well selected.

Pair Separation					
Training			Checking		
Class		Separability	Class		Separability
conifers 1	conifers 2	0.99	meadow 1	meadow 2	0.93
deciduous young	deciduous old	1.28	deciduous old	meadow 1	1.25
deciduous young	conifers 2	1.85	deciduous young	deciduous old	1.45
red-tile-roofs	shadow	1.94	conifers 2	shadow	1.75
deciduous old	conifers 2	1.95	red-tile-roofs	shadow	1.79
conifers 1	shadow	1.97	deciduous old	meadow 2	1.81
deciduous young	conifers 1	1.97	conifers 1	conifers 2	1.85
conifers 1	deciduous old	1.98	conifers 1	shadow	1.93
deciduous old	meadow 2	1.99	conifers 2	red-tile-roofs	1.98
conifers 2	shadow	1.99	deciduous young	meadow 1	1.98
conifers 1	red-tile-roofs	1.99	deciduous young	conifers 2	1.98
conifers 2	red-tile-roofs	1.99	deciduous old	conifers 2	1.99
deciduous old	meadow 1	1.99	conifers 1	red-tile-roofs	1.99
deciduous young	red-tile-roofs	1.99	deciduous young	meadow 2	1.99
deciduous old	red-tile-roofs	1.99	deciduous young	conifers 1	1.99
deciduous young	shadow	1.99	deciduous young	shadow	1.99
deciduous old	shadow	1.99	conifers 1	deciduous old	1.99
meadow 1	meadow 2	1.99	deciduous old	shadow	1.99
deciduous young	meadow 2	1.99	conifers 2	meadow 2	1.99
deciduous young	meadow 1	1.99	red-tile-roofs	meadow 2	1.99
conifers 2	meadow 2	1.99	deciduous young	red-tile-roofs	1.99
red-tile-roofs	meadow 2	1.99	conifers 2	meadow 1	1.99
conifers 1	meadow 2	2	deciduous old	red-tile-roofs	1.99
shadow	meadow 2	2	shadow	meadow 2	1.99
conifers 2	meadow 1	2	meadow 1	shadow	1.99
conifers 1	meadow 1	2	meadow 1	red-tile-roofs	1.99
meadow 1	shadow	2	conifers 1	meadow 2	1.99
meadow 1	red-tile-roofs	2	conifers 1	meadow 1	1.99

Table 5: Spectral separability of training and checking (=control) samples

### 7.3 Assessment of the cluster distributions in feature space

As a further step, the distribution of the points in the feature space is checked. It should be mentioned, that ENVI software provides a tool called n-D Visualizer, which is used to check the distribution of point clouds in the n-dimensional feature space, thus, all following figures in this section have been produced by the n-D Visualizer tool.

A 2D scatter plot is a plot where the distribution within one channel is plotted against the distribution in the other channel. An n-D scatter plot is a plot of n channels where the distribution of each channel is plotted against the distribution in the other channels. While 2D scatter plots can demonstratively be displayed as graphics, the n-D scatter plot needs animation in order to become understandable. Therefore, plots have been added here, where the axes in the n-D Visualizer have been rotated so that they resemble a 2D scatter plot.

In the first case three multispectral bands were investigated, namely, Red-Near-Infrared (R-NIR), Green-Near-Infrared (G-NIR) and Red-Green (R-G), while in the second case, the three texture parameters Mean, Contrast and Entropy were in the focus. The Blue channel was not included, firstly, because of its high correlation with the other visible light channel and, secondly, the restriction to 3 channels facilitates the visual inspection of the scatter plots.

### 7.3.1 Spectral case

Figures 9 and 10 display the distribution of all training and checking areas, respectively, in the 3D feature space. When comparing the distributions, one must be aware, that the colour of the same class differs in the plots of training and checking areas, as the legends show. Of course, also the shapes of the point clouds are different because of different spatial rotation of the axes. And one further point must be mentioned. As one can see, there are more classes (and colours) in the legend than colours can be recognized in the plot. The reason is the mutual occlusions of the point clouds if 3D clouds are projected onto a 2D plane. Again, animation would disclose this apparent shortcoming.

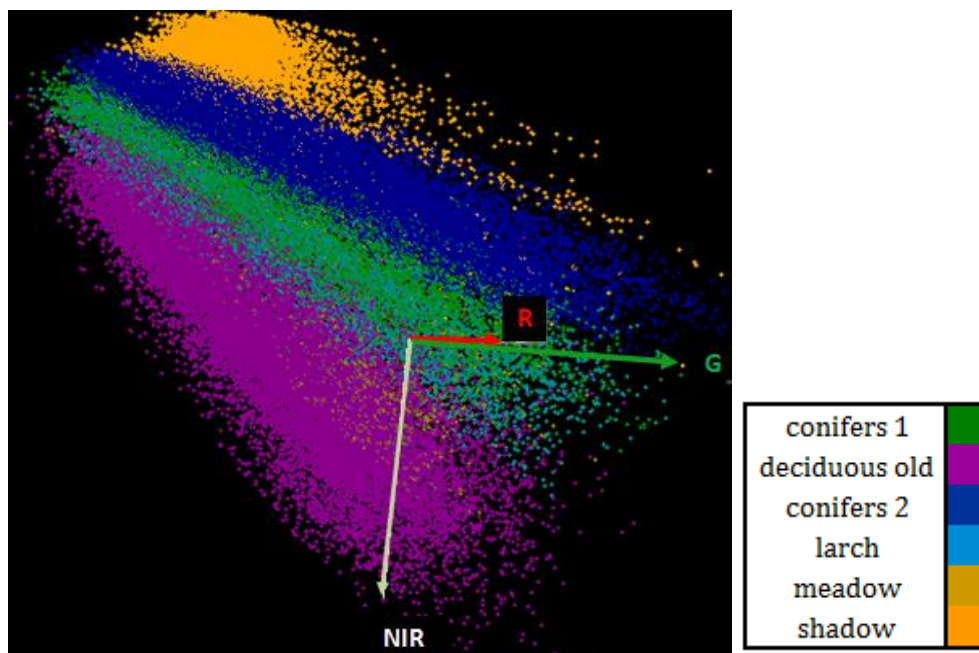


Fig.9: The distribution of the training areas in the feature space of multispectral channels R, G and NIR

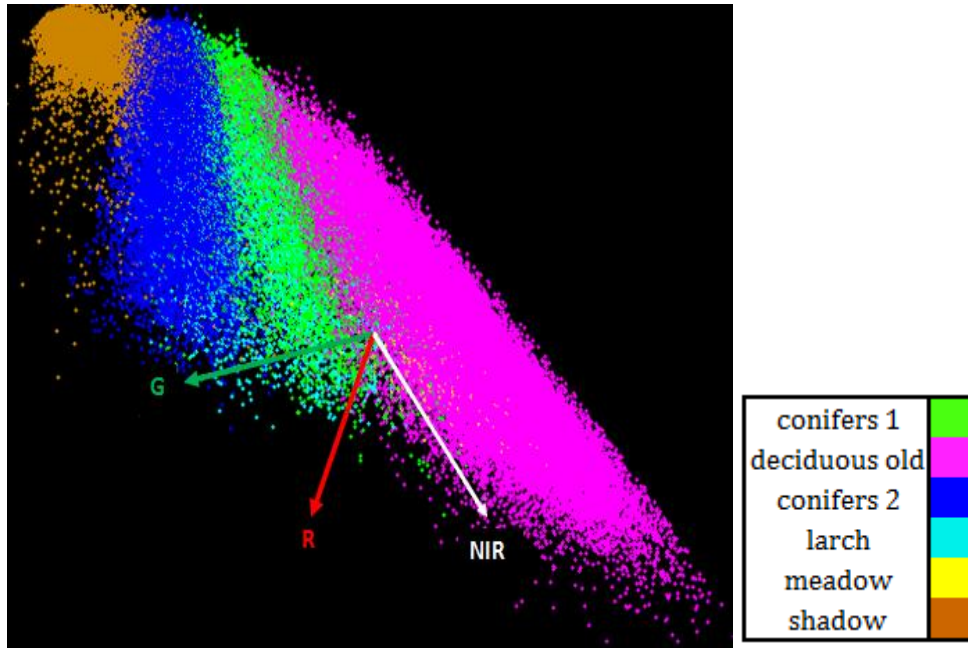


Fig.10: The distribution of the checking areas in the feature space of multispectral channels R, G and NIR

As already emphasized above, figures 9 and 10 must not be compared, because the plots are created in order to see the distribution of the points in the multispectral feature space. The clouds have a different position and different direction, therefore these two screenshots are not comparable, in order to see a relationship between training and checking areas.

The following figures, 11 to 13, show the same point cloud as in figure 9, but this time the axes have been rotated in positions in order to generate 2D scatter plots. The figures show all possible pairings of the three channels. One can clearly see that the channels are highly correlated, there is a linear dependence, especially between Green and Red, therefore, the cloud shapes are compact and may form elongated normal distributions. Deciduous old, conifers 1 and conifers 2 are distinguishable and the shape of the training areas do not overlap, thus, they come closer to the shape of an ellipse, and could be approximated by a multidimensional ellipse. The correlation is lower if NIR is involved.

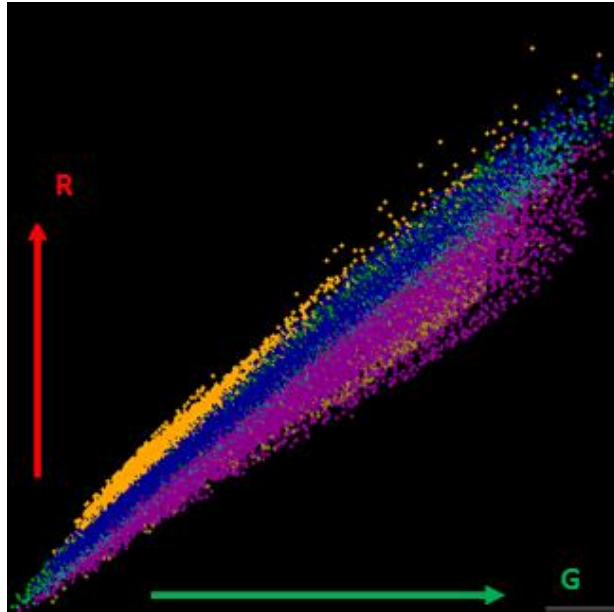


Fig.11: View of all training areas, R and G channels

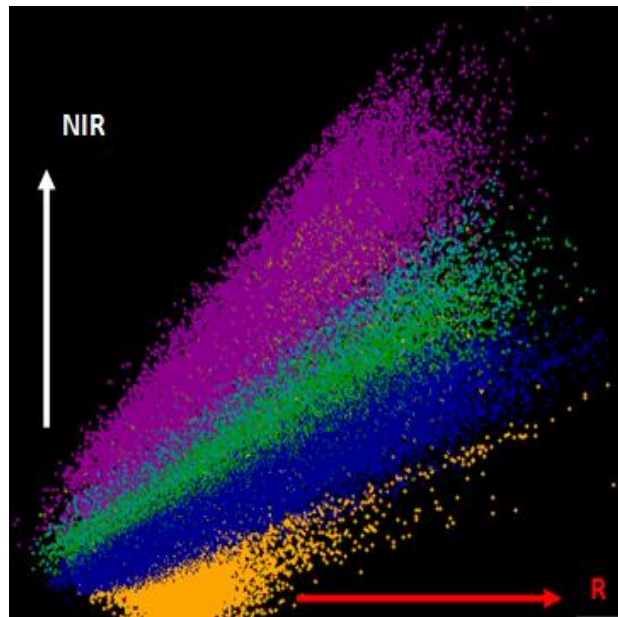


Fig.12: View of all training areas, R and NIR channels



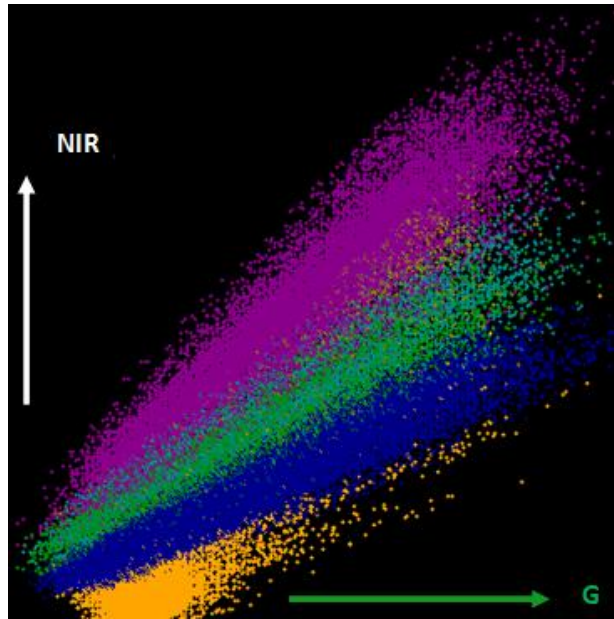


Fig.13: View of all training areas, G and NIR channels

### 7.3.2 Textural case

Figures 14 and 15 display the distribution of all training and checking areas in the 3D feature space of the texture features Mean, Contrast and Entropy. One must be aware, that the Entropy axis is rotated so that it runs vertically to the paper plane, thus generating a 2D scatter plot of the channels Mean versus Contrast. As already mentioned before, the colours of the same classes are different in the plots of training and checking areas, respectively. When comparing, the legends need to be consulted.

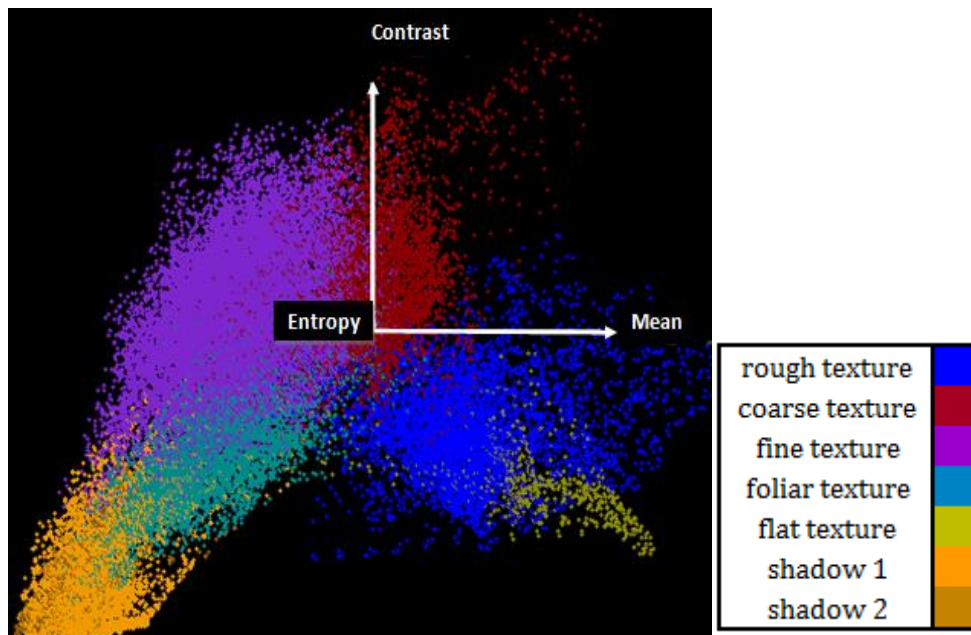


Fig.14: The distribution of all training areas in the feature space of textural channels Mean versus Contrast

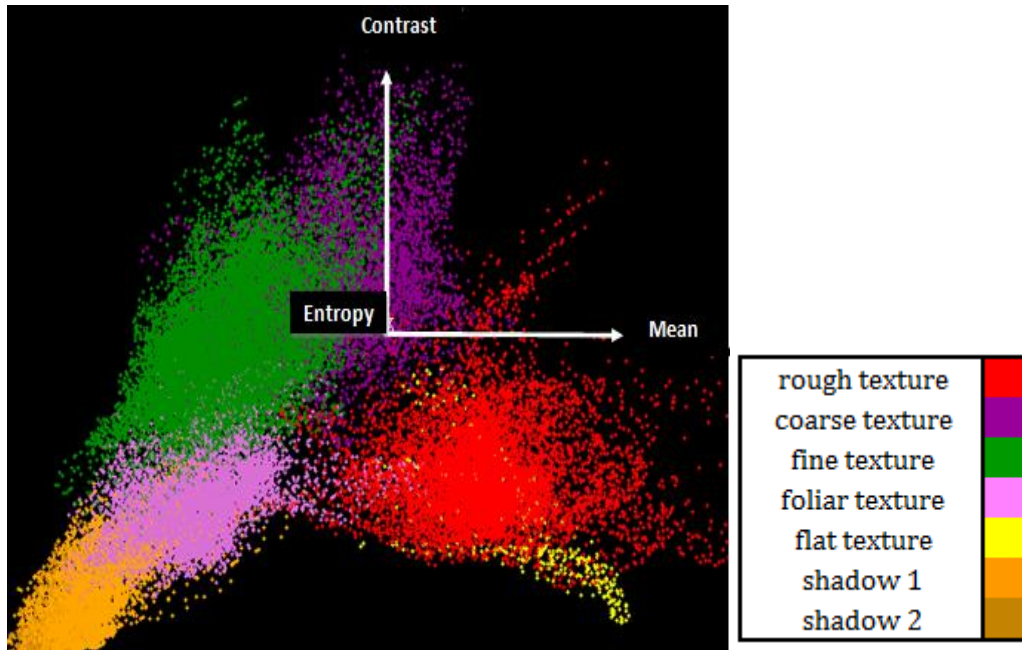


Fig.15: The distribution of all checking areas in the feature space of textural channels Mean versus Contrast

In the figures below, 16 to 18, the co-occurrence texture features already show that the classes are much more compressed and closer to each other.

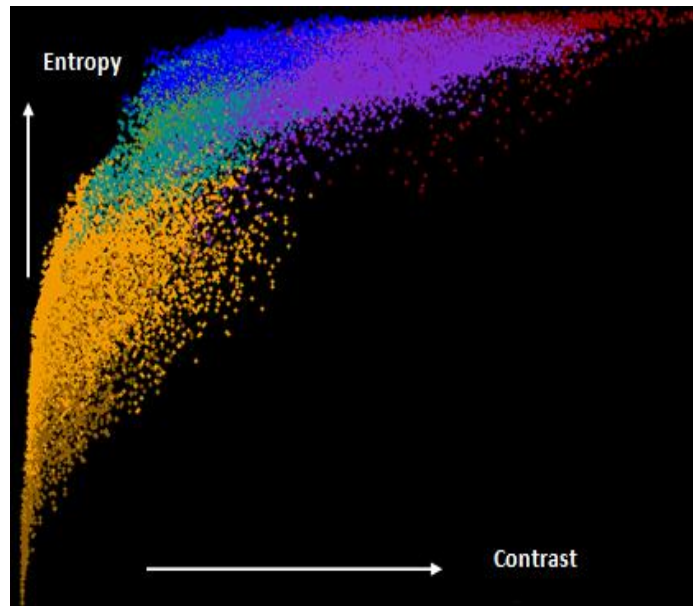


Fig.16: 2D scatter plot of Contrast versus Entropy of all training areas



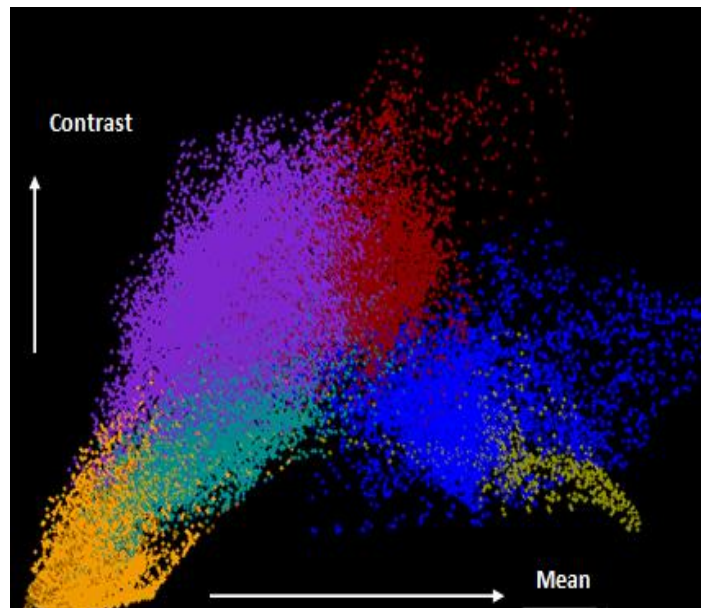


Fig.17: 2D scatter plot of Mean versus Contrast of all training areas (same as Fig. 14)

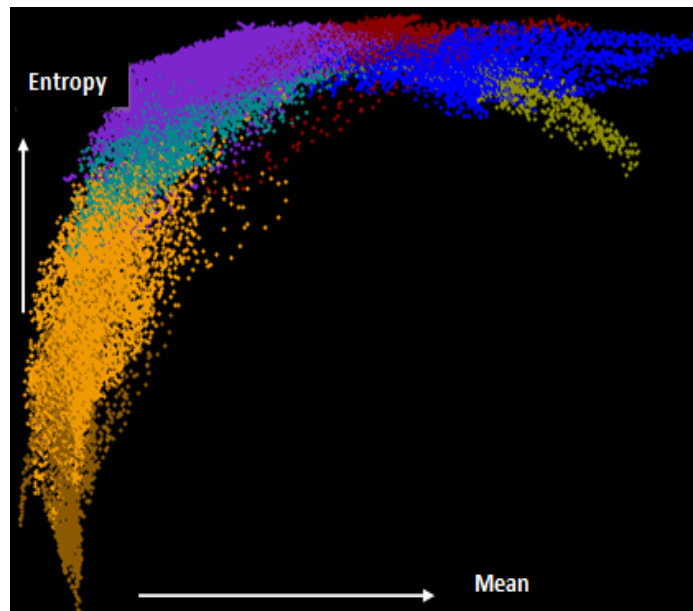


Fig.18: 2D scatter plot of Mean versus Entropy of all training areas

In figure number 17, it is easy to observe that, coarse texture is within fine texture, flat texture within rough texture, as well as foliar texture within shadow, being difficult to distinguish between the clouds. In some cases the elliptical shapes become recognizable but in other cases, the clouds are more compressed being hard to recognize their form. The variations of the pixels in the shadow classes are very low. Entropy expresses how many bits are used in order to store this sort of class. For shadow not many bits are needed because everything is dark. For other textures, in contrast, there are dark and bright areas, i.e. a much wider range of the gray values, therefore, much more bits per pixel are needed for these classes, hence, the entropy is higher.

The Maximum Likelihood classifier does a good job if the statistics of the ground truth areas within the training subset resemble a normal distribution. By visually analyzing the scatter plot, where the Entropy is involved, a non-linear dependence can be observed. One may assume that the required precondition of normal distribution might not be fulfilled. One work around could be a non-linear scaling of the Entropy axis, in order to generate a quasi-linear distribution and thus come close the normal distribution. In this investigation a scaling of that kind has not been taken into consideration. The Maximum Likelihood classifier has been applied to the original values.

In the first, the spectral case (see figures 9 and 10), the classes are better discernible than in the second, the textural case (figures 14 and 15).

In the following figures, from 19 to 26, a few classes are meticulously investigated and individually analyzed. As can be observed, for the classes fine texture (training sample), coarse texture (checking sample), rough texture (training sample) and foliar texture (checking sample), the clouds are rather homogenous and come close to the shape of an ellipse, although the afore mentioned non-linearity of Entropy is still recognizable in all respective figures. Still, we can assume that they are approximately normally distributed. Therefore, the images were inspected even closer. 2D scatter plots have been generated in order to allow a better estimation whether the clouds could be approximated by ellipses.

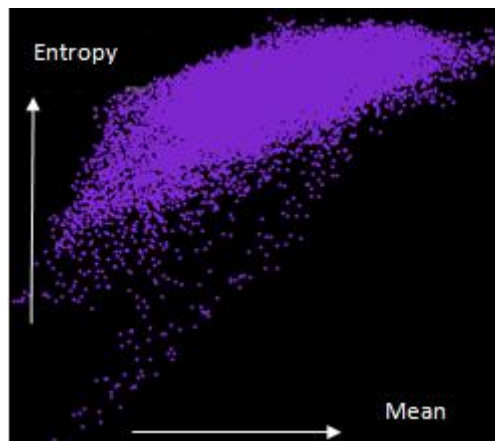


Fig. 19: 2D scatter plot of training area of fine texture, Mean vs. Entropy

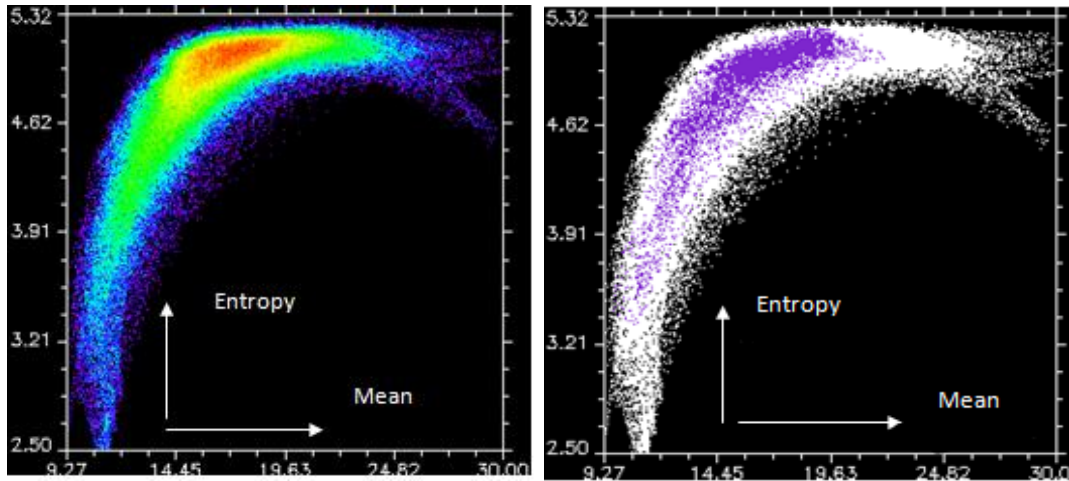


Fig. 20: Left side image: the density slice of the distribution in this feature space for the entire image (note: colours indicate point density in the cloud and not colour coded classes); Right side image: violet indicates where the point cloud of the sample for fine texture is located while white points belong to other classes (Note, the conspicuous non-linearity).

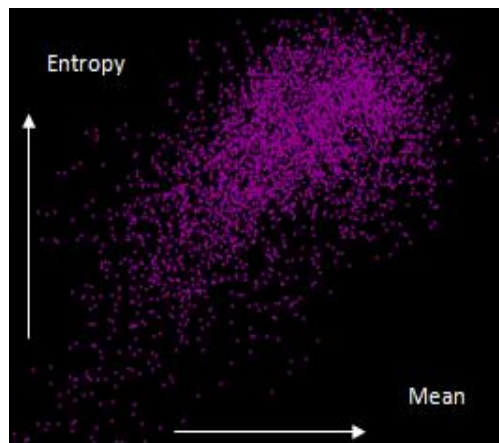


Fig. 21: 2D scatter plot of checking area of coarse texture, Mean vs. Entropy

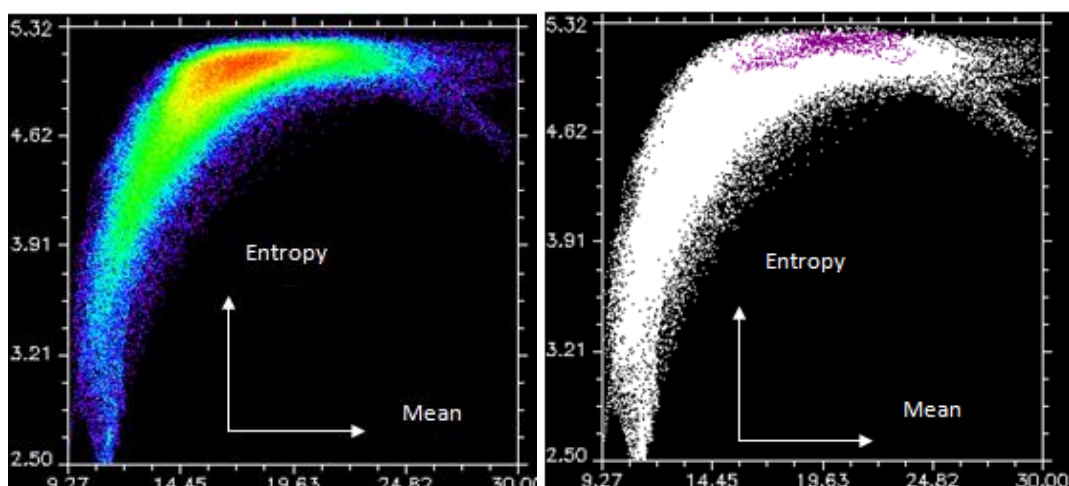


Fig. 22: Left side image: the density slice of the distribution in this feature space for the entire image (note: colours indicate point density in the cloud and not colour coded classes); Right side image: violet indicates where the point cloud of the sample for coarse texture is located, while white points belong to other classes.

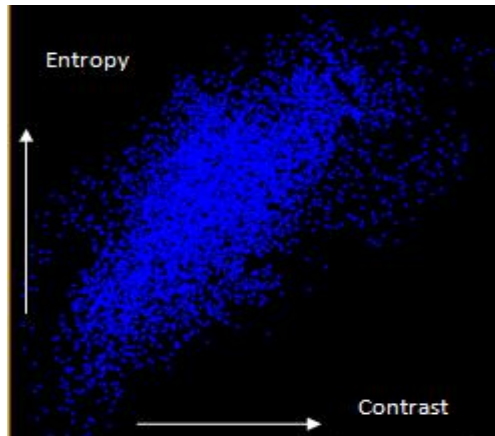


Fig. 23: 2D scatter plot of training area of rough texture, Contrast vs. Entropy

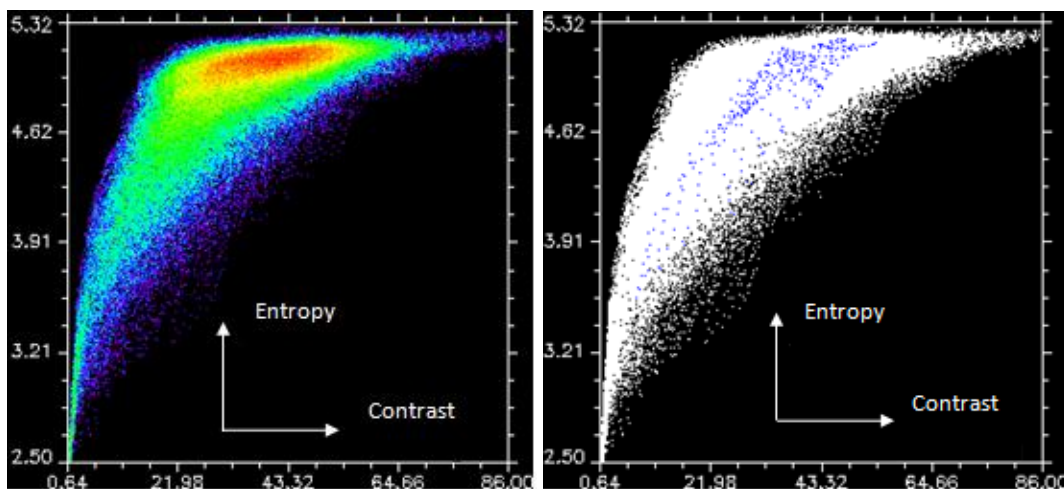


Fig. 24: Left side image: the density slice of the distribution in this feature space for the entire image (note: colours indicate point density in the cloud and not colour coded classes); Right side image: blue indicates where the point cloud of the sample for rough texture is located, while white points belong to other classes.

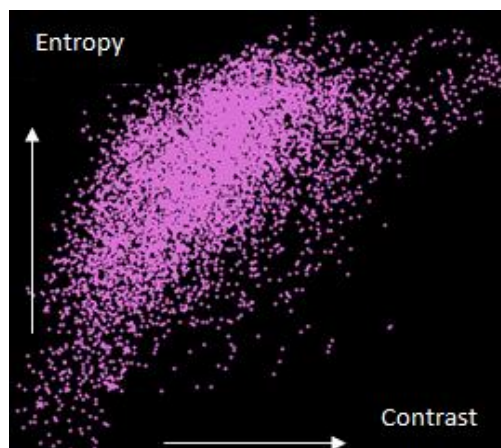


Fig. 25: 2D scatter plot of checking area of foliar texture, Contrast vs. Entropy

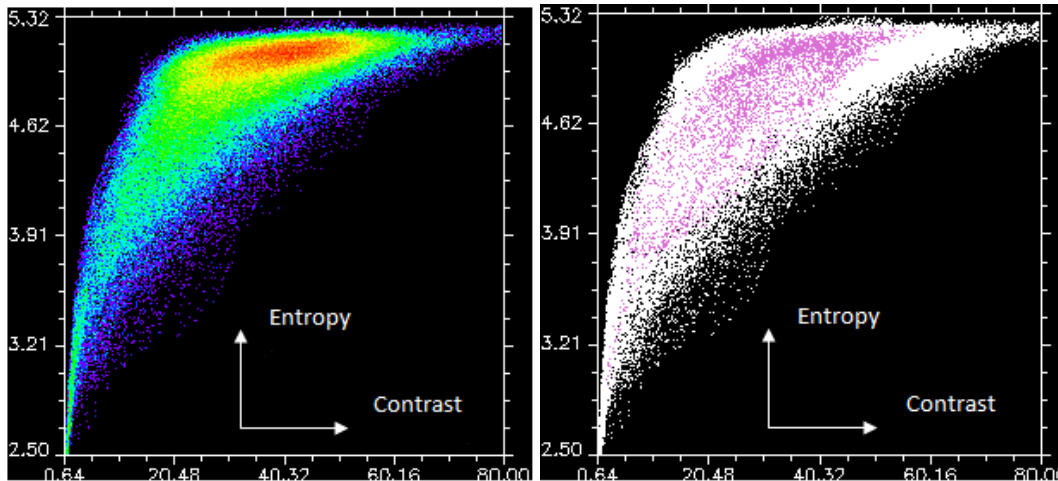


Fig. 26: Left side image: the density slice of the distribution in this feature space for the entire image (note: colours indicate point density in the cloud and not colour coded classes); Right side image: purple indicates where the point cloud of the sample for foliar texture is located, while white points belong to other classes.

The texture classes shadow have also been investigated here (see figures 27 to 30), although in practice it does not play a role, as already mentioned earlier. For classification reasons, on the other hand, it is advisable to introduce this sort of classes to improve the discrimination between other classes. As shadows are almost uniformly dark, their texture does not show much variation, and therefore, it has been expected that their clouds come closer to a normal distribution than clouds of other classes.

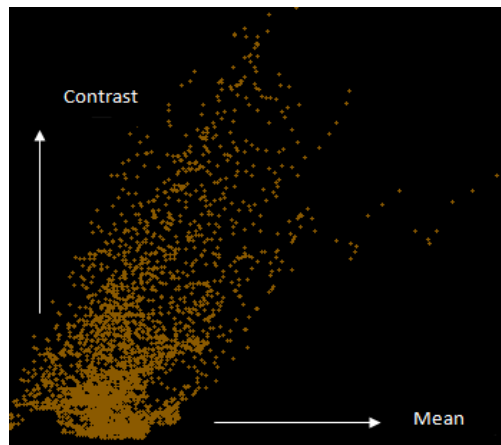


Fig. 27: 2D scatter plot of training area of shadow 2, Mean vs. Contrast



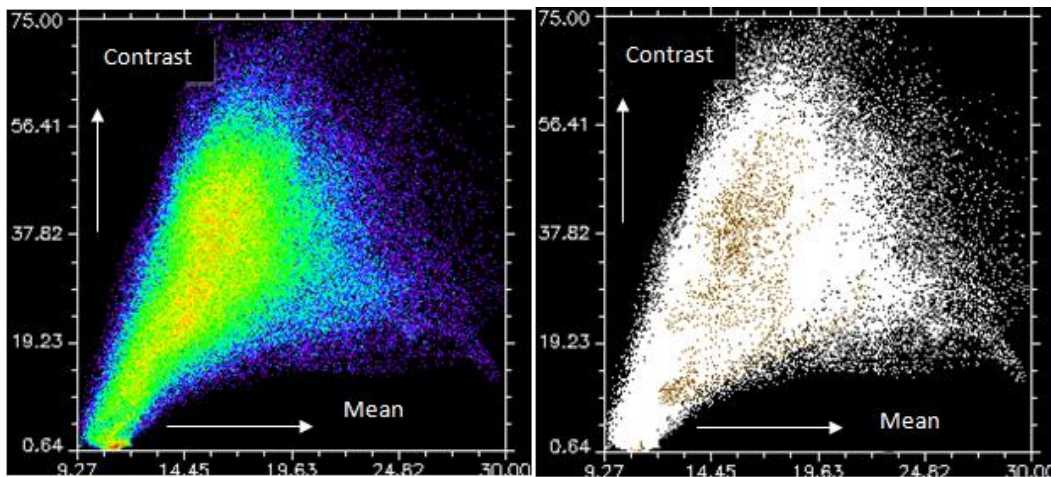


Fig. 28: Left side image: the density slice of the distribution in this feature space for the entire image (note: colours indicate point density in the cloud and not colour coded classes); Right side image: brown indicates where the point cloud of the training sample for shadow 2 is located, while white points belong to other classes.

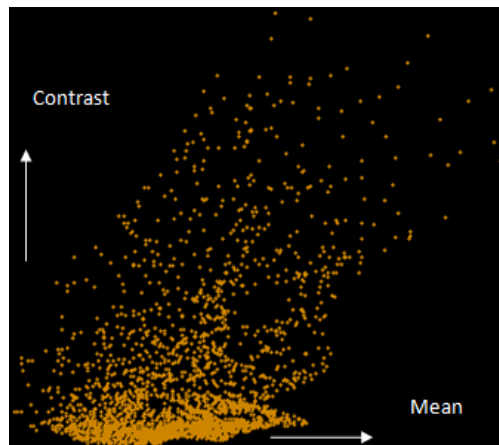


Fig. 29: 2D scatter plot of checking area of shadow 2, Mean vs. Contrast

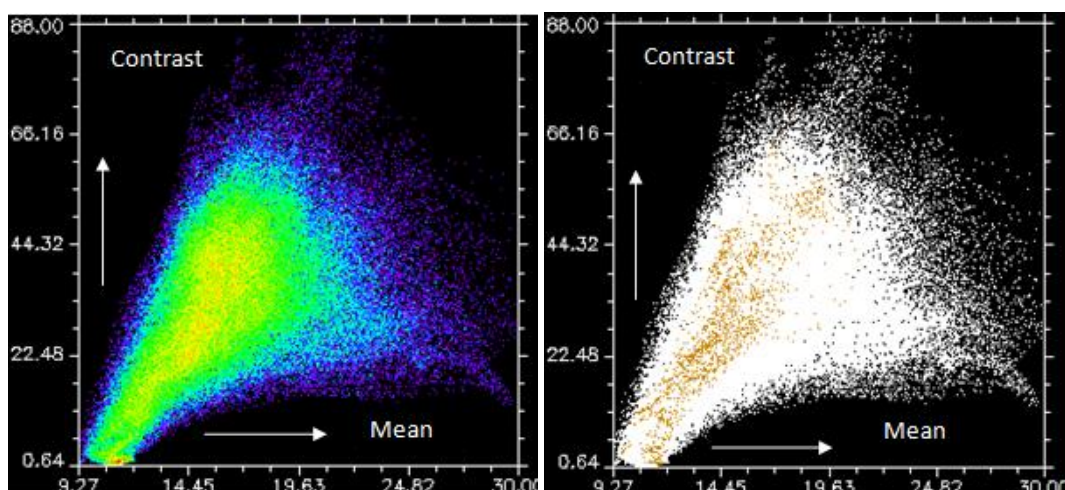


Fig. 30: Left side image: the density slice of the distribution in this feature space for the entire image (note: colours indicate point density in the cloud and not colour coded classes); Right side image: yellow indicates where the point cloud of the sample for shadow 2 is located, while white points belong to other classes.

As for the classification results based on Haralick's textural features, their quality is partly questionable. As already expected, the Maximum Likelihood classifier might not be a good choice for this sort of data, even though there are classes, for which the results are satisfactory. Several reasons may be considered responsible for the suboptimal quality. The shape of the clouds and its deviation from normal distributions is just one part, the other is the fact that already the selection of ground truth areas caused problems in finding homogeneously textured sample fields. The a priori investigation of separability already suspected that less satisfying results may be expected.

On the other hand, the Maximum Likelihood classifier is more suitable for the multispectral case. This algorithm has traditionally been applied to multispectral data in the past and, hence, has become a standard procedure for classifying multispectral data. As mentioned before, it immediately becomes evident that the Maximum Likelihood classification was not exceptionally appropriate in the textural case, but produces very good results for some classes like for the multispectral case.

## 7.4 Visual comparison of the real distribution with the normal distribution

In the following the training areas are abbreviated by IT for the area of interest of training regions and IC for the area of interest for checking regions.

In this subchapter, the real distribution is compared with the normal distribution derived from the real distribution. When classifying, there is usually a model behind that and this model is more or less a functional approximation of the real distribution. In the case of Maximum Likelihood, this model is the normal distribution, in other words, the real cloud is described by only a vector and a matrix. The vector describes the mean values and the matrix the variance-covariance properties of the data cloud spread out over the individual channels.

Images 31a to 31c represent the training areas for the fine texture class and images 32a to 32c are the checking areas for the same fine texture class. In all these figures, it is investigated how the point cloud looks like compared to that what the statistical analysis for a normal distribution would deliver. The colour-coded isolines represent the density of the point cloud and the black ellipses show the isolines for certain probabilities of a normal distribution derived from the point cloud. In other words, it can be seen a sort of compression by a functional approximation where the real point cloud is described by their statistical measures assuming that it is a normal distribution. The difference between the isolines and the ellipses is an indicator of how good a normal distribution would fit. If the isolines and the ellipses were identical, one could say that the normal distribution describes the real distribution in an ideal way. If the normal distribution would fit, also the mean value should lie close to the highest peak of the isolines. If this is not the case, it means, that the mean value is not representative.

In figure 31a one can see, that the mean value is far away from the peak of the distribution and also the direction of the isolines are different from that of the normal distribution. In other words, it means that the cloud does not fulfill the requirements of a normal distribution and therefore, one does not have to expect very good results when applying the Maximum Likelihood classifier. In contrast, figure 31b is a rather good case and one can

clearly see that the maximum density is at the position where the center of the ellipses is located.

The initial gray values in the range between minimum and maximum have been scaled from 0 to 1, hence, each of the texture features (Mean, Contrast and Entropy) has at least one point at 0 and one point at 1. The colour bar represents a measure of the point density, where the violet colour indicates the lowest density and the red one the highest density.

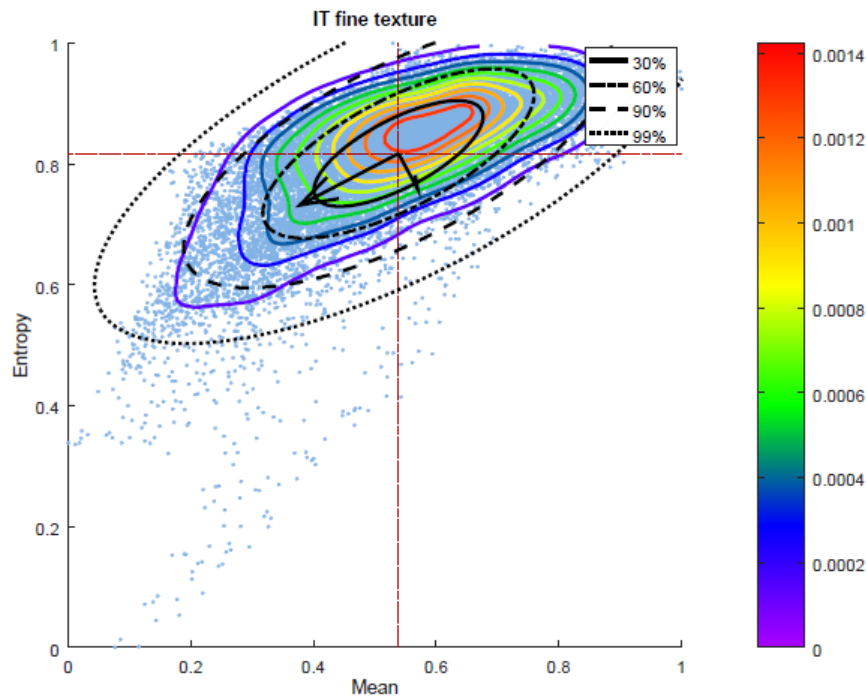


Fig. 31a : The representation of the 2D distribution in the feature space for Mean versus Entropy

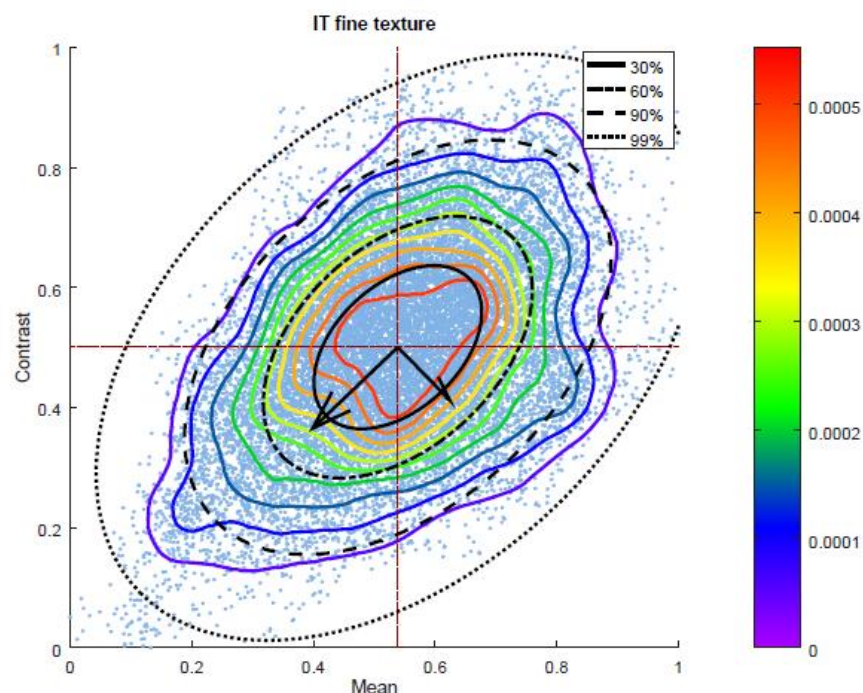


Fig. 31b : The representation of the 2D distribution in the feature for Mean versus Contrast



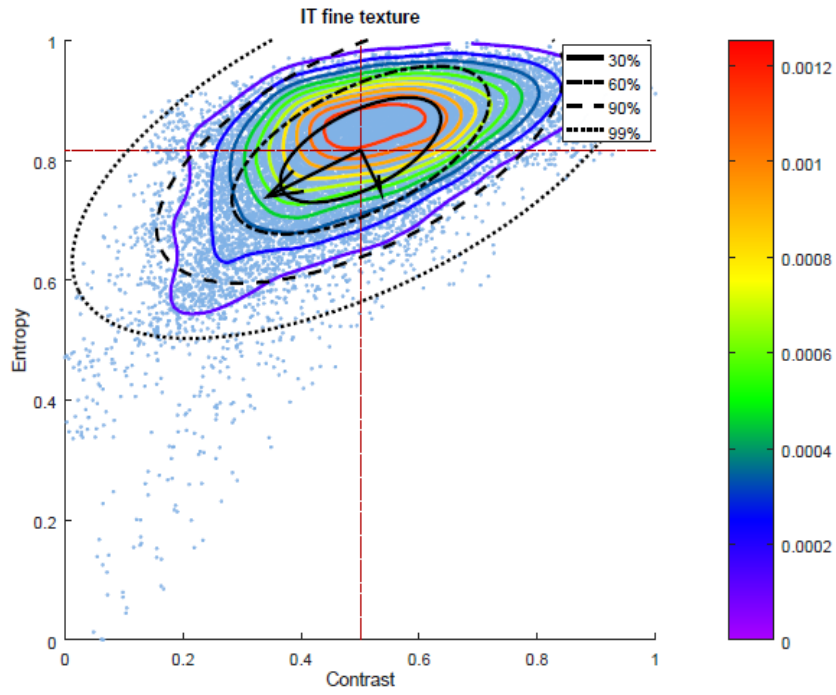


Fig. 31c : The representation of the 2D distribution in the feature space for Contrast versus Entropy

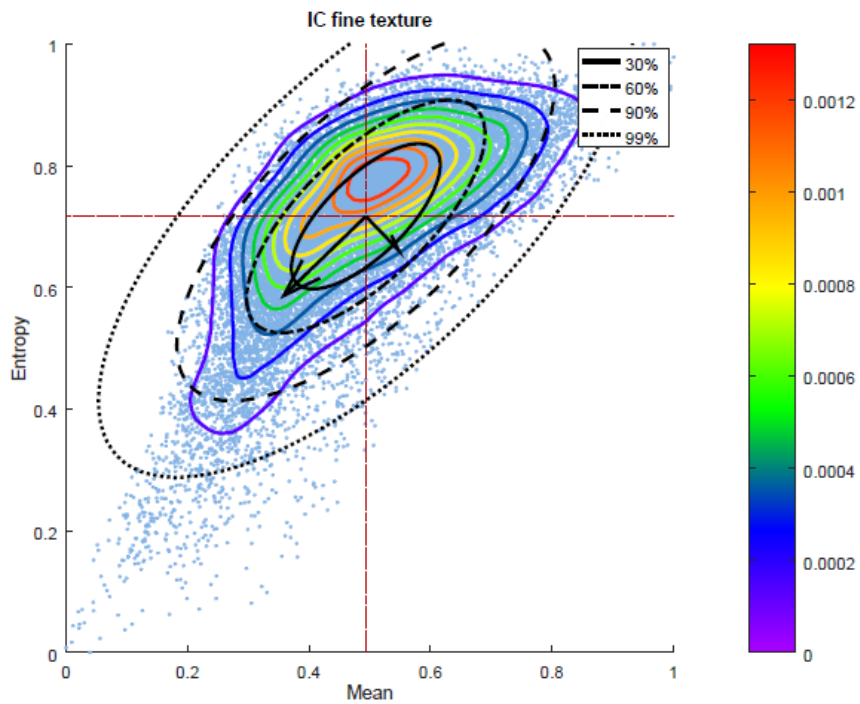


Fig. 32a : The representation of the 2D distribution in the feature space for Mean versus Entropy

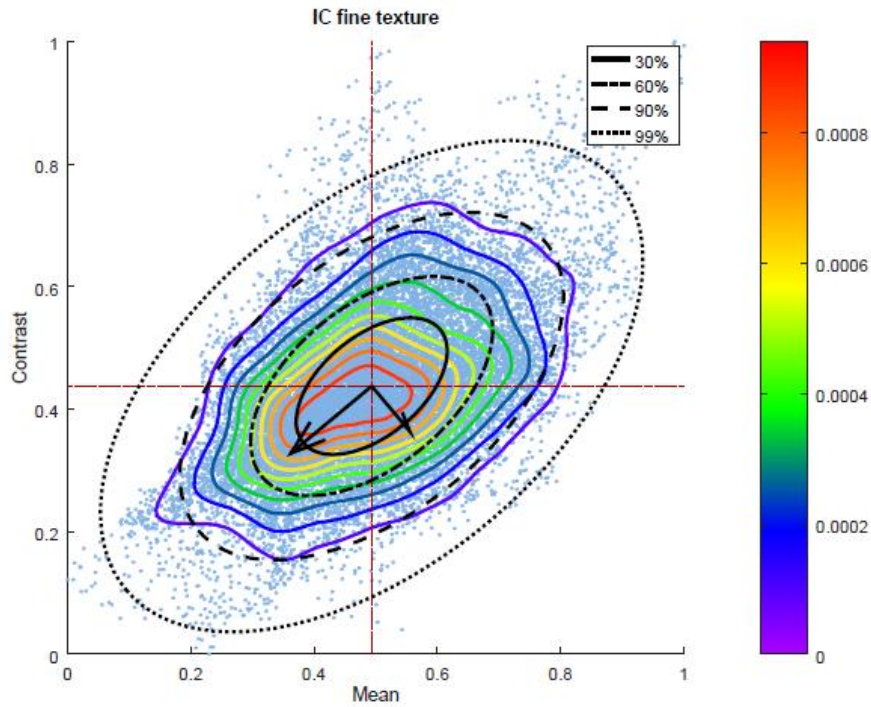


Fig. 32b : The representation of the 2D distribution in the feature space for Mean versus Contrast

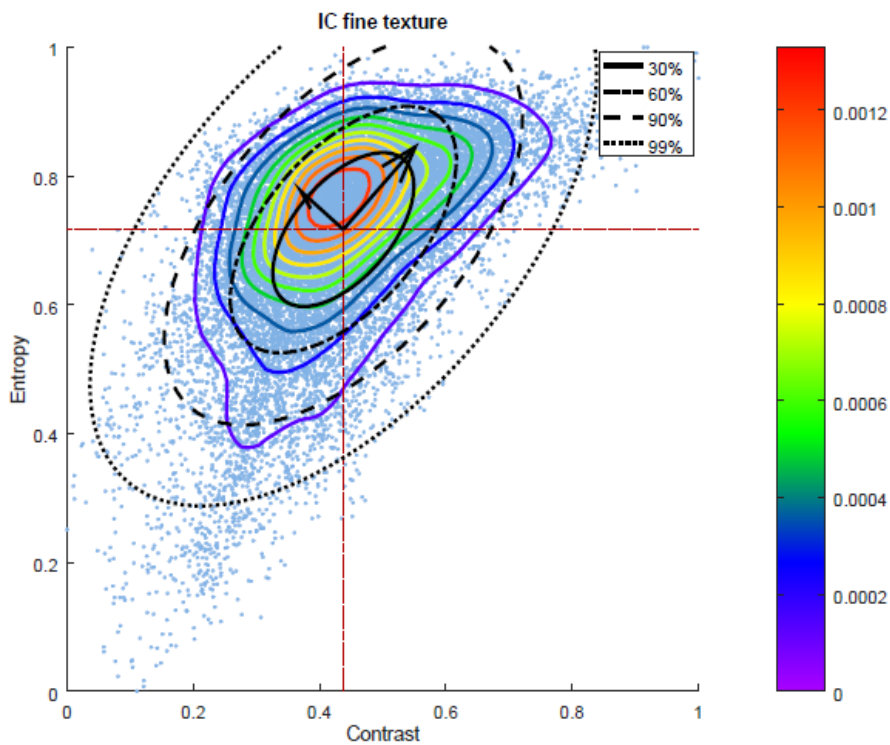
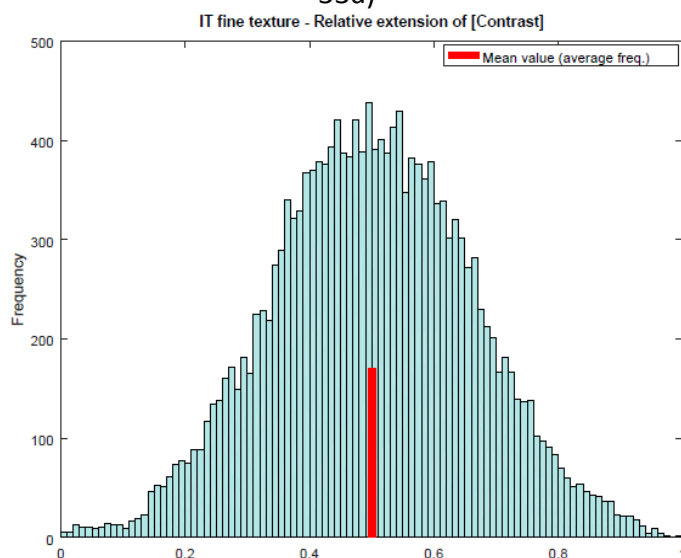
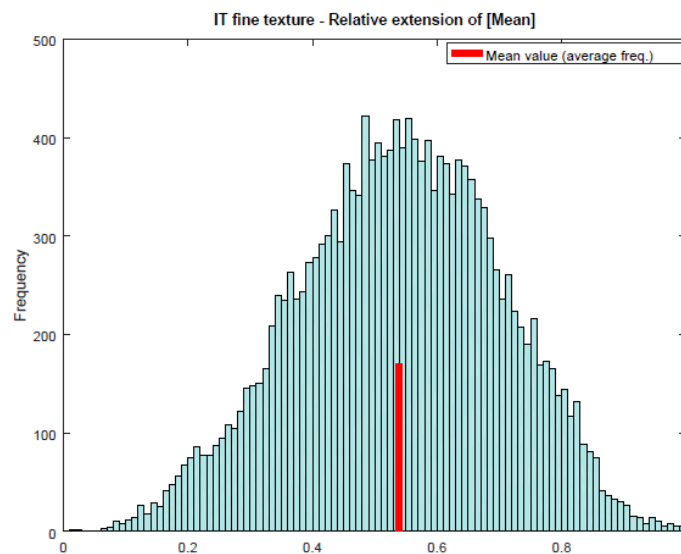


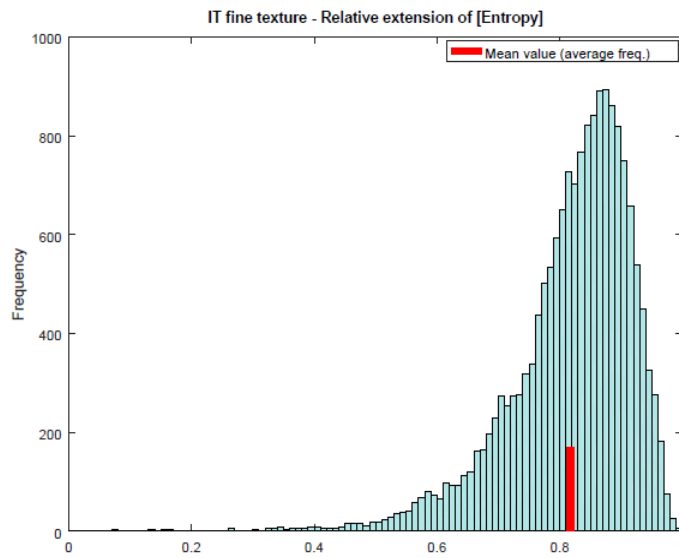
Fig. 32c : The representation of the 2D distribution in the feature space for Contrast versus Entropy

Concluding from the visual inspection of the above figures, the already afore mentioned significantly non-linear behaviour of the Entropy distribution can be confirmed. All scatter plots, where Entropy is involved, show, that the mean of the normal distribution does

conspicuously not match the area of the highest density of the data cloud. Even though the isolines are not matching the shape of the probability ellipses, they are not so far away, that an attempt to apply the Maximum Likelihood classification should immediately be abandoned. One should just be aware, that optimal results must not be expected.

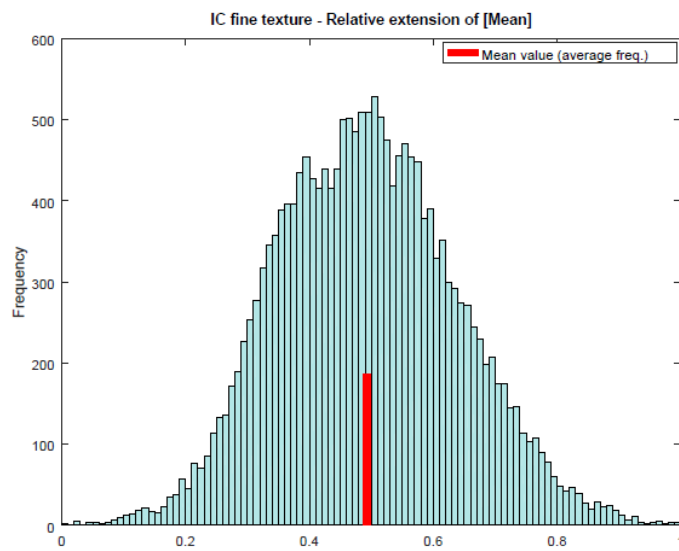
The following figures 33 (a,b,c) and 34 (a,b,c) display individual frequency histograms of Mean, Contrast and Entropy for the ground truth sample IT (training areas) and IC (checking areas). These histograms, represent the projection of the scattergrams onto the axis, and are cross views of the projection onto the axis. The histograms can be seen in one channel, where the length of the red bar represent the average frequency. The position of the bar shows the mean value and the lengths of the bar shows the average frequency.



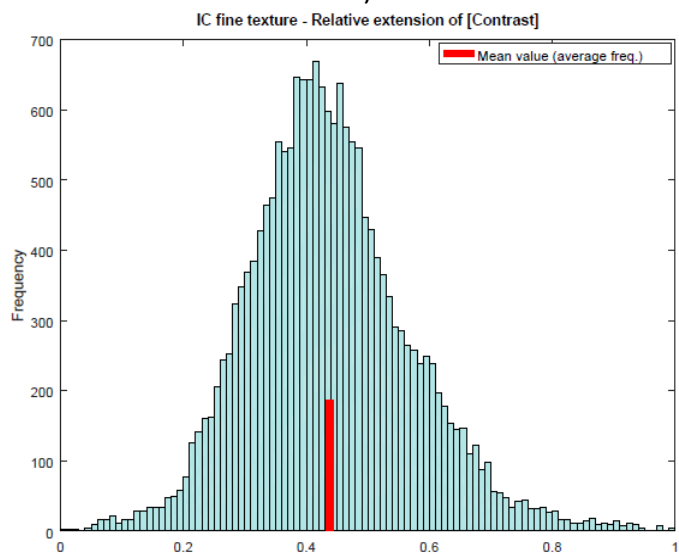


33c)

Figure 33 (a,b,c). Textural case: Frequencies of Mean, Contrast and Entropy for the training samples of class fine texture



34a)



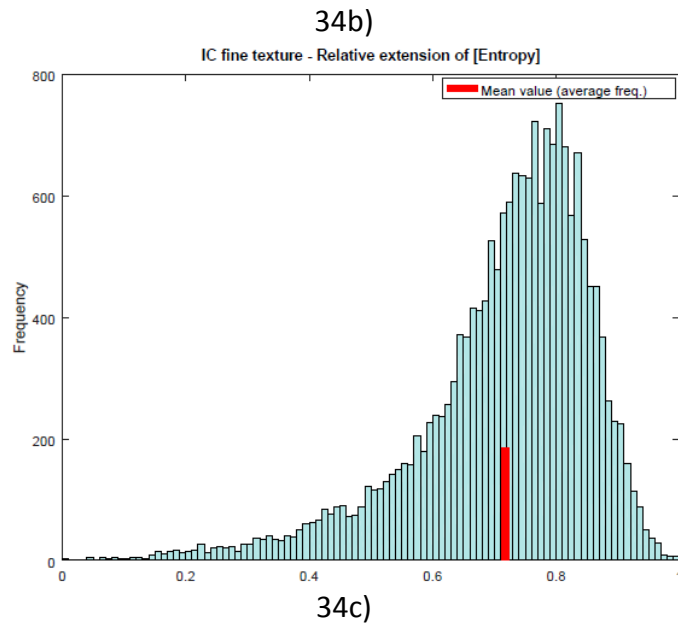


Figure 34 (a,b,c). Textural case: Frequencies of Mean, Contrast and Entropy for the checking samples of class fine texture

In the same way as in above figures, the data range of all channels in the figures 35 and 36 is scaled from 0 to 1 and therefore it represents just a subspace of the original data range. The scattergrams are intended to visually assess the data distributions within a certain class. They may also be used, to a certain degree, to compare the shape of the distributions between the training and checking regions of the same class. Since only one class is represented in one figure the scattergrams do not show, of course, possible cloud overlaps of different classes. These 2D plots of a 3D graphical representation, which are a certain projection from a certain eye point into a certain direction, do not allow an as thorough assessment as an animation would do.

**IT fine texture - Relative extension of [Mean vs Contrast vs Entropy]**

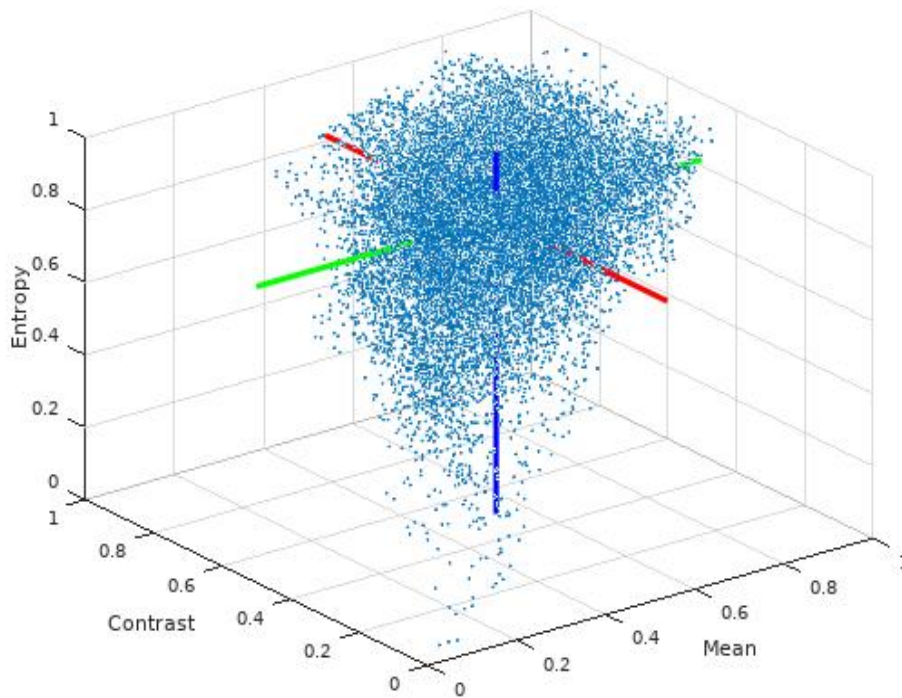


Fig. 35. Textural case: 3D Scattergram representing Mean vs. Contrast vs. Entropy for training samples of class fine texture

**IC fine texture - Relative extension of [Mean vs Contrast vs Entropy]**

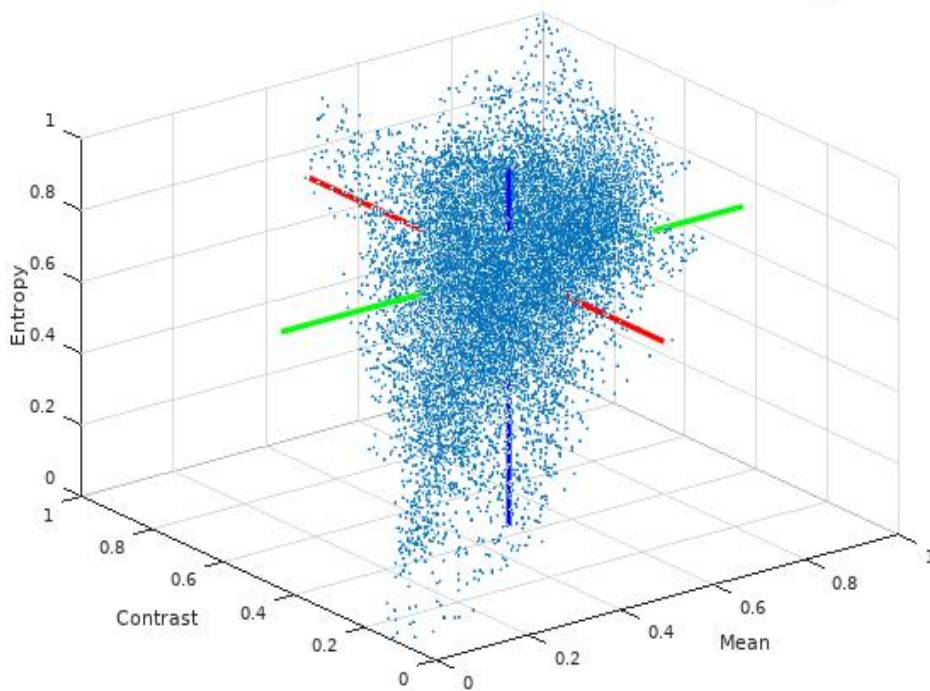


Fig. 36. Textural case: 3D Scattergram representing Mean vs. Contrast vs. Entropy for checking samples of class fine texture

## 7.5 Classification

The central objective of this practical example is to check the quality of the classification result by using checking samples, which are ground truth data other than the training data. Hence, it is obvious, that a careful selection of both the checking and training samples is a crucial prerequisite for a reliable assessment. Training and checking samples of a class must reliably cover the ground truth of the same class and in addition the samples must not overlap and should not lie in immediate neighbourhood. If these aspects are not accurately observed, the eventual quality assessment would be representative for the carelessness of sample selection rather than for the quality of classification. A test for the equivalence of checking and training areas could be carried out by a cross-validation, i.e. by once performing a classification with training samples and a second time with checking samples. In the ideal case both classifications would deliver the same result. A significant difference would indicate that training and the respective checking samples do not represent the same class, and therefore, a re-selection of ground truth data were necessary.

Both areas of interest have been classified, although the N-W area has been treated more thoroughly, while for the S-E area only a multispectral classification has been carried out. The N-W area, in the spectral case, training and checking samples for 6 classes have been chosen. Table 6 contains the name for the classes, in column 3 a colour infrared composite of a sample, and in the two right columns the number of pixels contained in the training and checking samples:

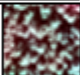




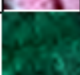
			Training samples	Checking samples
			Pixels	
Class 1	conifers 1		8,858	7,806
Class 2	deciduous old		20,375	38,355
Class 3	conifers 2		27,095	27,550
Class 4	larch		8,316	5,542
Class 5	meadow		783	709
Class 6	shadow		10,634	18,696

Table 6. Spectral case: training and checking samples

Table 7 contains the 7 selected texture classes, where the first picture column shows the green spectral band, on which the derivation of GLCM images has been based. The second picture column is a colour composite of the derived Haralick features Mean (as blue), Contrast (as green) and Entropy (as red).




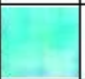










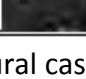
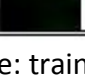
		Real world image	GLCM	Training samples	Checking samples
				Pixels	
Class 1	rough texture			5,492	8,553
Class 2	coarse texture			4,939	4,083
Class 3	fine texture			17,073	18,591
Class 4	foliar texture			7,678	7,638
Class 5	flat texture			618	367
Class 6	shadow 1			6,551	7,424
Class 7	shadow 2			3,139	2,625

Table 7. Textural case: training and checking samples

In the following, the classification has been carried out by applying the Maximum Likelihood rule for both the multispectral data and the textural data. Figures 37 and 38 and table 8 belong to the spectral case, figures 39 and 40 and table 9 to the textural case.

### 7.5.1 N-W area: Spectral case

Figure 37 shows the original image as colour-infrared composite (i.e. composed of Green, Red, Near Infrared) with the training areas superimposed in the colours as defined in the legend below, while figure 38 shows the respective result after a Maximum Likelihood classification which used all available four spectral channels (i.e. Blue, Green, Red, Near Infrared).



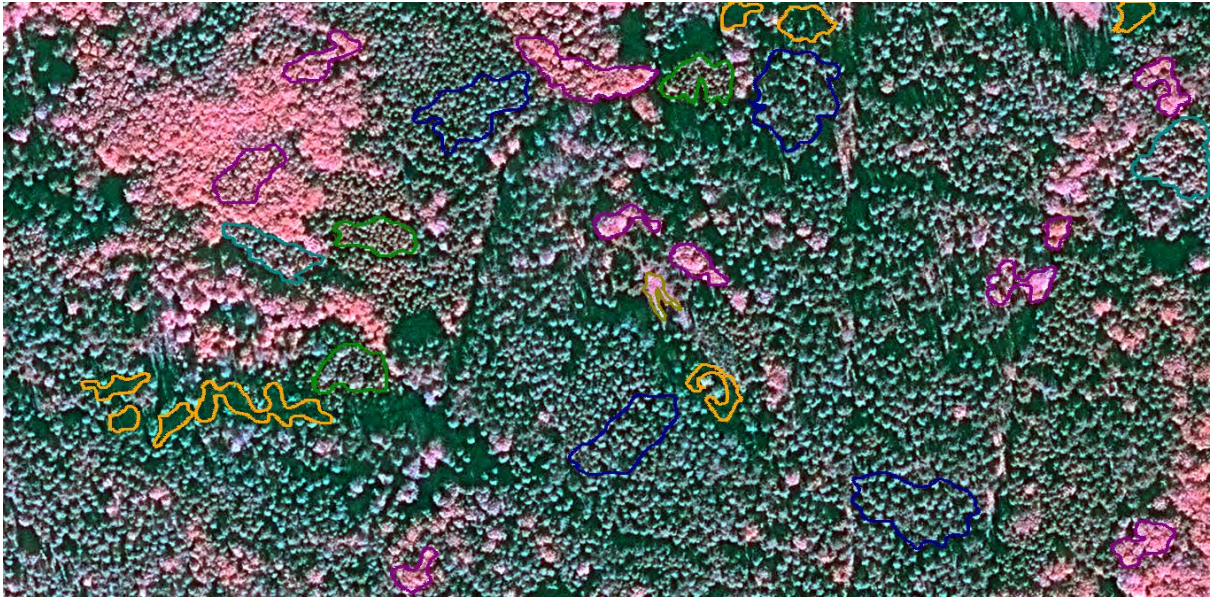


Fig.37: Original image as colour-infrared composite with training areas overlaid (IT)

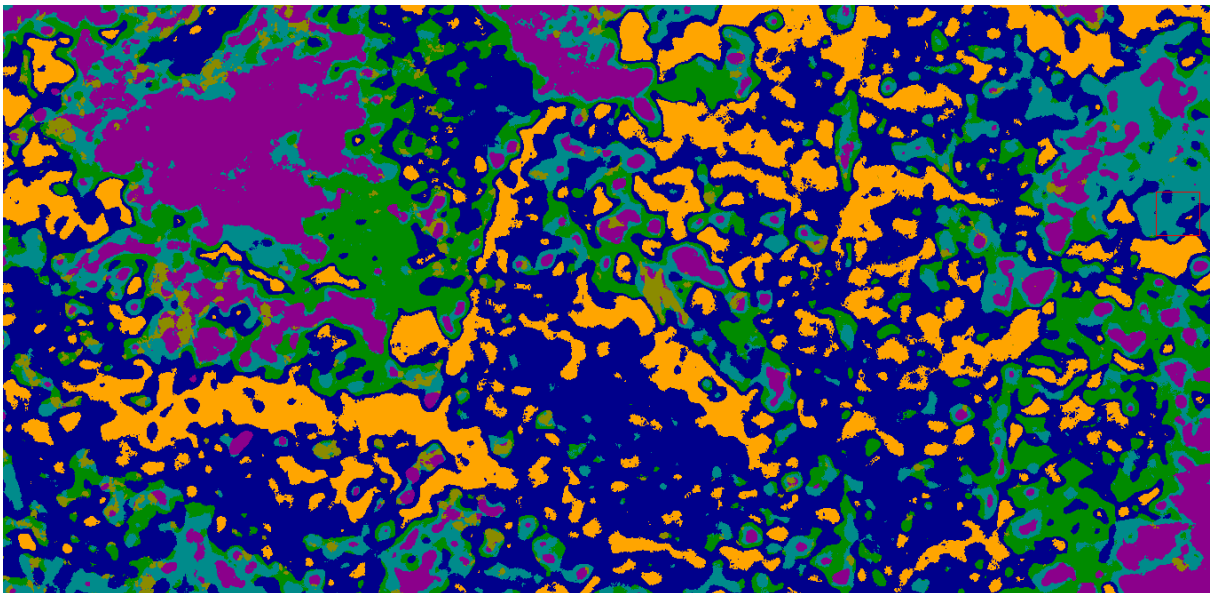


Fig.38: Result after a Maximum Likelihood classification based on the training areas

**Legend**

	<i>conifers 1</i>
	<i>deciduous old</i>
	<i>conifers 2</i>
	<i>larch</i>
	<i>meadow</i>
	<i>shadow</i>

Table 8 displays the means and standard deviations of the training areas and the checking areas.

The mean values show the estimated locations of the cloud centres in feature space. The better the centres are distributed over the entire feature space, the greater the chance for a good class discrimination. And the less the standard deviation, the smaller is the width of the clouds and again the better the chance that clouds do not overlap and, thus, allow a better class discrimination. In order to assess whether training areas and checking areas represent the same class, the statistics of training and checking samples should be compared. In the ideal case, they must be identical. In practice, they will not be identical, but too great differences provide an indicator that the final accuracy assessment may lack of reliability.

Table 8 shows the differences between the means of the training areas and of the checking areas. They are very close compared to the standard deviations of both values, therefore, these two training and checking areas could be assumed to represent the same samples.

		Training samples				Checking samples			
		Blue	Green	Red	NIR	Blue	Green	Red	NIR
conifers 1	<i>Mean</i>	114,4	213,6	293,4	622,3	112,9	211,8	288,9	653,5
	<i>Std.dev.</i>	31,60	56,45	75,68	186,72	31,12	56,77	75,98	203,50
deciduous old	<i>Mean</i>	148,2	252,3	316,3	1021,4	148,6	254,9	318,7	1089,5
	<i>Std.dev.</i>	34,70	54,92	65,06	262,52	31,01	50,66	59,98	253,64
conifers 2	<i>Mean</i>	114,2	208,6	285,9	483,6	114,5	209,1	286,1	479,4
	<i>Std.dev.</i>	33,04	57,25	75,62	155,23	32,79	57,09	75,61	151,91
larch	<i>Mean</i>	129,7	224,8	296,2	694,9	130,8	223,8	297,0	611,6
	<i>Std.dev.</i>	37,11	61,87	79,34	217,45	37,29	60,54	76,97	207,21
meadow	<i>Mean</i>	163,4	288,5	344,9	1038,9	166,8	283,4	339,9	1106,2
	<i>Std.dev.</i>	25,98	43,58	52,60	200,89	19,93	31,60	37,60	159,65
shadow	<i>Mean</i>	88,6	174,8	257,8	246,5	86,5	171,5	253,5	250,2
	<i>Std.dev.</i>	12,97	23,99	33,81	81,03	10,96	19,83	27,58	74,50

Table 8. Spectral case: statistical analysis of training and checking samples

### 7.5.2 N-W area: Textural case

As in the previous case, figure 39 shows the image used for the classification of the textural features. It is the result of the original image processed with the help of GLCM in order to derive the textural parameters Mean, Contrast and Entropy. Also here, the image has been overlaid by the training samples of the classes shown in the legend below figure 40.



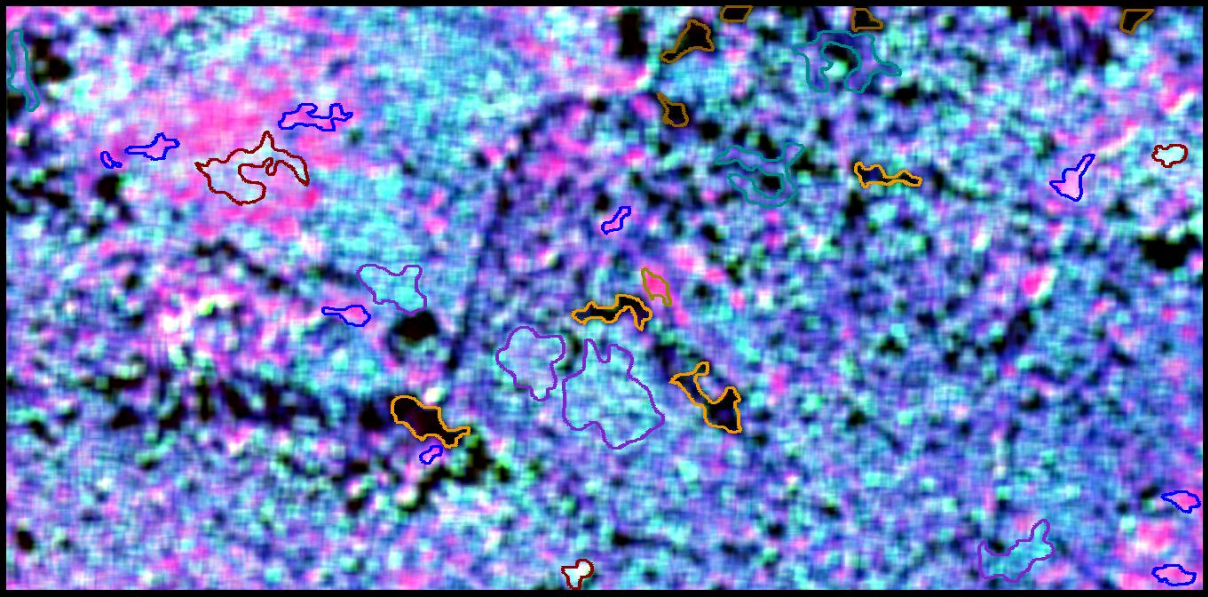


Fig.39: The textural image as colour composite of the channels Mean, Contrast and Entropy, overlaid by the training areas

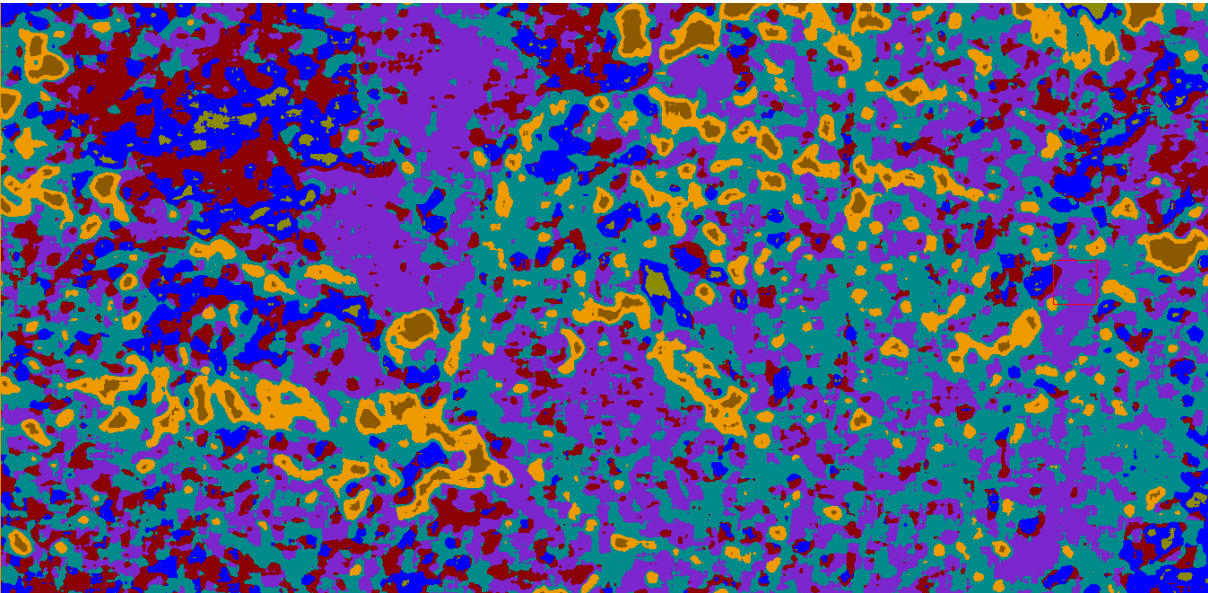


Fig. 40: Result after a Maximum Likelihood classification based on the training areas





Table 9 , as in the previous case, provides an overview of means and standard deviations of the training areas and checking areas.

		Training samples			Checking samples		
		Mean	Contrast	Entropy	Mean	Contrast	Entropy
rough texture	Mean	23,9	30,5	5,1	24,4	29,3	5,0
	Std.dev.	2,35	6,84	0,08	1,99	7,48	0,09
coarse texture	Mean	20,8	50,1	5,2	20,3	59,9	5,2
	Std.dev.	1,61	9,43	0,08	1,84	10,93	0,07
fine texture	Mean	16,6	46,1	5,1	16,7	48,6	5,1
	Std.dev.	1,77	8,86	0,13	1,63	8,93	0,09
foliar texture	Mean	15,4	26,2	4,8	15,2	24,2	4,8
	Std.dev.	2,00	7,93	0,23	1,62	5,64	0,17
flat texture	Mean	26,1	22,5	4,9	25,6	20,8	4,7
	Std.dev.	2,07	4,73	0,13	2,09	9,01	0,20
shadow 1	Mean	11,8	8,9	3,8	11,9	8,9	3,8
	Std.dev.	1,12	6,73	0,38	1,02	5,73	0,51
shadow 2	Mean	11,1	5,9	3,2	10,9	3,5	2,9
	Std.dev.	0,79	5,03	0,45	0,52	3,78	0,46

Table 9. Textural case: statistical analysis of training and checking samples

### 7.5.3 N-W area: Combination of spectral and textural properties

In the sections above, the classification has separately been carried out with a focus on spectral properties and on textural properties. Therefore, also the ground truth samples have been selected accordingly. Since spectral and textural properties together are characteristics of a certain class, for this reason it seems to be advisable to define a class by observing both properties at once and select ground truth samples, which are unique with respect to the combination of spectral and textural properties. Figure 41 shows the image with superimposed ground truth samples which have been selected according to the afore mentioned strategy.

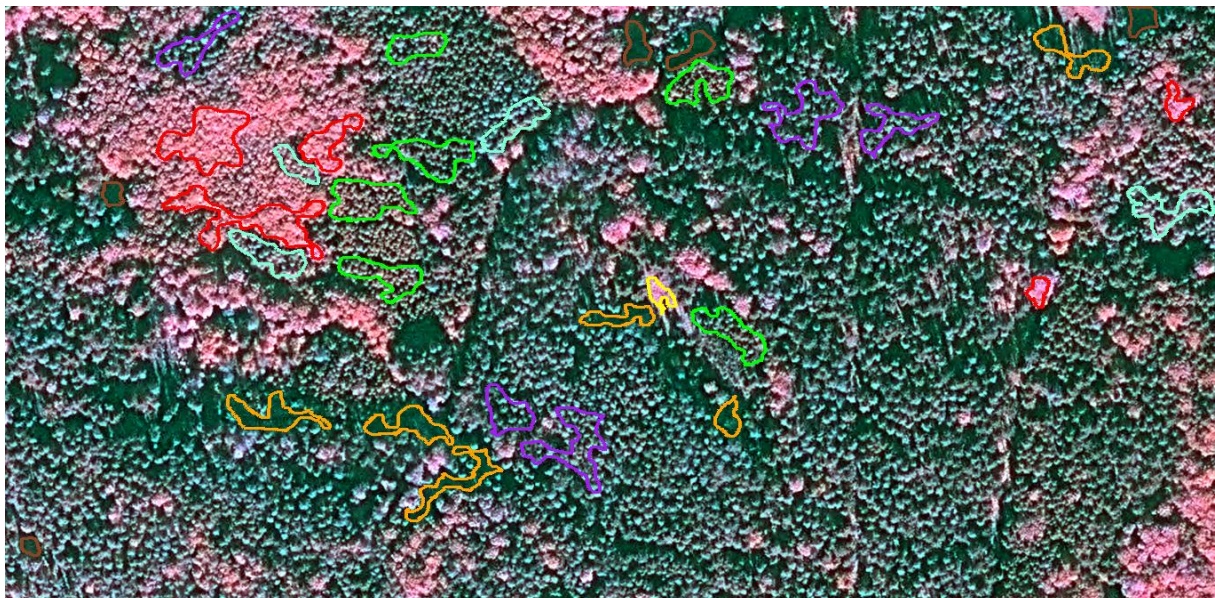


Fig. 41 : Image with ground truth samples according to spectral-textural properties

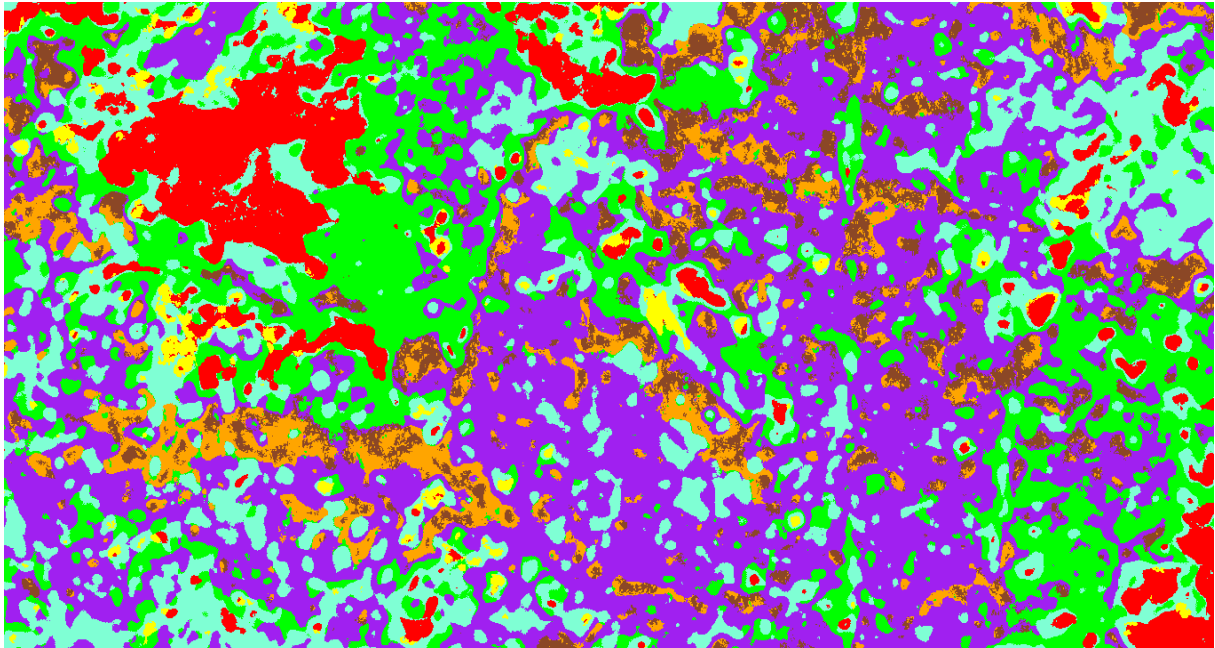


Fig. 42: Result of the Maximum Likelihood classification of the spectral-textural case



#### 7.5.4 S-E area: Spectral case

As already mentioned in section 1 the current research with the focus on the classification of high-resolution imagery has been split up into two parts: first, the classification based on spectral properties, second, the classification based on textural properties. The latter investigation was the more important, since texture plays a significant role for the interpretation of modern remote sensing images with their high geometric resolution.

At the beginning two areas of interest have been chosen, where the first one, the N-W area turned out to be more appropriate as far as forest classification is concerned. Still, also the second area of interest, the S-E area, should be processed eventually. Since there are not so great differences in texture, it has been decided to classify this area just based on spectral properties. Figure 43 shows a colour-infrared composite of that area with the ground truth areas superimposed.



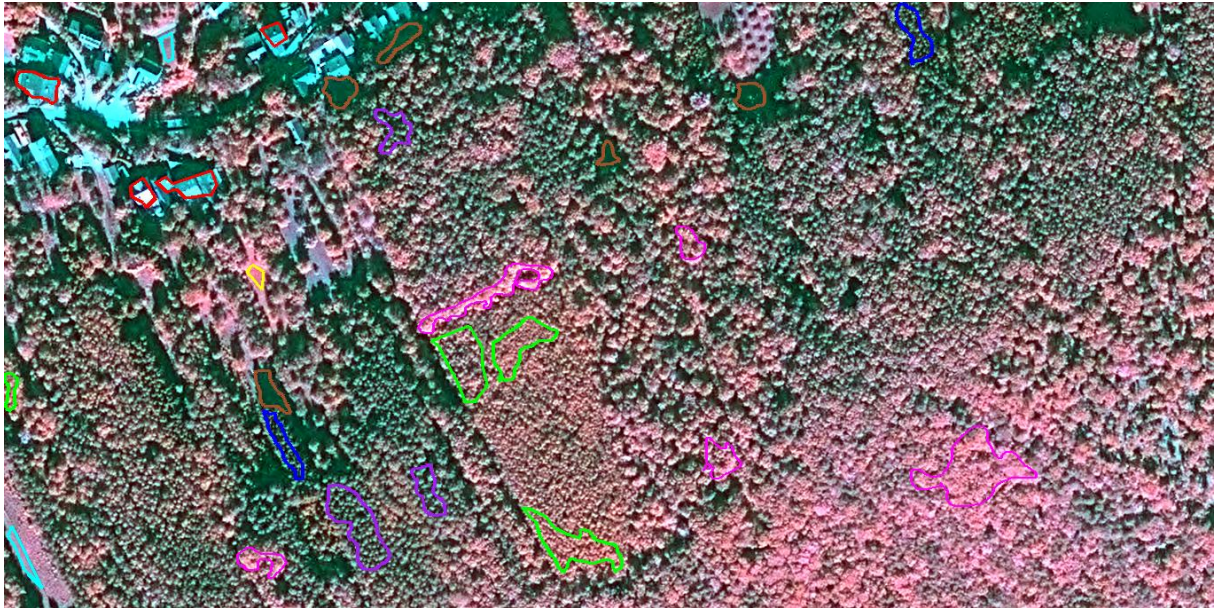


Fig.43: Colour-infrared composite of the S-E area with superimposed ground truth samples

Not only forest stands have been selected as ground truth but also built-up areas, meadows, and shadows. The latter ones, as already mentioned, are not in the main focus of this study, they are included for better class separability. Altogether 8 classes have been selected for each of the training areas as well as control areas. Before applying the classification algorithm one has to make sure that the classes are sufficiently separable, therefore, the decision has been made to apply the Jeffries-Matusita Distance as separability measure.

After the successful separability check (see section 7.2), the standard Maximum Likelihood classification method has been applied. Figure 44 shows the result.

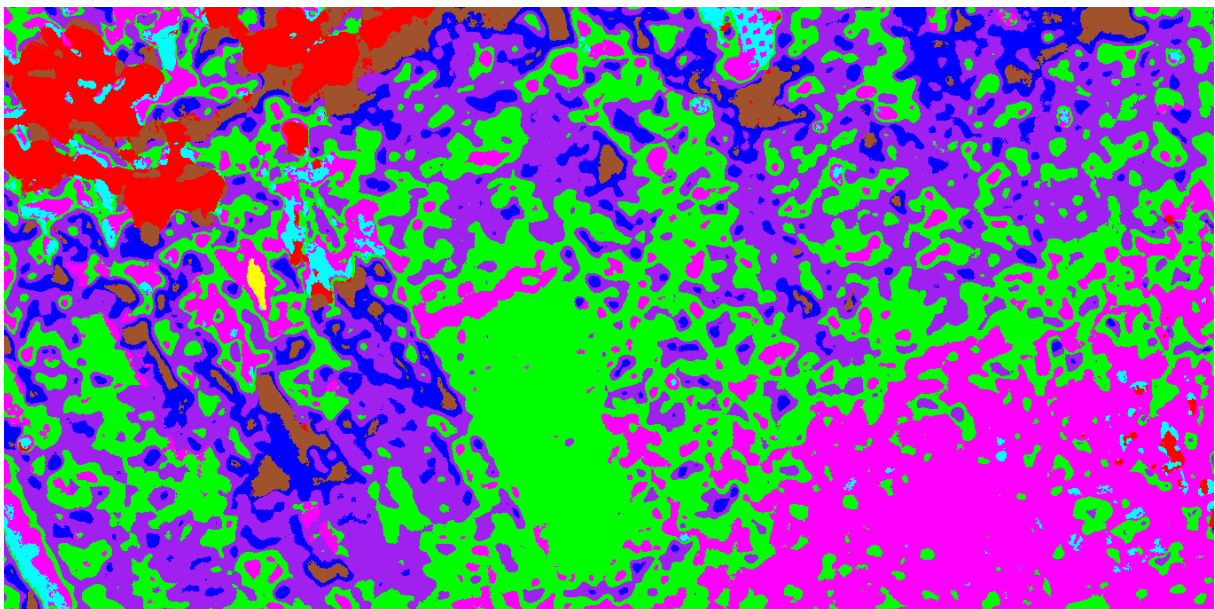


Figure 44 : Result of the Maximum Likelihood classification of the spectral image



## 7.6 Results of the quality assessment

Since training areas as well as checking areas represent ground truth, the classification could be carried out in two theoretically equivalent ways, i.e. by using the training areas for training and the checking areas for checking (that is the standard approach) or the checking areas for training and the training areas for checking (a cross-validation approach). In the ideal case both results should be identical. In the following a few abbreviations should be introduced for better readability. The result of a classification will be written as C(...). A classification based on training areas (IT), therefore, will be written as C(IT), a classification based on checking areas (IC) as C(IC). For the assessment with the help of a comparison within a confusion matrix the comparison operator  $\leftrightarrow$  will be introduced, in practice C(IT) $\leftrightarrow$ IC or C(IC) $\leftrightarrow$ IT denote classifications based on training areas, which are compared to checking data, and a classification based on checking areas, which are compared to training data, respectively. The comparison of two classifications - C(IT) based on training areas and C(IC) based on checking areas - is denoted as C(IT) $\leftrightarrow$ C(IC).

### 7.6.1 N-W area: Spectral case

In the first case, the original multispectral image with the Blue, Green, Red and Near-Infrared channels is taken into consideration. Table 10 shows the assessment of C(IT) $\leftrightarrow$ IC. The quality assessment with the help of confusion matrices compares the classified results with the ground truth results. The diagonals are filled with the correctly classified pixels and hopefully contain the highest values. In the following examples, (tables 10 to 18) the absolute values are not suited for providing information about the accuracy, but they show, how many pixels have been involved.

The ENVI Software, which has been used for classification, also provides a detailed overview of the achieved accuracy. The following tables show the ENVI listings, and therefore, it seems to be appropriate to provide a short description of the listings. They consist of five major parts:

- The first part consists of just two lines. The top line shows the Overall Accuracy as ratio correctly classified pixels to all assessed pixels, and the second line the Kappa coefficient.
- The second part shows the confusion matrix with the ground truth classes as columns and the classified classes as rows. The very last row contains the sum of the columns, the very last column the sum of the rows. The diagonal elements represent the correctly classified pixels. The number at the bottom right corner of the list is the number of all pixels involved in the assessment.

- The third part shows the confusion matrix in the same order as in the above one, but the columns show the class distribution after classification (expressed in percent) for the ground truth classes. Note, that in this case the diagonal elements are equivalent to the Producer's Accuracy. The very last column shows the class distribution after classification (expressed in percent).
- The fourth and the fifth part of the listing are mathematically related. The fourth part lists on the left the Error of Commission and Omission in percent and on the right as ratio of incorrectly classified pixels to all pixels of a classified class.
- The fifth part lists on the left the Producer's Accuracy and the User's Accuracy in percent and on the right as ratio of correctly classified pixels to all pixels of a classified class. The Producer's Accuracy is the complement of the Error of Omission, i.e. their sum is 100, and the User's Accuracy is the complement of Error of Commission, again their sum is 100, as one can easily see in the tables.

Table 10, 11, and 12 may be interpreted by keeping in mind that they are the assessment of three classifications, which more or less should, in the ideal case, deliver the same quality figures. Table 10 is based on  $C(IT) \leftrightarrow IC$ , table 11 on  $C(IC) \leftrightarrow IT$ , and eventually table 12 on  $C(IT) \leftrightarrow C(IC)$ . Just a remark need to be added here, since the latter comparison is not a genuine quality assessment, it is more a comparison of two classification results, which are expected to be highly identical. If one assumes that IT and IC both are highly representative for the classes, all three classification results would be more or less identical. The more the results differ, the less comparable were IT and IC, or in other words, the assessment of  $C(IT)$  by using IC may not be fully justified. Therefore, first, the quality figures of these three classifications must be compared:

- $C(IT) \leftrightarrow IC$ : Overall Accuracy 86.4%; Kappa 0.81
- $C(IC) \leftrightarrow IT$ : Overall Accuracy 77.4%; Kappa 0.71
- $C(IT) \leftrightarrow C(IC)$ : Overall Accuracy 83.4%; Kappa 0.78

Conclusion: There is a significant difference of 10% between the first two classifications, which indicates that training areas and checking areas do not ideally represent the same class, although an Overall Accuracy of some 80% is quite good and lie within the expectations of a multispectral classification. The quality of the third classification is somewhere, not unexpectedly, between the first two. If one looks a bit closer into the data, a significant greater number of checking pixels IC (greater by some 30%, i.e. 98658 compared to 76061) than training pixels IT exist. Thus, the first classification was less supported by training, but more thoroughly checked, while the second classification was better supported by training, but less checked, although this fact does not explain the difference of accuracies. If one looks at the individual classes, the major differences of pixels numbers are the classes "deciduous", "larch" and "shadow". By comparing the Producer's and User's Accuracies, the difference between classes within one classification are already very significant. The problem class is not really surprising "meadow", followed by "larch". For "meadow" only a bit more than 700 pixels have been selected and by the two classification a great part of the pixels has been assigned to the class "deciduous" (75% and 47%, respectively). Spectrally there was not a great difference between these classes with a dominating NIR channel. One could expect that the assignments for the class "deciduous" would be similarly bad. This is not the case and, therefore, the conclusion must be drawn that the ground truth areas for "meadow" were not representative enough. As for the class



“larch”, the classification decided once partly for “conifers 1” and in the second case for “conifers 2”. Finally, one can conclude, that the difference in the basic accuracy figures between these two classifications are mainly caused by the not well defined class “meadow” and to a lesser extent by the class “larch”.

Overall Accuracy = (85223/98658) 86.3822%  
 Kappa Coefficient = 0.8140

Class	Ground Truth (Pixels)				
	IC conifers 1	IC deciduous	IC conifers 2	IC meadow	IC shadow
Unclassified	0	0	0	0	0
IT conifers 1	6141	356	1248	0	138
IT deciduous	447	35136	0	532	21
IT conifers 2	614	4	23667	4	1351
IT meadow [Ye	195	884	38	158	0
IT shadow [Or	16	0	1837	0	17172
IT larch [Cya	393	1975	760	15	14
Total	7806	38355	27550	709	18696

Class	Ground Truth (Pixels)	
	IC larch	Total
Unclassified	0	0
IT conifers 1	449	8332
IT deciduous	98	36234
IT conifers 2	2022	27662
IT meadow [Ye	4	1279
IT shadow [Or	20	19045
IT larch [Cya	2949	6106
Total	5542	98658

Class	Ground Truth (Percent)				
	IC conifers 1	IC deciduous	IC conifers 2	IC meadow	IC shadow
Unclassified	0.00	0.00	0.00	0.00	0.00
IT conifers 1	78.67	0.93	4.53	0.00	0.74
IT deciduous	5.73	91.61	0.00	75.04	0.11
IT conifers 2	7.87	0.01	85.91	0.56	7.23
IT meadow [Ye	2.50	2.30	0.14	22.28	0.00
IT shadow [Or	0.20	0.00	6.67	0.00	91.85
IT larch [Cya	5.03	5.15	2.76	2.12	0.07
Total	100.00	100.00	100.00	100.00	100.00

Class	Ground Truth (Percent)	
	IC larch	Total
Unclassified	0.00	0.00
IT conifers 1	8.10	8.45
IT deciduous	1.77	36.73
IT conifers 2	36.49	28.04
IT meadow [Ye	0.07	1.30
IT shadow [Or	0.36	19.30
IT larch [Cya	53.21	6.19
Total	100.00	100.00

Class	Commission		Omission	
	(Percent)	(Percent)	(Pixels)	(Pixels)
IT conifers 1	26.30	21.33	2191/8332	1665/7806
IT deciduous	3.03	8.39	1098/36234	3219/38355
IT conifers 2	14.44	14.09	3995/27662	3883/27550
IT meadow [Ye	87.65	77.72	1121/1279	551/709
IT shadow [Or	9.83	8.15	1873/19045	1524/18696
IT larch [Cya	51.70	46.79	3157/6106	2593/5542
Class	Prod. Acc.		User Acc.	
	(Percent)	(Percent)	(Pixels)	(Pixels)
IT conifers 1	78.67	73.70	6141/7806	6141/8332
IT deciduous	91.61	96.97	35136/38355	35136/36234
IT conifers 2	85.91	85.56	23667/27550	23667/27662
IT meadow [Ye	22.28	12.35	158/709	158/1279
IT shadow [Or	91.85	90.17	17172/18696	17172/19045
IT larch [Cya	53.21	48.30	2949/5542	2949/6106

Table 10: Accuracy assessment C(IT) ↔ IC

Overall Accuracy = (58838/76061) 77.3563%  
 Kappa Coefficient = 0.7101

Class	Ground Truth (Pixels)				
	IT conifers 1	IT deciduous	IT conifers 2	IT meadow	IT shadow
Unclassified	0	0	0	0	0
IC conifers 1	6845	1430	1079	97	60
IC deciduous	0	15370	0	371	0
IC conifers 2	1115	48	20727	0	589
IC meadow [Ye	14	2632	0	315	0
IC shadow [Or	4	0	2506	0	9935
IC larch [Cya	880	895	2783	0	50
Total	8858	20375	27095	783	10634

Class	Ground Truth (Pixels)	
	IT larch	Total
Unclassified	0	0
IC conifers 1	1797	11308
IC deciduous	423	16164
IC conifers 2	295	22774
IC meadow [Ye	155	3116
IC shadow [Or	0	12445
IC larch [Cya	5646	10254
Total	8316	76061

Class	Ground Truth (Percent)				
	IT conifers 1	IT deciduous	IT conifers 2	IT meadow	IT shadow
Unclassified	0.00	0.00	0.00	0.00	0.00
IC conifers 1	77.27	7.02	3.98	12.39	0.56
IC deciduous	0.00	75.44	0.00	47.38	0.00
IC conifers 2	12.59	0.24	76.50	0.00	5.54
IC meadow [Ye	0.16	12.92	0.00	40.23	0.00
IC shadow [Or	0.05	0.00	9.25	0.00	93.43
IC larch [Cya	9.93	4.39	10.27	0.00	0.47
Total	100.00	100.00	100.00	100.00	100.00

Class	Ground Truth (Percent)	
	IT larch	Total
Unclassified	0.00	0.00
IC conifers 1	21.61	14.87
IC deciduous	5.09	21.25
IC conifers 2	3.55	29.94
IC meadow [Ye	1.86	4.10
IC shadow [Or	0.00	16.36
IC larch [Cya	67.89	13.48
Total	100.00	100.00

Class	Commission (Percent)	Omission (Percent)	Commission (Pixels)	Omission (Pixels)
	IC conifers 1	39.47	22.73	4463/11308
IC deciduous	4.91	24.56	794/16164	5005/20375
IC conifers 2	8.99	23.50	2047/22774	6368/27095
IC meadow [Ye	89.89	59.77	2801/3116	468/783
IC shadow [Or	20.17	6.57	2510/12445	699/10634
IC larch [Cya	44.94	32.11	4608/10254	2670/8316

Class	Prod. Acc. (Percent)	User Acc. (Percent)	Prod. Acc. (Pixels)	User Acc. (Pixels)
IC conifers 1	77.27	60.53	6845/8858	6845/11308
IC deciduous	75.44	95.09	15370/20375	15370/16164
IC conifers 2	76.50	91.01	20727/27095	20727/22774
IC meadow [Ye	40.23	10.11	315/783	315/3116
IC shadow [Or	93.43	79.83	9935/10634	9935/12445
IC larch [Cya	67.89	55.06	5646/8316	5646/10254

Table 11: Accuracy assessment C(IC)↔IT

An even better measure for estimating the ground truth quality can be found by comparing the two classification results, the first based on training areas, i.e. C(IT), and the second based on checking areas, i.e. C(IC). Table 12 shows the assessment C(IT)↔C(IC).

The following table represents the comparison of two images, therefore much more pixels are involved, but again one can see that class “meadow” could not be well discriminated. A great part has to be shared with class “deciduous”. And again the class “larch” is not well discriminated, too, and partly classified as “conifers 1” and “conifers 2”. This result is not unexpected, since this classification to a certain extent is based on both previous classifications.

Overall Accuracy = (766383/915936) 83.6721%  
 Kappa Coefficient = 0.7842

Class	Ground Truth (Pixels)					
	IC conifers 1	IC deciduous	IC conifers 2	IC meadow [Ye	IC shadow [Or	
IT conifers 1	112415	0	6332	0	0	
IT deciduous	5247	87680	0	14282	0	
IT conifers 2	2395	8	333806	0	15411	
IT meadow [Ye	4441	2025	642	11303	6	
IT shadow [Or	0	0	4047	0	143845	
IT larch [Cya	32295	11136	480	1368	0	
Total	156793	100849	345307	26953	159262	

Class	Ground Truth (Pixels)	
	IC larch [Cya	Total
IT conifers 1	8922	127669
IT deciduous	2898	110107
IT conifers 2	34709	386329
IT meadow [Ye	2434	20851
IT shadow [Or	475	148367
IT larch [Cya	77334	122613
Total	126772	915936

Class	Ground Truth (Percent)					
	IC conifers 1	IC deciduous	IC conifers 2	IC meadow [Ye	IC shadow [Or	
IT conifers 1	71.70	0.00	1.83	0.00	0.00	
IT deciduous	3.35	86.94	0.00	52.99	0.00	
IT conifers 2	1.53	0.01	96.67	0.00	9.68	
IT meadow [Ye	2.83	2.01	0.19	41.94	0.00	
IT shadow [Or	0.00	0.00	1.17	0.00	90.32	
IT larch [Cya	20.60	11.04	0.14	5.08	0.00	
Total	100.00	100.00	100.00	100.00	100.00	

Class	Ground Truth (Percent)	
	IC larch [Cya	Total
IT conifers 1	7.04	13.94
IT deciduous	2.29	12.02
IT conifers 2	27.38	42.18
IT meadow [Ye	1.92	2.28
IT shadow [Or	0.37	16.20
IT larch [Cya	61.00	13.39
Total	100.00	100.00

Class	Commission		Omission	
	(Percent)	(Percent)	(Pixels)	(Pixels)
IT conifers 1	11.95	28.30	15254/127669	44378/156793
IT deciduous	20.37	13.06	22427/110107	13169/100849
IT conifers 2	13.60	3.33	52523/386329	11501/345307
IT meadow [Ye	45.79	58.06	9548/20851	15650/26953
IT shadow [Or	3.05	9.68	4522/148367	15417/159262
IT larch [Cya	36.93	39.00	45279/122613	49438/126772

Class	Prod. Acc.		User Acc.	
	(Percent)	(Percent)	(Pixels)	(Pixels)
IT conifers 1	71.70	88.05	112415/156793	112415/127669
IT deciduous	86.94	79.63	87680/100849	87680/110107
IT conifers 2	96.67	86.40	333806/345307	333806/386329
IT meadow [Ye	41.94	54.21	11303/26953	11303/20851
IT shadow [Or	90.32	96.95	143845/159262	143845/148367
IT larch [Cya	61.00	63.07	77334/126772	77334/122613

Table 12: Accuracy assessment C(IT) ↔ C(IC)

## 7.6.2 N-W area: Textural case

Table 13, 14, and 15 may be interpreted in the same way as previous tables, by taking into consideration the textural classification. Table 13 is based on C(IT) ↔ IC, table 14 on C(IC) ↔ IT, and table 15 on C(IT) ↔ C(IC). The quality figures of these three classifications are as follows:

- C(IT) ↔ IC: Overall Accuracy 80.9%; Kappa 0.76
- C(IC) ↔ IT: Overall Accuracy 76.3%; Kappa 0.70
- C(IT) ↔ C(IC): Overall Accuracy 88.3%; Kappa 0.85

Conclusion: It can clearly be seen that the accuracies of these three classifications are quite high and lie within the expectations of a textural classification, although a significant improvement compared to pure multispectral classification cannot be observed. By comparing the Producer's and User's Accuracies, as in the multispectral case, the difference between classes within one classification is significant. For "flat" only 367 pixels have been selected and a significant part of the pixels has been assigned to the class "rough". Therefore, one can conclude, that "flat" is marginally represented, being too small and it cannot be determined very reliably, while all other classes are well represented.

Overall Accuracy = (39881/49281) 80.9257%  
 Kappa Coefficient = 0.7589

Ground Truth (Pixels)						
Class	IC rough text	IC coarse tex	IC fine textu	IC foliar tex	IC flat textu	
Unclassified	0	0	0	0	0	0
IT rough text	5854	9	0	171	80	
IT coarse tex	387	3306	1958	33	11	
IT fine textu	1	757	15849	294	0	
IT foliar tex	41	11	784	6999	0	
IT flat textu	2270	0	0	0	276	
IT shadow 1 [	0	0	0	141	0	
IT shadow 2 [	0	0	0	0	0	
Total	8553	4083	18591	7638	367	

Ground Truth (Pixels)			
Class	IC shadow 1	IC shadow 2	Total
Unclassified	0	0	0
IT rough text	5	0	6119
IT coarse tex	0	0	5695
IT fine textu	3	0	16904
IT foliar tex	599	0	8434
IT flat textu	0	0	2546
IT shadow 1 [	5255	283	5679
IT shadow 2 [	1562	2342	3904
Total	7424	2625	49281

Ground Truth (Percent)						
Class	IC rough text	IC coarse tex	IC fine textu	IC foliar tex	IC flat textu	
Unclassified	0.00	0.00	0.00	0.00	0.00	0.00
IT rough text	68.44	0.22	0.00	2.24	21.80	
IT coarse tex	4.52	80.97	10.53	0.43	3.00	
IT fine textu	0.01	18.54	85.25	3.85	0.00	
IT foliar tex	0.48	0.27	4.22	91.63	0.00	
IT flat textu	26.54	0.00	0.00	0.00	75.20	
IT shadow 1 [	0.00	0.00	0.00	1.85	0.00	
IT shadow 2 [	0.00	0.00	0.00	0.00	0.00	
Total	100.00	100.00	100.00	100.00	100.00	

Ground Truth (Percent)			
Class	IC shadow 1	IC shadow 2	Total
Unclassified	0.00	0.00	0.00
IT rough text	0.07	0.00	12.42
IT coarse tex	0.00	0.00	11.56
IT fine textu	0.04	0.00	34.30
IT foliar tex	8.07	0.00	17.11
IT flat textu	0.00	0.00	5.17
IT shadow 1 [	70.78	10.78	11.52
IT shadow 2 [	21.04	89.22	7.92
Total	100.00	100.00	100.00

Class	Commission (Percent)	Omission (Percent)	Commission (Pixels)	Omission (Pixels)
IT rough text	4.33	31.56	265/6119	2699/8553
IT coarse tex	41.95	19.03	2389/5695	777/4083
IT fine textu	6.24	14.75	1055/16904	2742/18591
IT foliar tex	17.01	8.37	1435/8434	639/7638
IT flat textu	89.16	24.80	2270/2546	91/367
IT shadow 1 [	7.47	29.22	424/5679	2169/7424
IT shadow 2 [	40.01	10.78	1562/3904	283/2625

Class	Prod. Acc. (Percent)	User Acc. (Percent)	Prod. Acc. (Pixels)	User Acc. (Pixels)
IT rough text	68.44	95.67	5854/8553	5854/6119
IT coarse tex	80.97	58.05	3306/4083	3306/5695
IT fine textu	85.25	93.76	15849/18591	15849/16904
IT foliar tex	91.63	82.99	6999/7638	6999/8434
IT flat textu	75.20	10.84	276/367	276/2546
IT shadow 1 [	70.78	92.53	5255/7424	5255/5679
IT shadow 2 [	89.22	59.99	2342/2625	2342/3904

Table 13: Accuracy assessment C(IT) ↔ IC

Overall Accuracy = (34713/45490) 76.3091%  
 Kappa Coefficient = 0.7025

Class	Ground Truth (Pixels)				
	IT rough text	IT coarse tex	IT fine textu	IT foliar tex	IT flat textu
Unclassified	0	0	0	0	0
IC rough text	5129	388	6	101	439
IC coarse tex	155	3991	2416	301	0
IC fine textu	12	437	12786	681	0
IC foliar tex	56	94	1815	5716	7
IC flat textu	140	23	0	7	172
IC shadow 1 [	0	6	50	872	0
IC shadow 2 [	0	0	0	0	0
Total	5492	4939	17073	7678	618

Class	Ground Truth (Pixels)		Total
	IT shadow 1	IT shadow 2	
Unclassified	0	0	0
IC rough text	0	0	6063
IC coarse tex	0	0	6863
IC fine textu	0	0	13916
IC foliar tex	201	7	7896
IC flat textu	0	0	342
IC shadow 1 [	4825	1038	6791
IC shadow 2 [	1525	2094	3619
Total	6551	3139	45490



Class	Ground Truth (Percent)				
	IT rough text	IT coarse tex	IT fine textu	IT foliar tex	IT flat textu
Unclassified	0.00	0.00	0.00	0.00	0.00
IC rough text	93.39	7.86	0.04	1.32	71.04
IC coarse tex	2.82	80.81	14.15	3.92	0.00
IC fine textu	0.22	8.85	74.89	8.87	0.00
IC foliar tex	1.02	1.90	10.63	74.45	1.13
IC flat textu	2.55	0.47	0.00	0.09	27.83
IC shadow 1 [	0.00	0.12	0.29	11.36	0.00
IC shadow 2 [	0.00	0.00	0.00	0.00	0.00
Total	100.00	100.00	100.00	100.00	100.00

Class	Ground Truth (Percent)		Total
	IT shadow 1	IT shadow 2	
Unclassified	0.00	0.00	0.00
IC rough text	0.00	0.00	13.33
IC coarse tex	0.00	0.00	15.09
IC fine textu	0.00	0.00	30.59
IC foliar tex	3.07	0.22	17.36
IC flat textu	0.00	0.00	0.75
IC shadow 1 [	73.65	33.07	14.93
IC shadow 2 [	23.28	66.71	7.96
Total	100.00	100.00	100.00

Class	Commission (Percent)	Omission (Percent)	Commission (Pixels)	Omission (Pixels)
IC rough text	15.40	6.61	934/6063	363/5492
IC coarse tex	41.85	19.19	2872/6863	948/4939
IC fine textu	8.12	25.11	1130/13916	4287/17073
IC foliar tex	27.61	25.55	2180/7896	1962/7678
IC flat textu	49.71	72.17	170/342	446/618
IC shadow 1 [	28.95	26.35	1966/6791	1726/6551
IC shadow 2 [	42.14	33.29	1525/3619	1045/3139

Class	Prod. Acc. (Percent)	User Acc. (Percent)	Prod. Acc. (Pixels)	User Acc. (Pixels)
IC rough text	93.39	84.60	5129/5492	5129/6063
IC coarse tex	80.81	58.15	3991/4939	3991/6863
IC fine textu	74.89	91.88	12786/17073	12786/13916
IC foliar tex	74.45	72.39	5716/7678	5716/7896
IC flat textu	27.83	50.29	172/618	172/342
IC shadow 1 [	73.65	71.05	4825/6551	4825/6791
IC shadow 2 [	66.71	57.86	2094/3139	2094/3619

Table 14: Accuracy assessment C(IC)↔IT

Overall Accuracy = (808410/915936) 88.2605%  
 Kappa Coefficient = 0.8464

Ground Truth (Pixels)					
Class	IC rough text	IC coarse tex	IC fine textu	IC foliar tex	IC flat textu
IT rough text	76267	10	0	8935	1923
IT coarse tex	14987	105737	3870	4093	2869
IT fine textu	0	6646	214193	20333	19
IT foliar tex	10	1472	16321	286346	182
IT flat textu	5103	0	0	0	1321
IT shadow 1 [	0	0	0	3709	0
IT shadow 2 [	0	0	0	0	0
Total	96367	113865	234384	323416	6314

Ground Truth (Pixels)			
Class	IC shadow 1 [	IC shadow 2 [	Total
IT rough text	0	0	87135
IT coarse tex	0	0	131556
IT fine textu	5	0	241196
IT foliar tex	13769	0	318100
IT flat textu	0	0	6424
IT shadow 1 [	110139	619	114467
IT shadow 2 [	2651	14407	17058
Total	126564	15026	915936

Ground Truth (Percent)					
Class	IC rough text	IC coarse tex	IC fine textu	IC foliar tex	IC flat textu
IT rough text	79.14	0.01	0.00	2.76	30.46
IT coarse tex	15.55	92.86	1.65	1.27	45.44
IT fine textu	0.00	5.84	91.39	6.29	0.30
IT foliar tex	0.01	1.29	6.96	88.54	2.88
IT flat textu	5.30	0.00	0.00	0.00	20.92
IT shadow 1 [	0.00	0.00	0.00	1.15	0.00
IT shadow 2 [	0.00	0.00	0.00	0.00	0.00
Total	100.00	100.00	100.00	100.00	100.00

Ground Truth (Percent)			
Class	IC shadow 1 [	IC shadow 2 [	Total
IT rough text	0.00	0.00	9.51
IT coarse tex	0.00	0.00	14.36
IT fine textu	0.00	0.00	26.33
IT foliar tex	10.88	0.00	34.73
IT flat textu	0.00	0.00	0.70
IT shadow 1 [	87.02	4.12	12.50
IT shadow 2 [	2.09	95.88	1.86
Total	100.00	100.00	100.00

Class	Commission (Percent)	Omission (Percent)	Commission (Pixels)	Omission (Pixels)
IT rough text	12.47	20.86	10868/87135	20100/96367
IT coarse tex	19.63	7.14	25819/131556	8128/113865
IT fine textu	11.20	8.61	27003/241196	20191/234384
IT foliar tex	9.98	11.46	31754/318100	37070/323416
IT flat textu	79.44	79.08	5103/6424	4993/6314
IT shadow 1 [	3.78	12.98	4328/114467	16425/126564
IT shadow 2 [	15.54	4.12	2651/17058	619/15026

Class	Prod. Acc. (Percent)	User Acc. (Percent)	Prod. Acc. (Pixels)	User Acc. (Pixels)
IT rough text	79.14	87.53	76267/96367	76267/87135
IT coarse tex	92.86	80.37	105737/113865	105737/131556
IT fine textu	91.39	88.80	214193/234384	214193/241196
IT foliar tex	88.54	90.02	286346/323416	286346/318100
IT flat textu	20.92	20.56	1321/6314	1321/6424
IT shadow 1 [	87.02	96.22	110139/126564	110139/114467
IT shadow 2 [	95.88	84.46	14407/15026	14407/17058

Table 15: Accuracy assessment C(IT)↔C(IC)

### 7.6.3 N-W area: Combination of spectral and textural properties

Table 16, 17, and 18 represent the combination by taking into consideration both, spectral and textural properties already at the selection of training and checking samples. Table 16 is based on C(IT)↔IC, table 17 on C(IC)↔IT, and table 18 on C(IT)↔C(IC). The quality figures of these three classifications are as follows:

- C(IT)↔IC: Overall Accuracy 76.0%; Kappa 0.69
- C(IC)↔IT: Overall Accuracy 73.2%; Kappa 0.67
- C(IT)↔C(IC): Overall Accuracy 83.0%; Kappa 0.78

Conclusion: By combining spectral and textural properties, the Overall Accuracy is quite good, although, there is a significant difference of 10% between the last two classifications, which again indicates that the training areas and checking areas do not ideally represent the same class. By comparing the Producer`s and User`s Accuracies, the problem class is again "flat", followed by "shadow 1" and "shadow 2". For "flat" only 645 pixels have been selected and a great part of the pixels has been assigned to class "old deciduous very dense". Also in this case, the ground truth areas for "flat" were not representative enough, therefore, the difference in the accuracy between the last two classifications are caused by the not well defined class "flat".

Overall Accuracy = (37196/48937) 76.0079%  
Kappa Coefficient = 0.6949

Class	Ground Truth (Pixels)					
	IC old decidu	IC conifers v	IC conifers l	IC larch rare	IC shadow 1	IC shadow 2
Unclassified	0	0	0	0	0	0
IT old decidu	11528	0	0	223	0	0
IT conifers v	80	5456	742	247	10	0
IT conifers l	0	3508	12068	1006	131	0
IT larch rare	429	920	987	4962	0	0
IT shadow 1 [	0	0	67	35	1284	0
IT shadow 2 [	0	19	119	0	1668	0
IT flat [Yell	329	0	0	89	0	0
Total	12366	9903	13983	6562	3093	0

Class	Ground Truth (Pixels)		Total
	IC shadow 2	IC flat	
Unclassified	0	0	0
IT old decidu	0	333	12084
IT conifers v	6	0	6541
IT conifers l	22	0	16735
IT larch rare	0	16	7314
IT shadow 1 [	755	0	2141
IT shadow 2 [	1602	0	3408
IT flat [Yell	0	296	714
Total	2385	645	48937

Class	Ground Truth (Percent)				
	IC old decidu	IC conifers v	IC conifers l	IC larch rare	IC shadow 1
Unclassified	0.00	0.00	0.00	0.00	0.00
IT old decidu	93.22	0.00	0.00	3.40	0.00
IT conifers v	0.65	55.09	5.31	3.76	0.32
IT conifers l	0.00	35.42	86.30	15.33	4.24
IT larch rare	3.47	9.29	7.06	75.62	0.00
IT shadow 1 [	0.00	0.00	0.48	0.53	41.51
IT shadow 2 [	0.00	0.19	0.85	0.00	53.93
IT flat [Yell	2.66	0.00	0.00	1.36	0.00
Total	100.00	100.00	100.00	100.00	100.00

Class	Ground Truth (Percent)		Total
	IC shadow 2	IC flat	
Unclassified	0.00	0.00	0.00
IT old decidu	0.00	51.63	24.69
IT conifers v	0.25	0.00	13.37
IT conifers l	0.92	0.00	34.20
IT larch rare	0.00	2.48	14.95
IT shadow 1 [	31.66	0.00	4.38
IT shadow 2 [	67.17	0.00	6.96
IT flat [Yell	0.00	45.89	1.46
Total	100.00	100.00	100.00

Class	Commission (Percent)	Omission (Percent)	Commission (Pixels)	Omission (Pixels)
IT old decidu	4.60	6.78	556/12084	838/12366
IT conifers v	16.59	44.91	1085/6541	4447/9903
IT conifers l	27.89	13.70	4667/16735	1915/13983
IT larch rare	32.16	24.38	2352/7314	1600/6562
IT shadow 1 [	40.03	58.49	857/2141	1809/3093
IT shadow 2 [	52.99	32.83	1806/3408	783/2385

Class	Prod. Acc. (Percent)	User Acc. (Percent)	Prod. Acc. (Pixels)	User Acc. (Pixels)
IT old decidu	93.22	95.40	11528/12366	11528/12084
IT conifers v	55.09	83.41	5456/9903	5456/6541
IT conifers l	86.30	72.11	12068/13983	12068/16735
IT larch rare	75.62	67.84	4962/6562	4962/7314
IT shadow 1 [	41.51	59.97	1284/3093	1284/2141
IT shadow 2 [	67.17	47.01	1602/2385	1602/3408
IT flat [Yell	45.89	41.46	296/645	296/714

Table 16: Accuracy assessment C(IT) ↔ IC

Overall Accuracy = (41938/57279) 73.2171%  
 Kappa Coefficient = 0.6748

Class	Ground Truth (Pixels)				
	IT old decidu	IT conifers v	IT conifers l	IT larch rare	IT shadow 1
Unclassified	0	0	0	0	0
IC old decidu	10672	55	0	20	0
IC conifers v	1	10062	561	653	149
IC conifers l	0	3024	9901	993	262
IC larch rare	221	785	597	5347	63
IC shadow 1 [	0	115	416	0	3843
IC shadow 2 [	0	0	0	0	4777
IC flat [Yell	733	0	0	52	0
Total	11627	14041	11475	7065	9094

Class	Ground Truth (Pixels)		Total
	IT shadow 2	IT flat	
Unclassified	0	0	0
IC old decidu	0	356	11103
IC conifers v	14	0	11440
IC conifers l	66	0	14246
IC larch rare	0	2	7015
IC shadow 1 [	1426	0	5800
IC shadow 2 [	1908	0	6685
IC flat [Yell	0	205	990
Total	3414	563	57279

Class	Ground Truth (Percent)				
	IT old decidu	IT conifers v	IT conifers l	IT larch rare	IT shadow 1
Unclassified	0.00	0.00	0.00	0.00	0.00
IC old decidu	91.79	0.39	0.00	0.28	0.00
IC conifers v	0.01	71.66	4.89	9.24	1.64
IC conifers l	0.00	21.54	86.28	14.06	2.88
IC larch rare	1.90	5.59	5.20	75.68	0.69
IC shadow 1 [	0.00	0.82	3.63	0.00	42.26
IC shadow 2 [	0.00	0.00	0.00	0.00	52.53
IC flat [Yell	6.30	0.00	0.00	0.74	0.00
Total	100.00	100.00	100.00	100.00	100.00

Class	Ground Truth (Percent)		Total
	IT shadow 2	IT flat	
Unclassified	0.00	0.00	0.00
IC old decidu	0.00	63.23	19.38
IC conifers v	0.41	0.00	19.97
IC conifers l	1.93	0.00	24.87
IC larch rare	0.00	0.36	12.25
IC shadow 1 [	41.77	0.00	10.13
IC shadow 2 [	55.89	0.00	11.67
IC flat [Yell	0.00	36.41	1.73
Total	100.00	100.00	100.00

Class	Commission (Percent)	Omission (Percent)	Commission (Pixels)	Omission (Pixels)
IC old decidu	3.88	8.21	431/11103	955/11627
IC conifers v	12.05	28.34	1378/11440	3979/14041
IC conifers l	30.50	13.72	4345/14246	1574/11475
IC larch rare	23.78	24.32	1668/7015	1718/7065
IC shadow 1 [	33.74	57.74	1957/5800	5251/9094
IC shadow 2 [	71.46	44.11	4777/6685	1506/3414



Class	Prod. Acc. (Percent)	User Acc. (Percent)	Prod. Acc. (Pixels)	User Acc. (Pixels)
IC old decidu	91.79	96.12	10672/11627	10672/11103
IC conifers v	71.66	87.95	10062/14041	10062/11440
IC conifers l	86.28	69.50	9901/11475	9901/14246
IC larch rare	75.68	76.22	5347/7065	5347/7015
IC shadow 1 [	42.26	66.26	3843/9094	3843/5800
IC shadow 2 [	55.89	28.54	1908/3414	1908/6685
IC flat [Yell	36.41	20.71	205/563	205/990

Table 17: Accuracy assessment C(IC)↔IT

Overall Accuracy = (760376/915936) 83.0163%

Kappa Coefficient = 0.7783

Class	Ground Truth (Pixels)				
	IC old decidu	IC conifers v	IC conifers l	IC larch rare	IC shadow 1 [
IT old decidu	66999	0	0	782	0
IT conifers v	1901	154904	8402	16996	0
IT conifers l	0	9566	323815	2841	12988
IT larch rare	3585	6803	5726	153002	0
IT shadow 1 [	0	617	5776	1699	37384
IT shadow 2 [	0	170	1588	19	43727
IT flat [Yell	2404	14	10	383	0
Total	74889	172074	345317	175722	94099

Class	Ground Truth (Pixels)		Total
	IC shadow 2 [	IC flat [Yell	
IT old decidu	0	8151	75932
IT conifers v	0	1729	183932
IT conifers l	2	0	349212
IT larch rare	0	4914	174030
IT shadow 1 [	14767	0	60243
IT shadow 2 [	12744	0	58248
IT flat [Yell	0	11528	14339
Total	27513	26322	915936

Class	Ground Truth (Percent)				
	IC old decidu	IC conifers v	IC conifers l	IC larch rare	IC shadow 1 [
IT old decidu	89.46	0.00	0.00	0.45	0.00
IT conifers v	2.54	90.02	2.43	9.67	0.00
IT conifers l	0.00	5.56	93.77	1.62	13.80
IT larch rare	4.79	3.95	1.66	87.07	0.00
IT shadow 1 [	0.00	0.36	1.67	0.97	39.73
IT shadow 2 [	0.00	0.10	0.46	0.01	46.47
IT flat [Yell	3.21	0.01	0.00	0.22	0.00
Total	100.00	100.00	100.00	100.00	100.00

Class	Ground Truth (Percent)		Total
	IC shadow 2 [	IC flat [Yell	
IT old decidu	0.00	30.97	8.29
IT conifers v	0.00	6.57	20.08
IT conifers l	0.01	0.00	38.13
IT larch rare	0.00	18.67	19.00
IT shadow 1 [	53.67	0.00	6.58
IT shadow 2 [	46.32	0.00	6.36
IT flat [Yell	0.00	43.80	1.57
Total	100.00	100.00	100.00

Class	Commission		Omission	
	(Percent)	(Percent)	(Pixels)	(Pixels)
IT old decidu	11.76	10.54	8933/75932	7890/74889
IT conifers v	15.78	9.98	29028/183932	17170/172074
IT conifers l	7.27	6.23	25397/349212	21502/345317
IT larch rare	12.08	12.93	21028/174030	22720/175722
IT shadow 1 [	37.94	60.27	22859/60243	56715/94099
IT shadow 2 [	78.12	53.68	45504/58248	14769/27513
IT flat [Yell	19.60	56.20	2811/14339	14794/26322
Class	Prod. Acc.	User Acc.	Prod. Acc.	User Acc.
	(Percent)	(Percent)	(Pixels)	(Pixels)
IT old decidu	89.46	88.24	66999/74889	66999/75932
IT conifers v	90.02	84.22	154904/172074	154904/183932
IT conifers l	93.77	92.73	323815/345317	323815/349212
IT larch rare	87.07	87.92	153002/175722	153002/174030
IT shadow 1 [	39.73	62.06	37384/94099	37384/60243
IT shadow 2 [	46.32	21.88	12744/27513	12744/58248
IT flat [Yell	43.80	80.40	11528/26322	11528/14339

Table 18: Accuracy assessment C(IT)↔C(IC)

In the following table (table 19), the accuracies achieved so far are summarised. Concluding from these results one can see that the expectations that by considering the texture in the classification does not significantly improve the quality, in contrast even, in this case, is lower, but one should be aware that this difference is not very significant.

	C(IT) $\leftrightarrow$ IC		C(IC) $\leftrightarrow$ IT		C(IT) $\leftrightarrow$ C(IC)	
	OA	Kappa	OA	Kappa	OA	Kappa
Spectral	86,4	0,81	77,4	0,71	83,4	0,78
Textural	80,7	0,76	76,3	0,70	88,3	0,85
Spectral + Textural	76	0,79	73,2	0,67	83	0,78

Table 19 : General overview of the quality assessment

#### 7.6.4 S-E area: Spectral case

Table 20, represents the assessment of the spectral classification and shows the assessment of  $C(IT) \leftrightarrow IC$ , with an Overall Accuracy of 88.8% and Kappa 0.86. By comparing the Producer`s and User`s Accuracies, one can clearly see that “meadow 1” is unreliable and equal to 0, which means that it has been classified but the training areas have different properties than the checking areas. Therefore, the conclusion must be drawn that this is an indicator that the training statistics and the checking statistics are not equivalent and the properties of checking and training areas are different.

Since from the very beginning the decision has been made not to concentrate on the S-E area because of the suboptimal image content, the classification has been carried out with multispectral data alone in order to investigate whether a good quality could be achieved. The accuracy assessment showed no unexpected difficulties. In practice, the entire classification process should be repeated by looking carefully at those object classes which caused the problems. In the case of the current investigation, a second run has not been carried out due to the fact that the entire S-E area was not in the focus anymore.

Overall Accuracy = (30960/34880) 88.7615%  
 Kappa Coefficient = 0.8590

Ground Truth (Pixels)					
Class	IC Deciduos y	IC Conifers 1	IC Deciduos o	IC Conifers 2	IC Meadow 1
Unclassified	0	0	0	0	0
IT Deciduos y	9226	0	951	14	1
IT Conifers 1	0	472	0	805	0
IT Deciduos o	83	0	8355	0	335
IT Conifers 2	0	6	0	5554	0
IT Meadow 1 [	0	0	0	0	0
IT Red-tile-r	0	0	0	0	0
IT Shadow [Si	0	0	0	0	0
IT Meadow 2 [	0	0	0	0	103
Total	9309	478	9306	6373	439

Ground Truth (Pixels)				
Class	IC Red-tile-r	IC Shadow	IC Meadow 2	Total
Unclassified	0	0	0	0
IT Deciduos y	7	37	4	10240
IT Conifers 1	0	311	0	1588
IT Deciduos o	11	5	687	9476
IT Conifers 2	1	167	0	5728
IT Meadow 1 [	0	0	0	0
IT Red-tile-r	3906	351	4	4261
IT Shadow [Si	36	2211	0	2247
IT Meadow 2 [	0	1	1236	1340
Total	3961	3083	1931	34880

Ground Truth (Percent)					
Class	IC Deciduos y	IC Conifers 1	IC Deciduos o	IC Conifers 2	IC Meadow 1
Unclassified	0.00	0.00	0.00	0.00	0.00
IT Deciduos y	99.11	0.00	10.22	0.22	0.23
IT Conifers 1	0.00	98.74	0.00	12.63	0.00
IT Deciduos o	0.89	0.00	89.78	0.00	76.31
IT Conifers 2	0.00	1.26	0.00	87.15	0.00
IT Meadow 1 [	0.00	0.00	0.00	0.00	0.00
IT Red-tile-r	0.00	0.00	0.00	0.00	0.00
IT Shadow [Si	0.00	0.00	0.00	0.00	0.00
IT Meadow 2 [	0.00	0.00	0.00	0.00	23.46
Total	100.00	100.00	100.00	100.00	100.00

Ground Truth (Percent)				
Class	IC Red-tile-r	IC Shadow	IC Meadow 2	Total
Unclassified	0.00	0.00	0.00	0.00
IT Deciduos y	0.18	1.20	0.21	29.36
IT Conifers 1	0.00	10.09	0.00	4.55
IT Deciduos o	0.28	0.16	35.58	27.17
IT Conifers 2	0.03	5.42	0.00	16.42
IT Meadow 1 [	0.00	0.00	0.00	0.00
IT Red-tile-r	98.61	11.39	0.21	12.22
IT Shadow [Si	0.91	71.72	0.00	6.44
IT Meadow 2 [	0.00	0.03	64.01	3.84
Total	100.00	100.00	100.00	100.00

Class	Commission (Percent)	Omission (Percent)	Commission (Pixels)	Omission (Pixels)
IT Deciduos y	9.90	0.89	1014/10240	83/9309
IT Conifers 1	70.28	1.26	1116/1588	6/478
IT Deciduos o	11.83	10.22	1121/9476	951/9306
IT Conifers 2	3.04	12.85	174/5728	819/6373
IT Meadow 1 [	0.00	100.00	0/0	439/439
IT Red-tile-r	8.33	1.39	355/4261	55/3961
IT Shadow [Si	1.60	28.28	36/2247	872/3083
IT Meadow 2 [	7.76	35.99	104/1340	695/1931

Class	Prod. Acc. (Percent)	User Acc. (Percent)	Prod. Acc. (Pixels)	User Acc. (Pixels)
IT Deciduos y	99.11	90.10	9226/9309	9226/10240
IT Conifers 1	98.74	29.72	472/478	472/1588
IT Deciduos o	89.78	88.17	8355/9306	8355/9476
IT Conifers 2	87.15	96.96	5554/6373	5554/5728
IT Meadow 1 [	0.00	0.00	0/439	0/0
IT Red-tile-r	98.61	91.67	3906/3961	3906/4261
IT Shadow [Si	71.72	98.40	2211/3083	2211/2247
IT Meadow 2 [	64.01	92.24	1236/1931	1236/1340

Table 20: Accuracy assessment C(IT) ↔ IC

## 7.7 Combination of spectral and textural classifications

In this subchapter, with the help of the ENVI function “band mathematics”, pixel values from the spectral classification have been combined with pixel values from textural classification, yielding new classes of combinations, like “conifers1 - rough texture”, “meadow - flat”, “conifers 2 - fine texture” and so on. The combination has been done on a pixel basis, thus, for each pixel the spectral classification result has been combined with the textural classification result. This combination leads to a class that in its name contains the respective spectral class and the respective textural class. The result of the combination is presented in figure 45:

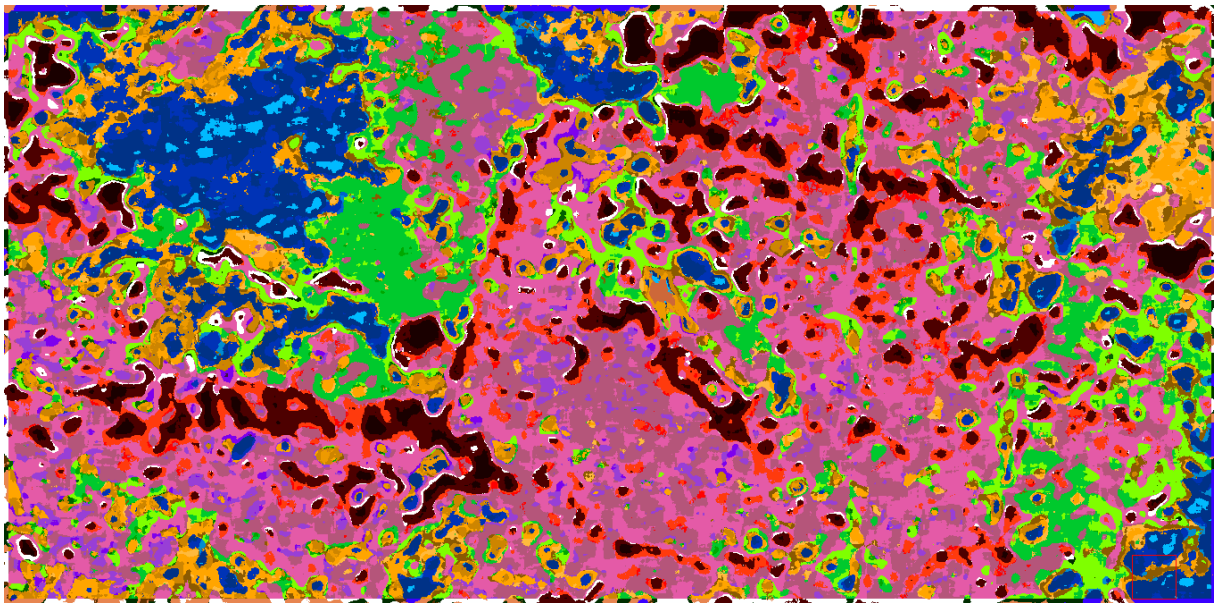


Fig. 45: Result of the mathematical combination of spectral and textural classification



Legend

<b>class</b>	<b>color</b>		
<i>unclassified</i>		<i>conifers 2-shadow 1</i>	
<i>conifers 1-rough texture</i>		<i>conifers 2-shadow 2</i>	
<i>conifers 1-coarse texture</i>		<i>meadow-rough texture</i>	
<i>conifers 1-fine texture</i>		<i>meadow-coarse texture</i>	
<i>conifers 1-foliar texture</i>		<i>meadow-fine texture</i>	
<i>conifers 1-flat</i>		<i>meadow-foliar texture</i>	
<i>conifers 1-shadow 1</i>		<i>meadow-flat</i>	
<i>deciduous old-rough texture</i>		<i>meadow-shadow 1</i>	
<i>deciduous old-coarse texture</i>		<i>meadow-shadow 2</i>	
<i>deciduous old-fine texture</i>		<i>shadow-fine texture</i>	
<i>deciduous old-foliar texture</i>		<i>shadow-foliar texture</i>	
<i>deciduous old-flat</i>		<i>shadow-shadow 1</i>	
<i>deciduous old-shadow 1</i>		<i>shadow-shadow 2</i>	
<i>conifers 2-rough texture</i>		<i>larch-rough texture</i>	
<i>conifers 2-coarse texture</i>		<i>larch-coarse texture</i>	
<i>conifers 2-fine texture</i>		<i>larch-fine texture</i>	
<i>conifers 2-foliar texture</i>		<i>larch-foliar texture</i>	
<i>conifers 2-flat</i>		<i>larch-flat</i>	
		<i>larch-shadow 1</i>	

The mathematical combination yielded a great number of classes so that their use in practice would be of very limited value. By analyzing the mathematically found classes, it turned out, that many of the classes contained only a few pixels or appeared only in rather small and scattered patches or were located at the boundaries of major classes, and therefore, it can be assumed that they do not play a significant role. These classes, yielded by mathematical combinations, are just caused by the slight inaccuracies of class discriminations by the classification algorithm and it is almost impossible to match them with class assignments by visual inspection. Therefore, this sort of classes should not be used for the assessment of the accuracies.

In order to apply the usual quality assessment using the confusion matrix, both classifications need to have the same number of classes. One classification has 36 classes and the other classification only seven classes, therefore, individual classes have to be selected for the comparison. A cross-reference table (table 21) has been created, which shows the complicated relationship between the two classifications. There are two different approaches possible for class selection. The first is based on a visual evaluation and the second one is based on a cross-reference table showing the pairing frequencies and proposes the maximum frequency of a class pairing. The red fields in the cross-reference table represent the maximum values, while the red numbers were independently selected by visual impression. For five of the seven classes, the visual and the mathematical selection is identical. Still, it has been decided to use only the visual selection for the quality assessment with the help of the confusion matrix, where the classification from manual selected spectral-textural training samples serves as a sort of ground truth.

The following table 22, shows the comparison of a classification based on training samples of the spectral together with the textural properties, and a classification, which is the result of the mathematical operation between a classification based on spectral training samples and a classification based on textural training samples. It should be mentioned explicitly, that the comparison is one of two classifications rather than of checking areas with a classified image.  $IT_{sp+tx}$  means training samples considering both spectral and textural properties, while  $IT_{sp}$  means training samples considering spectral, and  $IT_{tx}$  training samples considering textural properties. The ring symbol stands for a mathematical operation, and brackets [...] for the result of that operation. In the following this comparison is written as  $C(IT_{sp+tx}) \Leftrightarrow [C(IT_{sp}) \circ C(IT_{tx})]$ .

One must keep in mind, that in table 22 the comparison must not be interpreted as a real accuracy assessment. The attention should also be drawn at the class names for the “reference” classes (the columns) and the “classified” classes (the rows): they are not identical due to the two different classifications.

As one example the class pair “meadow-flat” versus “flat” should be discussed. Firstly, only the small number of 730 pixels have been correctly classified, but more conspicuous is the great difference between Producer’s and User’s Accuracy of 22.1% and 97.1%, respectively. The reference class “flat” consisted of 3282 pixels, which is not large, but still by far larger than the classified class “meadow-flat”, which has only 752 pixels. Keeping this ratio in mind, it can already be expected that the Producer’s Accuracy cannot be higher than  $752/3282=22.9\%$ , while the User’s Accuracy could even reach 100%. From this point of view, the achieved results lie quite close to the achievable maxima and, therefore, they have to be considered as very good. This example shows impressively that the User’s and Producer’s Accuracy of a certain class depend a lot on the number of pixels in the reference areas of that class and the number of pixels classified into this class. The greater the difference the more may the accuracies differ from 100%.

Conclusion: In this special case, the accuracy assessment table is just an attempt for an accuracy assessment; therefore, it is much more important to take a look into the cross-reference table of these two classifications, because there all classes are taken into consideration and not only a more or less reliably selected subset.

		<i>old decid very dense</i>	<i>conif very dense</i>	<i>conif less dense</i>	<i>larch rarefied</i>	<i>shad1</i>	<i>shad2</i>	<i>flat</i>	
	<i>sptx_36+1</i>	1	2	3	4	5	6	7	
0	0	840004	732004	566724	741906	855693	857688	901597	
<i>shad-foliar</i>	1	49853	0	811	19785	169	17302	11786	0
<i>conif2-fine</i>	2	154684	0	12423	128079	13819	4	359	0
<i>decid old-coarse</i>	3	39013	22485	2518	3	12502	0	0	1505
<i>larch-foliar</i>	4	27010	0	8515	2089	16406	0	0	0
<i>conif1-foliar</i>	5	55522	0	52838	1654	1030	0	0	0
<i>conif1-fine</i>	6	58510	0	56096	1658	756	0	0	0
<i>shad-shad1</i>	7	75426	0	607	7020	137	36313	31349	0
<i>decid old-rough</i>	8	54744	43206	1069	0	7930	0	0	2539
<i>larch-coarse</i>	9	50649	0	5563	610	44463	0	0	13
<i>conif2-foliar</i>	10	179534	0	14126	147838	16187	18	1365	0
<i>conif2-coarse</i>	11	25650	0	286	13209	12155	0	0	0
<i>conif2-shad1</i>	12	21711	0	1808	17566	1462	15	860	0
<i>larch-rough</i>	13	19151	0	1812	61	17265	0	0	13
<i>larch-fine</i>	14	18989	0	4498	2585	11906	0	0	0
<i>shad-shad2</i>	15	17016	0	1	38	0	5272	11705	0
<i>mead-coarse</i>	16	9204	24	2028	227	2751	0	0	4174
<i>conif1-coarse</i>	17	7040	0	5386	615	1039	0	0	0
<i>larch-shad1 *</i>	18	6592	0	726	259	5601	0	0	6
<i>mead-rough</i>	19	6661	24	635	72	1438	0	0	4492
<i>shad-fine</i>	20	6072	0	122	3810	20	1316	804	0
<i>decid old-flat</i>	21	5416	5073	8	0	132	0	0	203
<i>decid old-shad1 *</i>	22	5378	4130	326	0	647	0	0	275
<i>conif2-rough</i>	23	4688	0	29	1640	3019	0	0	0
<i>conif1-shad1</i>	24	4700	0	4363	179	158	0	0	0
<i>decid old-foliar</i>	25	4161	795	1861	1	1504	0	0	0
<i>mead-foliar</i>	26	2020	0	1650	57	233	0	0	80
<i>conif1-rough</i>	27	1891	0	1588	86	217	0	0	0
<i>mead-fine</i>	28	1546	0	1316	44	168	0	0	18
<i>decid old-fine</i>	29	1395	193	698	0	504	0	0	0
<i>mead-flat</i>	30	752	1	6	1	14	0	0	730
<i>mead-shad1</i>	31	660	1	200	13	157	0	0	289
<i>larch-flat</i>	32	222	0	7	0	213	0	0	2
<i>conif2-shad2</i>	33	34	0	1	13	0	0	20	0
<i>conif2-flat</i>	34	28	0	0	0	28	0	0	0
<i>mead-shad2</i>	35	8	0	5	0	0	3	0	0
<i>conif1-flat</i>	36	6	0	6	0	0	0	0	0
		75932	183932	349212	174030	60243	58248	14339	
Max		43206	56096	147838	44463	36313	31349	4492	

Table 21: Cross-reference table

Overall Accuracy = (340351/436631) 77.9493%  
 Kappa Coefficient = 0.7162

Ground Truth (Pixels)					
Class	Unclassified	IT old decidu	IT conifers vIT conifers	IIT larch	rare
Unclassified	0	0	0	0	0
Decidold_roug	0	43206	1069	0	7930
Conif1_fine	0	0	56096	1658	756
Conif2_foliar	0	0	14126	147838	16187
Larch_coarse	0	0	5563	610	44463
Shadow_shadow	0	0	607	7020	137
Shadow_shadow	0	0	1	38	0
Meadow_flat	0	1	6	1	14
Total	0	43207	77468	157165	69487

Ground Truth (Pixels)				
Class	IT shadow 1	[IT shadow 2	[IT flat [Yell	Total
Unclassified	0	0	0	0
Decidold_roug	0	0	2539	54744
Conif1_fine	0	0	0	58510
Conif2_foliar	18	1365	0	179534
Larch_coarse	0	0	13	50649
Shadow_shadow	36313	31349	0	75426
Shadow_shadow	5272	11705	0	17016
Meadow_flat	0	0	730	752
Total	41603	44419	3282	436631

Ground Truth (Percent)					
Class	Unclassified	IT old decidu	IT conifers vIT conifers	IIT larch	rare
Unclassified	0.00	0.00	0.00	0.00	0.00
Decidold_roug	0.00	100.00	1.38	0.00	11.41
Conif1_fine	0.00	0.00	72.41	1.05	1.09
Conif2_foliar	0.00	0.00	18.23	94.07	23.30
Larch_coarse	0.00	0.00	7.18	0.39	63.99
Shadow_shadow	0.00	0.00	0.78	4.47	0.20
Shadow_shadow	0.00	0.00	0.00	0.02	0.00
Meadow_flat	0.00	0.00	0.01	0.00	0.02
Total	0.00	100.00	100.00	100.00	100.00

Ground Truth (Percent)				
Class	IT shadow 1	[IT shadow 2	[IT flat [Yell	Total
Unclassified	0.00	0.00	0.00	0.00
Decidold_roug	0.00	0.00	77.36	12.54
Conif1_fine	0.00	0.00	0.00	13.40
Conif2_foliar	0.04	3.07	0.00	41.12
Larch_coarse	0.00	0.00	0.40	11.60
Shadow_shadow	87.28	70.58	0.00	17.27
Shadow_shadow	12.67	26.35	0.00	3.90
Meadow_flat	0.00	0.00	22.24	0.17
Total	100.00	100.00	100.00	100.00

Class	Commission (Percent)	Omission (Percent)	Commission (Pixels)	Omission (Pixels)
Unclassified	0.00	0.00	0/0	0/0
Decidold_roug	21.08	0.00	11538/54744	1/43207
Conif1_fine	4.13	27.59	2414/58510	21372/77468
Conif2_foliar	17.65	5.93	31696/179534	9327/157165
Larch_coarse	12.21	36.01	6186/50649	25024/69487
Shadow_shadow	51.86	12.72	39113/75426	5290/41603
Shadow_shadow	31.21	73.65	5311/17016	32714/44419
Meadow_flat	2.93	77.76	22/752	2552/3282

Class	Prod. Acc. (Percent)	User Acc. (Percent)	Prod. Acc. (Pixels)	User Acc. (Pixels)
Unclassified	0.00	0.00	0/0	0/0
Decidold_roug	100.00	78.92	43206/43207	43206/54744
Conif1_fine	72.41	95.87	56096/77468	56096/58510
Conif2_foliar	94.07	82.35	147838/157165	147838/179534
Larch_coarse	63.99	87.79	44463/69487	44463/50649
Shadow_shadow	87.28	48.14	36313/41603	36313/75426
Shadow_shadow	26.35	68.79	11705/44419	11705/17016
Meadow_flat	22.24	97.07	730/3282	730/752

Table 22:  $C(IT_{sp+tx}) \Leftrightarrow [C(IT_{sp}) \circ C(IT_{tx})]$

## 8 Conclusions

This research was intended to investigate whether taking into consideration textural features alone or together with spectral features may bear the potential to improve the classification accuracy when discriminating between forest stands in high-resolution satellite images. Images from the Pleiades satellites served as the data source. Any other of today's highly resolving images captured from space would have been suitable, too.

In order to limit the number of possible approaches, some restrictions have been defined in advance and during the first steps of investigations:

- First, only the well-known Haralick features, based on the Greylevel Co-occurrence Matrix (GLCM), should be used for deriving textural features;
- Second, only one set of parameters has been applied for deriving the textural features;
- Third, only a very limited set of Haralick features has been selected for the eventual investigations;
- Fourth, as classification algorithm only the Maximum Likelihood approach has been used.

Due to these limitations, several investigations were necessary at the beginning. There is no doubt, that it is justified to base investigations on the Haralick approach, therefore, not too much attention has been paid to other approaches. Although the Haralick textural features have been well known for decades and have successfully served as basic texture measures for a great many research projects, some further testing was needed in order to understand their practical behavior in forested areas in the Pleiades images.

Besides checking the influences of the GLCM's quantization parameters, direction, and distance setting, the window size seemed to be quite important. The generation of texture images can be compared to non-linear filtering in the spatial domain. A moving window is

shifted over the image and in each window Haralick features are calculated. Therefore, it is obvious, that the window size may have a significant influence on distinguishing between areas of uniform textures. Small windows do not smear the boundary between texture classes on the one hand, but on the other hand, small windows bear very little information about typical texture properties, since the texture is a property of a more or less large image patch rather than the property of an individual pixel. Increasing the window size offers by far more possibilities to derive reliable texture parameters at the cost of uncertainties on texture boundaries and, later on, of the accuracy of class boundaries. Small texture areas will be smoothed and incorrectly analyzed. By deriving the textural features for a series of window sizes from 5x5 pixel to 25x25 pixels, the visual impression was in favor of 15x15 pixels. This window size has then been used for all further investigations. A size of 15x15 pixels would also have allowed varying the setting of the directional and even of the distance parameter. These parameters have not been changed, the direction was left at "South-East" and the distance at 1, i.e. "Neighboring Pixel". The question arises whether a too strict limitation has been imposed on the investigations. As for the direction, one should first be aware of the sensitivity of that parameter to a derived textural feature. For all image textures with a typical directional, non-isotropic behavior, such as rows in vineyards, for instance, the directional parameter is quite important. In forested areas, one usually observes an isotropic behavior and, therefore, varying the directional parameter seemed to be superfluous. As for the distance parameter, a variation makes only sense, first, if the window size is big enough, possibly greater than 7 or 9, and second, if a series of distance settings are compared to each other, which would allow drawing conclusions regarding the spatial frequency of the texture. In order to limit the calculations in this investigation, the distance setting has been left constant, although it would be worth to check also other settings because young and old forests show quite different spatial frequencies. Hence, it might help to achieve a better distinction between old and young forest stands. Future investigations should take this fact into account.

There are quite a lot of Haralick features, which could be used. In order to keep the effort low, only three of them have been selected, i.e. the mean, the contrast, and the entropy. Of course, the question arises, whether these features provide the optimum choice for forest analysis. A rough comparison with other features showed partly high correlations, and it was hard to determine, which set of features is optimal. The selection of the above-mentioned features was supported by other research, who successfully used these three features for analyzing satellite images. No further checking has taken place, but certainly, it should be kept in mind for future research.

Finally, a choice has been made regarding the classification algorithm. For the classification of multispectral satellite images, the Maximum Likelihood (ML) approach has become one of the most used standards. There are several prerequisites which need to be fulfilled in order to successfully apply ML. Most importantly, training data must be normally distributed and the distribution should form not too big clouds, in order to guarantee good class separability. By careful selection of training data in spectral images, the preconditions are fulfilled to a great extent. Textural features may behave differently, and therefore, it was a must to investigate closer how the data clouds of the training areas behave in the feature space. A first visual inspection did not look that nice and, therefore, the shape of the clouds and the derived parameters of the normal distribution have been carefully compared. As a result, one comes to the following conclusion: The ML approach is certainly not the optimal



for this sort of texture classification since individual training data deviate significantly from an ideal normal distribution. On the other hand, there are features which come quite close to the ideal conditions. This investigation, therefore, dared to stick to ML and to find out which accuracy would be achievable. A careful separability analysis and the accuracy assessment showed weak points but also proved that ML may yield good, though not excellent results. The assumption that including textural parameters in the classification would significantly improve the accuracy of the classified data could not be confirmed. There is a slight improvement compared to the classification based on spectral features, if only textural features are analysed. Unfortunately, the achieved accuracy of a classification based on spectral together with textural features was even slightly worse. But in any case, the degradations as well as the improvements are far from any significance. The great advantage of ML is its implementation in almost each remote sensing software package and its comparably simple handling, but it needs a lot of effort for careful selection of training data, especially as far as texture selection is concerned. Still, future research should focus on other classification approaches as well, which allow a more general data distribution.

Summarizing, one can state, that this investigation leads to an insight of how Haralick textural parameters behave in the classification of forested areas in images acquired by modern high-resolution space sensors. Although the results are not as perfect as one would have preferred, several points could be found, which certainly need further research. But there is no question, that textural parameter will play an increasingly important role when analyzing modern remotely sensed images.

## References

- Anys H., Bannari A., He D.C., and Morin D., (1994). Texture Analysis for the Mapping of Urban Areas Using Airborne MEIS-II images. Proceedings of the First International Airborne Remote Sensing Conference and Exhibition, Strasbourg, France, Vol. 3, pp. 231-245;
- Buntilov V.M., (2013). Pan-Sharpener of Multispectral Imagery Using Content-Specific Orthogonal Linear Transform. International Journal of Computer and Communication Engineering, Vol. 2, No. 3;
- Chen C. H., Pau L. F., and Wang P. S. P., (1998). Chapter: Texture Analysis. In The Handbook of Pattern Recognition and Computer Vision (2nd Edition), pp. 207-248;
- Coburn C. A., and Roberts A. C. B., (2004). A Multiscale Texture Analysis Procedure for Improved Forest Stand Classification. International Journal of Remote Sensing 25: 4287–4308;
- Fisher A., (1923). The Mathematical Theory of Probabilities. Vol.1, The Macmillan Company, New York;
- Franklin S. E., Wulder M. A., and Gerylo G. R., (2001). Texture Analysis of IKONOS Panchromatic Data for Douglas-Fir Forest Age Class Separability in British Columbia. International Journal of Remote Sensing 22: 2627–2632;
- Grigorescu S.E., Petkov N., and Kruizing P., (2002). Comparison of Texture Features Based on Gabor Filters; IEEE Transactions on Image Processing, 11(10), 1160-1167;
- Gonzales R.C., and Woods R.E., (2001). Digital Image Processing. Prentice Hall International. Chapter: Image Enhancement in Spatial Domain pp 88-93, Chapter: Representation and Description, pp. 665-674;
- Hall-Beyer M., (2017). GLCM Texture: A Tutorial, v.3.0 March 2017. [https://prism.ucalgary.ca/bitstream/handle/1880/51900/texture%20tutorial%20v%203\\_0%20180206.pdf](https://prism.ucalgary.ca/bitstream/handle/1880/51900/texture%20tutorial%20v%203_0%20180206.pdf). Accessed on 10 May 2019;
- Hall-Beyer M., (2017). Practical Guidelines for Choosing GLCM Textures to Use in Landscape Classification Tasks Over a Range of Moderate Spatial Scales. International Journal of Remote Sensing, 38:5, 1312-1338;
- Haralick R. M., Shanmugam K., and Dinstein I., (1973). Textural Features for Image Classification. IEEE Transactions on Systems, Man, and Cybernetics, Vol.3, No.6, pp. 610–621;
- Jensen J.R., (2005). Introductory Digital Image Processing: A Remote Sensing Perspective - 3rd ed. Prentice Hall, United States of America. p. 526;
- Jenicka S. and Suruliandi A., (2014). A Textural Approach for Land Cover Classification of Remotely Sensed Image. CSI Transactions on ICT, Vol. 2, pp. 1-9;

Kerroum M.A., Hammouch A., and Aboutajdine D., (2009). Textural Feature Selection by Joint Mutual Information Based on Gaussian Mixture Model for Multispectral Image Classification. *Pattern Recognition Letters* 31(10):1168-1174;

Kidiyo K., Miloud C. E. M., and Nasreddine T., (2014 ). Recent Trends in Satellite Image Pan-sharpening Techniques. 1st International Conference on Electrical, Electronic and Computing Engineering, June 2014, Vrnjacka Banja, Serbia;

Lillesand T. M., and Kiefer R. W., (2000). *Remote Sensing and Image Interpretation*, 4th Edition, Wiley & Sons, New York, 724 p.;

Mausel P.W., Kramber W.J., and Lee J.K., (1990). Optimum Band Selection of Supervised Classification of Multispectral Data. *Photogrammetric Engineering and Remote Sensing*, Vol.56(1), pp. 55-60;

Poli D., Remondino F., Angiuli E., and Agugiaro G., (2015). Radiometric and Geometric Evaluation of GeoEye-1, WorldView-2 and Pléiades-1A Stereo Images for 3D Information Extraction. *ISPRS Journal of Photogrammetry and Remote Sensing*, Volume 100, February 2015, pp. 35-47;

Puetz A.M. and Olsen R.C., (2006). Haralick Texture Features Expanded into the Spectral Domain; *Proc. SPIE 6233, Algorithms and Technologies for Multispectral, Hyperspectral, and Ultraspectral Imagery XII*;

Richards J.A., (1999). *Remote Sensing Digital Image Analysis*, Springer-Verlag, Berlin, p.133, p. 240;

Sidhu A.S. and Dillon T.S., (2009). Biomedical Data and Applications. Content-Based Visual Query on Texture Feature in Multimedia Medical Databases, pp.108 -109;

Vansteenkiste E., Schoutteet A.,Gautama S., and Philips W., (2004). Comparing Color and Textural Transformation in very High-Resolution Satellite Image Classification. *Conference: Image Processing, ICIP'04, Vol.5, pp. 3351-3354*;

Wang L., Chen S., Chunyuan D., Wenjie J., and Dameng Y., (2016). A Survey of Methods Incorporating Spatial Information in Image Classification and Spectral Unmixing. *International Journal of Remote Sensing*. Vol. 37(16), pp. 3870-3910;

Zhao P., Zhao J., Wu J., Yang Y., Xue W., and Hou Y., (2016). Integration of Multi-Classifiers in Object-Based Methods for Forest Classification in the Loess Plateau, China, pp. 283-289.

## Internet sources

- [1] [http://www.landinfo.com/products\\_satellite.htm](http://www.landinfo.com/products_satellite.htm) (last access: 3.3.2019);
- [2] <https://directory.eoportal.org/web/eoportal/satellite-missions/p/pleiades> (last access: 3.3.2019);
- [3] <https://pannatura.at/wald/daten-und-fakten/> (last access: 15.03.2019);
- [4] <http://region-rosalia.at> (last access:3.3.2019);
- [5] [http://www.intelligence-airbusds.com/files/pmedia/public/r49228\\_9\\_pleiades\\_product.pdf](http://www.intelligence-airbusds.com/files/pmedia/public/r49228_9_pleiades_product.pdf) (last access: 4.3.2019);
- [6] <https://earth.esa.int/web/eoportal/satellite-missions/p/pleiades> (last access: 4.3.2019);
- [7] <http://desktop.arcgis.com/en/arcmap/latest/manage-data/raster-and-images/fundamentals-of-panchromatic-sharpening.htm> (last access: 4.3.2019);
- [8] <https://apollomapping.com/imagery/high-resolution-imagery/pleiades-1> (last access: 4.3.2019);
- [9] <https://www.sciencedirect.com/topics/earth-and-planetary-sciences/spatial-resolution> (last access: 4.3.2019);
- [10] <https://www.sciencedirect.com/topics/earth-and-planetary-sciences/spectral-resolution> (last access: 4.3.2019);
- [11] <https://www.sciencedirect.com/topics/earth-and-planetary-sciences/radiometric-resolution> (last access: 4.3.2019);
- [12] <https://www.sciencedirect.com/topics/earth-and-planetary-sciences/temporal-resolution> (last access: 4.3.2019);
- [13] [https://en.wikipedia.org/wiki/Stand\\_level\\_modelling](https://en.wikipedia.org/wiki/Stand_level_modelling) (last access: 4.3.2019);
- [14] [https://en.wikipedia.org/wiki/Crown\\_closure](https://en.wikipedia.org/wiki/Crown_closure) (last access: 4.3.2019).